Lelio Orci · Alain Perrelet

Freeze-Etch Histology

A Comparison between Thin Sections and Freeze-Etch Replicas

With 82 Figures

Springer-Verlag
Berlin Heidelberg New York 1975

LELIO ORCI, M. D.
ALAIN PERRELET, M. D.
Institute of Histology and Embryology, School of Medicine, University of Geneva, Geneva, Switzerland

ISBN 978-3-642-66022-1 ISBN 978-3-642-66020-7 (eBook)
DOI 10.1007/978-3-642-66020-7

Library of Congress Cataloging in Publication Data. Orci, Lelio. Freeze-Etch Histology. Bibliography: p. Includes index. 1. Freeze-Etching. 2. Mammals-Cytology. I. Perrelet, Alain, joint author. II. Title. QH236.072 599'.08'7 74-22379

Softcover reprint of the hardcover 1st edition 1975

Preface

The development of the electron microscope brought in a new era, in which cell structures could be visualized down to a macromolecular level. It is of course well recognized that some cell components can be modified or even completely lost during the complex sequence of fixation, dehydration, staining and plastic embedding which is essential before a thin section can be obtained. Further, only these cell components which can be made electron opaque can be visualized. For these reasons, the morphologist and cell biologist alike have to explore alternative techniques of specimen preparation which may avoid some of the artefacts inherent in conventional thin-section electron microscopy, and at the same time give a totally different view of the cell.

Such a new technique is freeze-etching. The aspect of the freeze-etched cell is, however, so different from that seen in a thin section that it requires both time and experience to move from one to the other. The purpose of this book is to provide a bridge, to help those who are familiar with conventional electron microscopy, to cross into the less familiar freeze-etching. This has been done by providing paired photographs wherever possible, one showing the thin section of a tissue or a cell, the other a freeze-etch replica of a similar material. At the same time we have tried to provide a basis for interpretation of freeze-etched structures, and we hope the reader will find the first 23 Plates especially useful in this respect. Because there are many excellent atlases of cell structure available at the present time, we felt there was no need to provide lengthy discussions of each plate. Captions are therefore kept to a strict minimum, as are the references provided for each tissue studied with the freeze-etching technique.

Geneva, January 1975 THE AUTHORS

Contents

Key to Symbols and Abbreviations

$\overline{A}$	A-Face
$\overline{B}$	B-Face
A	Axon (Nerve Fiber)
AA	Non-Myelinated Axon
AL	Alveolar Lumen (Lung)
BB	Basal Body
BC	Bile Canaliculus
BI	Basal Infolding
BL	Basal Lamina
CC	Cell Coat
CF	Collagen Fiber
CL	Capillary Lumen
CO	Cytoplasmic Organelle
CW	Cell Web
Cy	Cytoplasm
D	Space of Disse
EC	Endothelial Cell
EP	Endothelial Pore
eu	Euchromatin
EV	Endocytotic (Micropinocytotic) Vesicle
F	Filament
FP	Foot Process
G	Golgi Complex
GJ	Gap Junction (Nexus)
Gl	Glycogen
H	Hepatocyte (Liver Cell)
he	Heterochromatin
ICS	Intercellular Space
Ki	Kinocilium
LB	Multilamellar Body (Lung)
M	Mitochondrion
Mb	Microbody
Mf	Myofilament
MD	Mucous Droplet
Mt	Microtubule
Mv	Microvillus
MVB	Multivesicular Body
My	Myelin Sheath (Schwann Cell)
N	Nucleus
NP	Nuclear Pore
nu	Nucleolus
P	Endocytotic (Micropinocytotic) Pit
R	Ribosome
RBC	Red Blood Cell
RER	Rough Endoplasmic Reticulum
SC	Schwann Cell
SER	Smooth Endoplasmic Reticulum
SG	Secretory Granule
SM	Smooth Muscle Cell
TJ	Tight Junction
TL	Tubular Lumen (Kidney)
UM	Unit Membrane
US	Urinary Space (Renal Corpuscle)
V	Vacuole
ZG	Zymogen Granule

⊖ Direction of Platinum Evaporation (Shadowing)

Introduction

The principle and the technical feasibility of freeze-etching were described by R.L. STEERE in 1957. This ingenious technique remained, however, of little practical use until 1961, when H. MOOR and coll. brought decisive practical improvements to the original design and made it a commercially available device which is now common equipment of electron microscopy laboratories.

Briefly outlined, the freeze-etching technique allows a very thin platinum-carbon replica to be made from the surface of a frozen-fractured tissue. The replica follows with great precision, down to 20 Å, surface details of the frozen-fractured tissue and it is transparent to electrons. It can thus be observed with the usual transmission electron microscope.

There are five preparative steps involved in the preparation of a freeze-etch replica.

1. Freezing of the Specimen

Freezing ensures the preservation of tissue components and is carried out by dipping the specimen in an inert gas (Freon 22) cooled and liquefied with liquid nitrogen.

To prevent the formation of ice crystals during freezing of the extra and intracellular water present in the tissue, the latter is infiltrated with a solution of 20–30% glycerol in distilled water or any buffer solution (0.1 M). Glycerol acts as a cryoprotectant preventing the growth of destructive ice crystals within the tissue*.

* Before treatment with the cryoprotectant, the tissue can also be fixed with buffered glutaraldehyde. This step has proven to be an important one since it has been shown that cryoprotectant used alone can induce a clustering of the membrane-associated particles (see reference at the end of this section: MCINTYRE *et al.* 1974).

2. Fracturing of the Frozen Specimen

Once frozen, the piece of tissue is transferred to a high vacuum chamber housing a special microtome in which the specimen support, the arm and the blade are also cooled with liquid nitrogen to avoid thawing of the preparation. The chamber is evacuated down to a vacuum of about 10^{-6} Torr and will remain so for this and the two next steps. The fracturing step is of utmost importance since it is during this phase that membranes will be split and the tridimensional picture of the tissue be produced. Indeed, the frozen tissue is not actually cut with the microtome knife but split or broken away along certain planes of fracture. One of these planes is formed by the cellular membranes and gives the freeze-etching technique its main relevance to cell biology.

3. Etching of the Frozen-Fractured Specimen

This step is optional and allows ice to be sublimated away from the tissue. In a given tissue, the extracellular space, rich in water, as well as the ground matrix of the cell cytoplasm are the most affected by etching. Membranes are not etchable. By removing differentially ice from the tissue, etching can reveal structures which are not normally exposed by the fracturing process, for example the true surface of membranes (see below). The use of glycerol as cryoprotectant will reduce the amount of ice which can be removed by etching.

4. Replication of the Frozen-Fractured and Etched Specimen

This step produces a replica of the tissue which is to be examined in the electron microscope. A replica

is made by evaporating a thin layer of platinum on the fractured tissue under a certain angle. The angle (usually 45% above the plane of the tissue) gives a shadowing effect which enhances the relief differences and is important for the proper orientation of the final electron micrographs. The platinum replica is reinforced with a layer of carbon evaporated perpendicularly.

5. Removing and Cleaning of the Replica

After the platinum-carbon evaporation has been performed, air is introduced in the vacuum chamber, the frozen specimen underlying the replica is thawed and the replica floated on a corrosive solution (strong alkali or acid) which will dissolve the thawed tissue adhering to the replica. The platinum and the carbon layers are inert to the corrosive solution. The cleaned replica is then washed by several floatings on distilled water and finally recovered on a copper mesh screen identical to those used for picking up thin-sections. The replica is ready for observation in the electron microscope. In summary, the main differences existing between a freeze-etch replica and a thin-section are as follows:

a) the platinum replica does not contain any actual component of the tissue: it is only a casting of the tissue surface;

b) any piece of frozen tissue will yield only one single replica as compared with the many successive sections which can be cut from an embedded specimen;

c) it is not possible to predict nor to control exactly the path that the fracture plane will follow in the frozen specimen.

The two last points sometimes make the obtention of a valuable replica a matter of luck... All replicas presented in this book have been obtained according to a standard procedure involving the fixation of the tissue in phosphate-buffered glutaraldehyde and infiltration with a 30% glycerol solution in the same buffer as for fixation. Etching time was 2 min at $-100\,^{\circ}C$.

Interpretation of Freeze-Etch Replicas

As briefly outlined above, the freeze-etching technique not only allows the observation of biological specimens without dehydration or embedding, but also reveals their ultrastructural organization in a tridimensional fashion. The tridimensional image is given essentially by a succession of fracture planes occurring in any given direction and separated one from another by identifiable steps or ridges. In a compact tissue (see Plate 1), the fracture planes are of two kinds: some occur at random without following natural boundary lines and expose for example the cell cytoplasm, the nucleoplasm, the extracellular space, whereas others follow preexistent boundaries within the cells or the tissue. Such boundaries are the membranes of the nucleus, the cytoplasmic organelles or the cell itself. The first kind of fracture is of relatively limited interest since, in most cases, it shows a more or less coarse granular substructure representing the frozen cytoplasmic matrix or the extracellular fluid and, in this respect, does not add much information as compared to conventional thin-section electron microscopy. It is therefore the fracture occurring along membranes which represents the capital advantage of freeze-etching over thin-sectioning, since it allows the visualization of the membrane inner structure, described now in more detail.

Once it was recognized that freeze-fracturing was exposing large pieces of intra and extracellular membranes, the question then arose as to which part of the membranes were revealed – where did the fracture occur in frozen membranes? The first hypothesis was that it followed the natural boundary of the membrane, that is, in the case of a plasma membrane, the interface existing between the outer leaflet and the extracellular space or between the inner leaflet and the cytoplasmic matrix. Such a fracture would have thus exposed the true outer and inner surfaces of the membrane. Reevaluation of this hypothesis was carried out principally by BRANTON, who first offered experimental evidence that the fracture process involving membranes would not be at the membrane interfaces but within the membrane itself. This latter interpretation, referred to as the membrane splitting hypothesis, suggested therefore that the freeze-fracture process exposes the inside of the membranes, their true surfaces being revealed only upon deep etching of the extra or intracellular ice. Since its original statement, the membrane splitting hypothesis has received many experimental confirmations and is now widely accepted among researchers in the field of freeze-etching. In the interpretation of the replicas presented in this book, we will also assume a membrane splitting and there are simple rules to remember when looking at membrane faces produced by freeze-etching (see Plates 2 and 3):

a) upon splitting, any given membrane produces two complementary and distinctive fracture faces. One of these faces (corresponding to the inner leaflet) remains associated with the cytoplasmic matrix and it is called by convention the fracture face A, or A-face; the other (corresponding to the outer leaflet) remains associated with the extracellular space in the case of a plasma membrane or with an intracisternal space in the case of a cytoplasmic organelle bound by a single membrane, and it is called the fracture face B, or B-face;

b) all membrane faces so far examined share the common basic appearance of a smooth surface in which small particles, 60–180 Å in diameter, are present. These particles are currently thought to be proteins incorporated in the lipid bilayer.

c) the two complementary fracture faces produced by the splitting of the membrane have an unequal number of particles: fracture face A has usually more particles than fracture face B.

d) the total number of particles present in a given membrane face varies to a great extent from one membrane type to another.

Selected References

BRANTON, D.: Fracture faces of frozen membranes. Proc. nat. Acad. Sci. (Wash.) **55**, 1048–1056 (1966).

BRANTON, D.: Membrane structure. Ann. Rev. Plant Physiol. **20**, 209–238 (1969).

BRANTON, D.: Freeze-etching studies of membrane structure. Phil. Trans. Roy. Soc. Lond. B **261**, 133–138 (1971).

KOEHLER, J.G.: The technique and application of freeze-etching in ultrastructure research. Advanc. biol. med. Phys. **12**, 1–84 (1968).

MCINTYRE, J.A., GILULA, N.B., KARNOVSKY, M.J.: Cryoprotectant induced redistribution of intramembranous particles in mouse lymphocytes. J. Cell Biol. **60**, 192–203 (1974).

MOOR, H., MÜHLETHALER, K., WALDNER, H., FREY-WYSSLING, A.: A new freezing ultramicrotome. J. biophys. biochem. Cytol. **10**, 1–13 (1961).

MOOR, H.: Use of freeze-etching in the study of biological ultrastructure. Int. Rev. exp. Path. **5**, 179–216 (1966).

MOOR, H.: Freeze-etching. Int. Rev. Cytol. **25**, 391–412 (1969).

MÜHLETHALER, K.: Studies on freeze-etching of cell membranes. Int. Rev. Cytol. **31**, 1–19 (1971).

PINTO DA SILVA, P., BRANTON, D.: Membrane splitting in freeze-etching. J. Cell Biol. **45**, 598–605 (1970).

STEERE, R.L.: Electron microscopy of structural detail in frozen biological specimens. J. biophys. biochem. Cytol. **3**, 45–60 (1957).

TILLACK, T.W., MARCHESI, V.T.: Demonstration of the outer surface of freeze-etched red blood cell membranes. J. Cell Biol. **45**, 649–653 (1970).

WEHRLI, E., MÜHLETHALER, K., MOOR, H.: Membrane structure as seen with a double replica method for freeze-fracturing. Exp. Cell Res. **59**, 336–339 (1970).

Plate 1 Neurosecretory Cell from the Posterior Pituitary of the Spiny Mouse

This picture illustrates the main features of a freeze-etch replica. In this cell, the fracture plane has exposed both the cytoplasm and the plasma membrane. In the cytoplasm, visible in the upper part of the figure, the fracture shows a coarse background representing the frozen cytoplasmic matrix. In the matrix, several smooth and rounded profiles can be seen. These are cytoplasmic organelles (CO)* whose limiting membrane is preferentially exposed by the freeze-etching. Depending upon which leaflet of the membrane has been taken away by the fracturing process, a rounded organelle will thus appear either as a convex profile or as a concave one. Below the cytoplasmic fracture a large area of the plasma membrane (Ā) has been exposed. It appears as a smooth surface on which many globular particles are standing. These are the membrane-associated particles; they project tiny shadows (white) which are most useful for the proper orientation of the picture since they indicate the direction of the platinum evaporation. Usually, the picture is oriented with the source of platinum evaporation at the bottom as indicated by the encircled arrow. In the lower right-hand corner of the picture, part of the cytoplasm of another neurosecretory cell can be seen. It is separated from the large cell profile by a coarse fracture face representing the frozen ice of the intercellular space (ICS).

Magnification × 113,000

* In this case, neurosecretory granules.

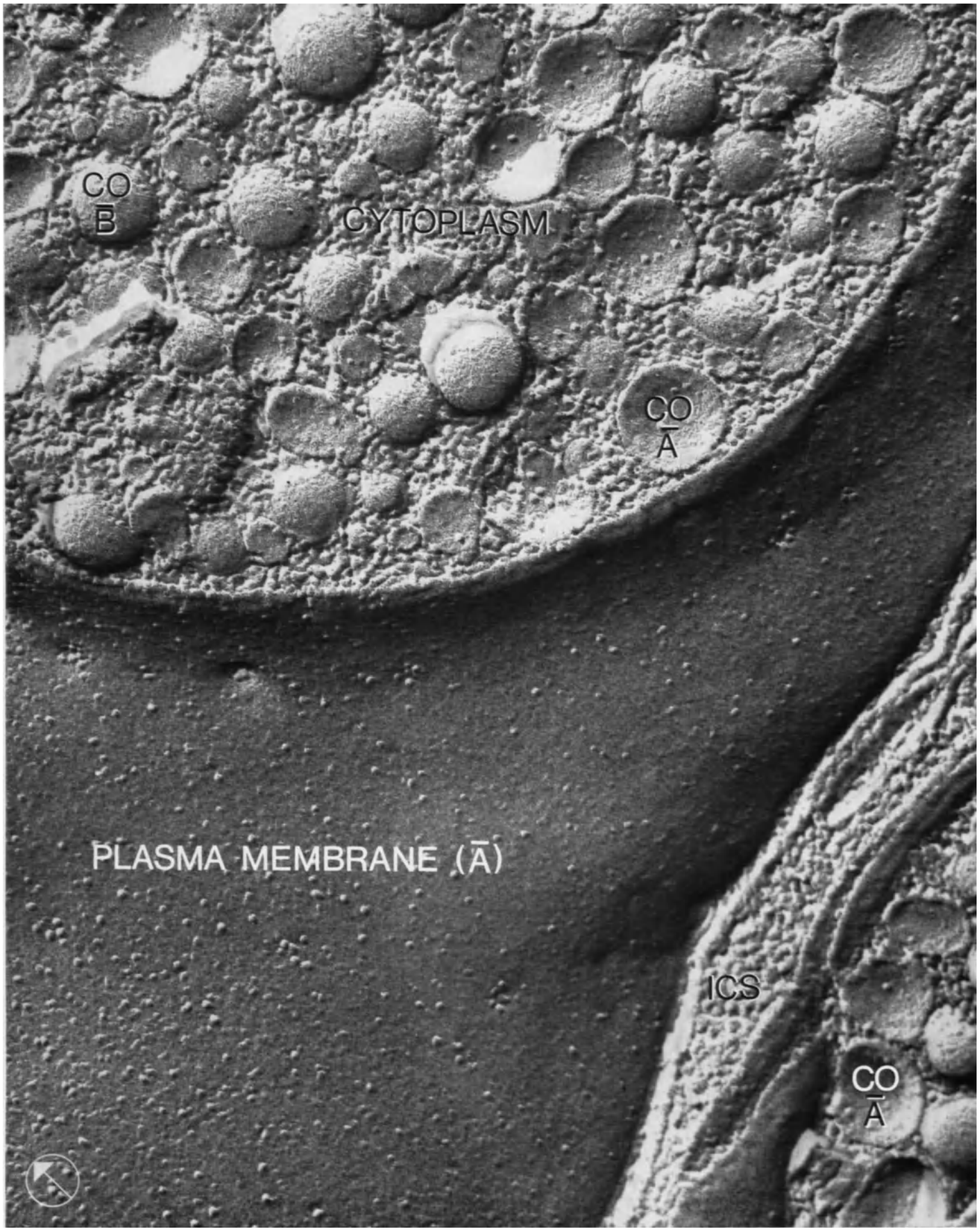
CO
B
CYTOPLASM
CO
A
PLASMA MEMBRANE (Ā)
ICS
CO
A

Plate 2 Endocrine Cells from the Rat Pancreas (Isolated Islet of Langerhans)

As pointed out in the Introduction, freeze-fracturing, splits membranes along their hydrophobic interior and this picture illustrates the two faces of the membrane thus produced. On the left-hand side of the picture, the fracture face is smooth and shows a few particles whereas on the right-hand side it is similarly smooth but contains numerous particles. It has been demonstrated that in the case of a plasma membrane the face having less particles corresponds to the outer leaflet of the membrane. It becomes visible when the cytoplasm and the membrane's inner leaflet have been removed upon fracturing, that is, when the observer is situated inside the cell. This face is the B-face ($\bar{B}$). Similarly the face having more particles has been shown to correspond to the inner leaflet of the membrane; it becomes visible when the outer leaflet and the associated intercellular matrix have been taken away, that is, when the observer is situated outside the cell. The more richly particulated face is the A-face ($\bar{A}$). From these considerations, it becomes thus apparent that for having one A- and one B-face side by side as seen in this picture, one must look at two neighboring cells*, one having its cytoplasm and membrane's inner leaflet removed, the other, its outer leaflet and the associated intercellular space. Accordingly, B-faces are always separated from adjacent A-faces by a step ($\rightarrow$) as evidenced here and representing the thickness of the fractured intercellular space.

Magnification $\times$ 163,000

* or only one if its cytoplasm is very thin as in endothelial cells. In this case (see Plate 7), the step represents the thickness of the cytoplasm.

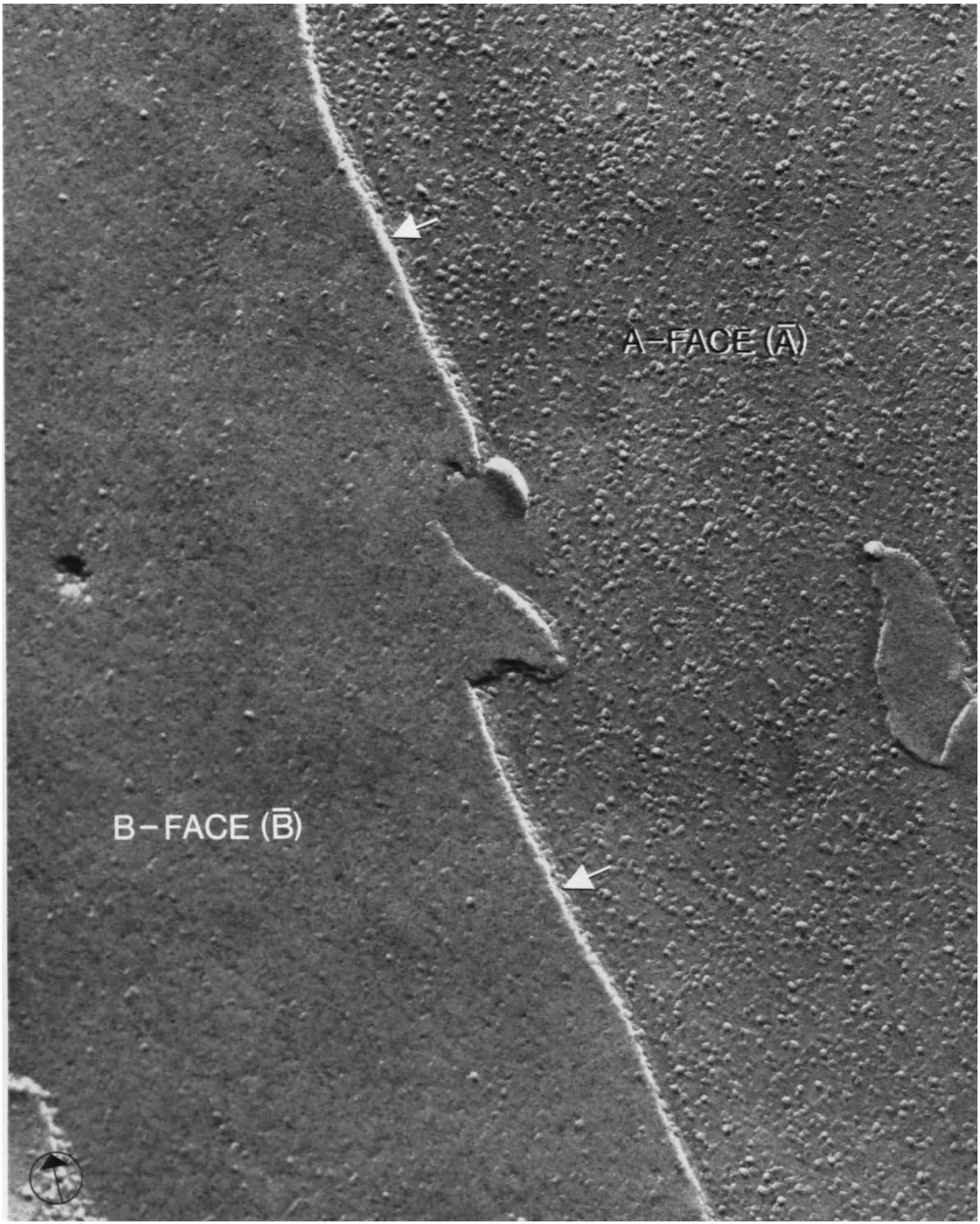

Plate 2

Plate 3 Myelin Sheath from the Mouse Sciatic Nerve

The appearance of membranes in freeze-etching varies greatly as far as the number of membrane-associated particles is concerned. Indeed, it has been shown that this number varies from several thousand per square micrometer to a few hundred, and that there is a definite relationship between the metabolic activity (that is, the protein content) of a given membrane and the number of its membrane-associated particles. Here we present a membrane which is rather inert metabolically, has a low protein content (20%) and accordingly a very small number of membrane-associated particles. It is the Schwann cell membrane wrapped around the axon in the form of a myelin sheath. (For picture of the myelin sheath in conventional thin section, see Plate 77). This picture shows a succession of fracture faces occurring across (darker zones of the picture), or in the plane of the layered membranes. Fracture faces in the plane of the membrane have an extremely smooth appearance and one can distinguish A- and B-faces separated by steps determined by the cross fracture of several membrane layers.

Magnification $\times 45{,}000$

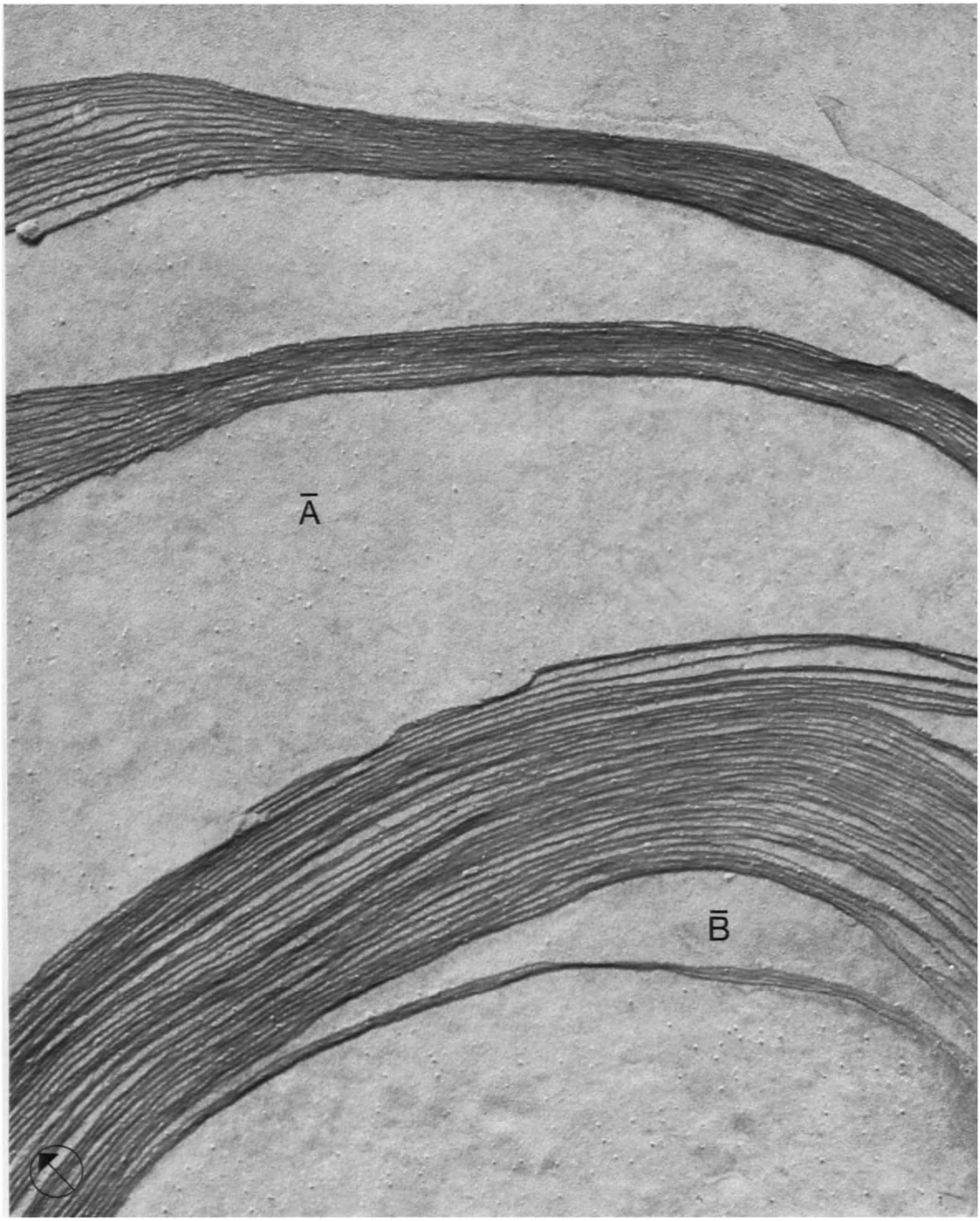
$\bar{A}$
$\bar{B}$

Plate 4 Capillary Endothelium from the Rat Pancreas

The freeze-fracture has exposed a large segment of the capillary wall which is formed in this region by parts of three endothelial cells (EC). On the cell membrane, there are numerous small rimmed circles, some of them raised above the fracture face. These circles represent endothelial pores or fenestrae and their fine structure is shown in Plates 5 to 7. In the upper left-hand corner of the picture, one sees a large circular profile representing another capillary (CL) in cross-fracture. This orientation of the capillary with respect to the fracture plane is of less informative value since it does not reveal surface features of the endothelial cells.

Magnification $\times 20{,}000$

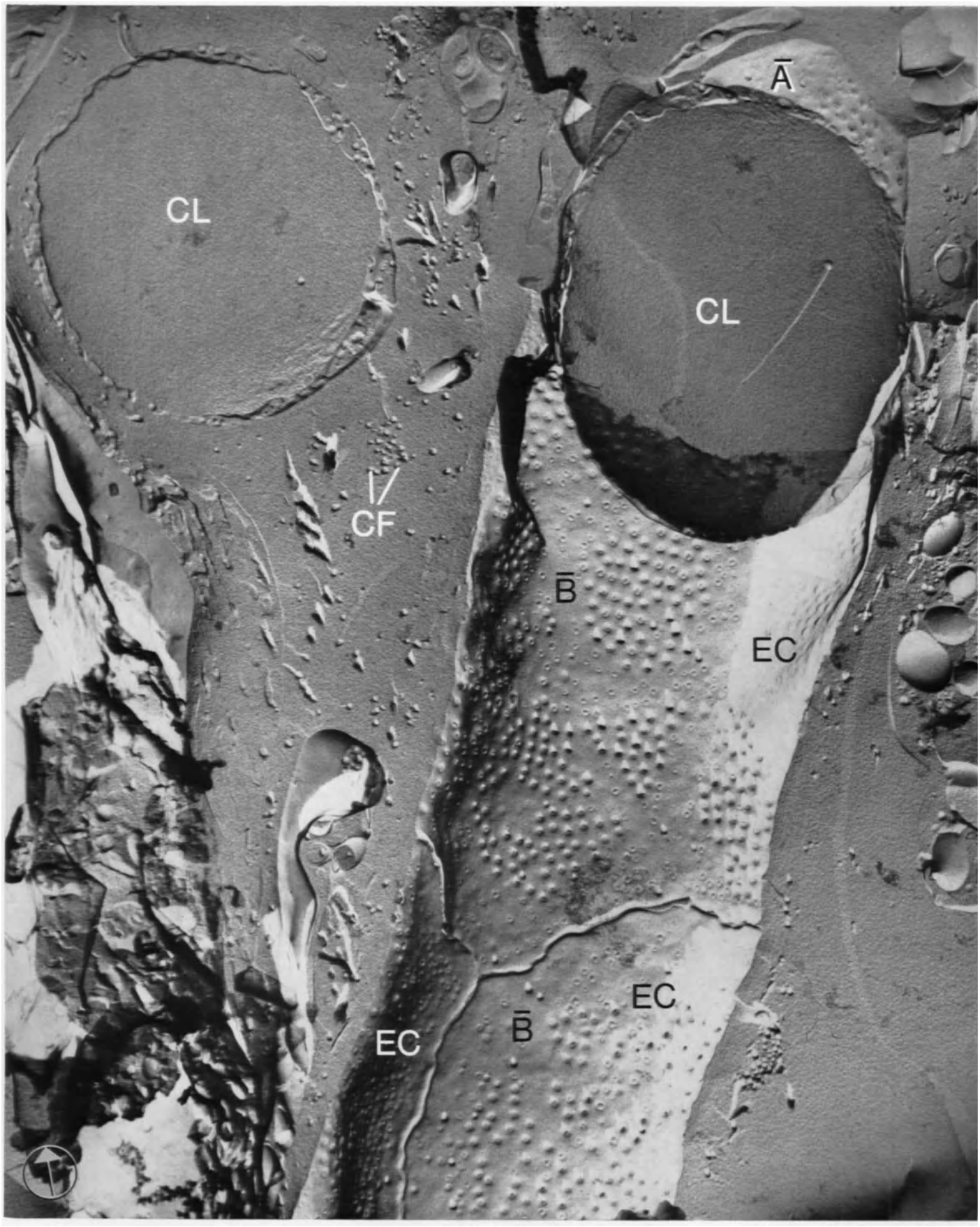
CL
CL
Ā
CF
B̄
EC
EC
B̄
EC

Plate 5 Capillary Endothelium from the Spiny Mouse Kidney

This picture illustrates parts of the membrane of two endothelial cells which present numerous differentiations characteristic of endothelial pores or fenestrae (EP). Pores have all a fairly regular appearance and when exposed on the membrane A-face, as it is the case here, they appear as depressions. Depressions do not project shadows on the fracture face but instead accumulate platinum (black) in the recesses facing the evaporating source. The floor of each depression has an uneven, slightly granular background. It might be noticed that the pores are absent from a region extending for several nanometers on each side of the intercellular line (→) between the two endothelial cells.

Magnification × 38,000

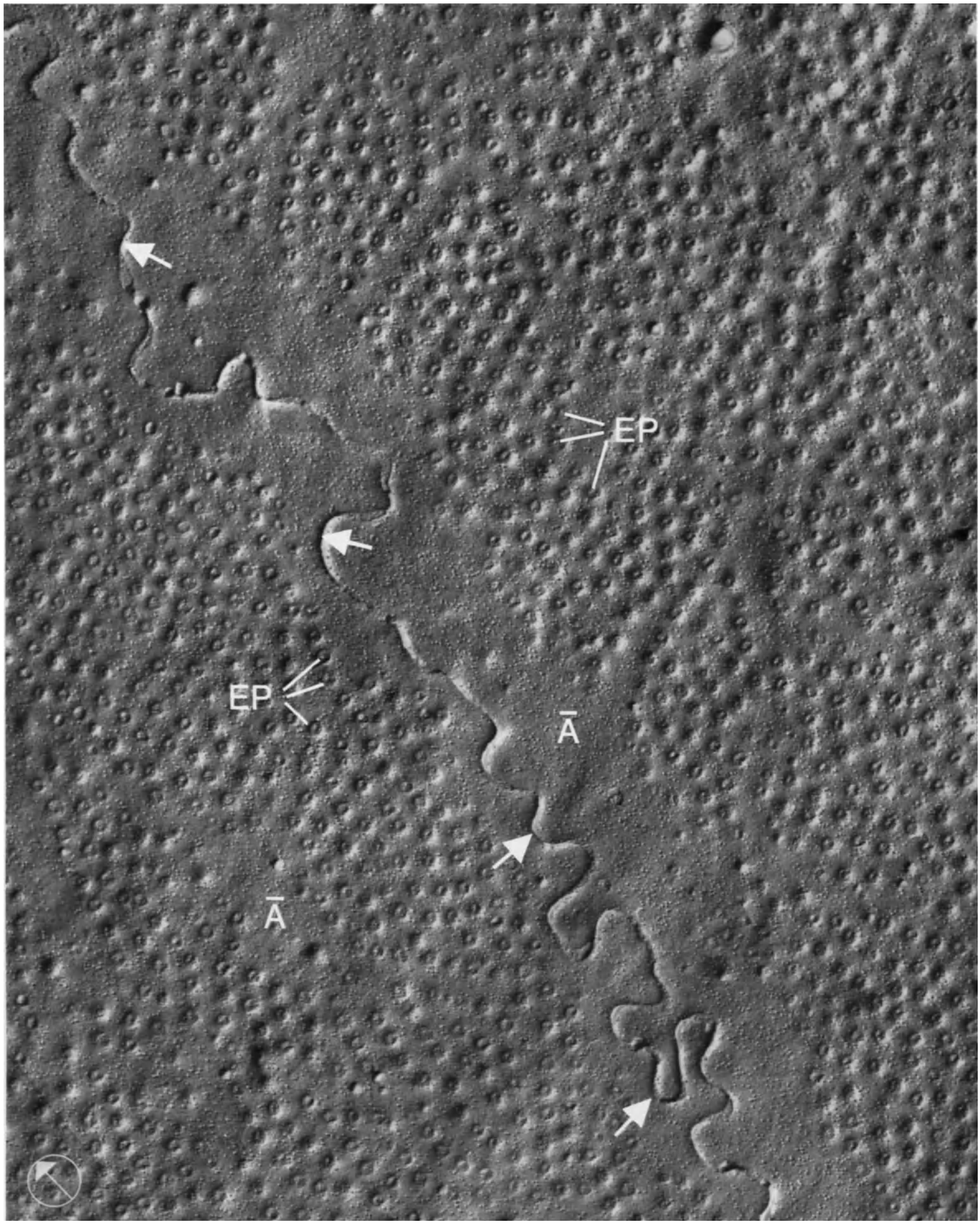
EP
EP
Ā
Ā

Plate 6 Capillary Endothelium from the Spiny Mouse Kidney

A large part of an endothelial cell membrane has been exposed showing numerous shallow depressions characteristic of the endothelial pores (EP) on A-faces. This picture is useful to distinguish between the freeze-etch appearance of endothelial pores and that of endocytotic figures. These latter differ from the pores by the fact that they appear as simple hemispherical pits (P) which represent the openings of endocytotic vesicles in the membrane face. They do not have the flat floor characterizing the pore depression. A higher magnification of the endocytotic pits is presented in Plate 10.

Magnification $\times 39{,}000$

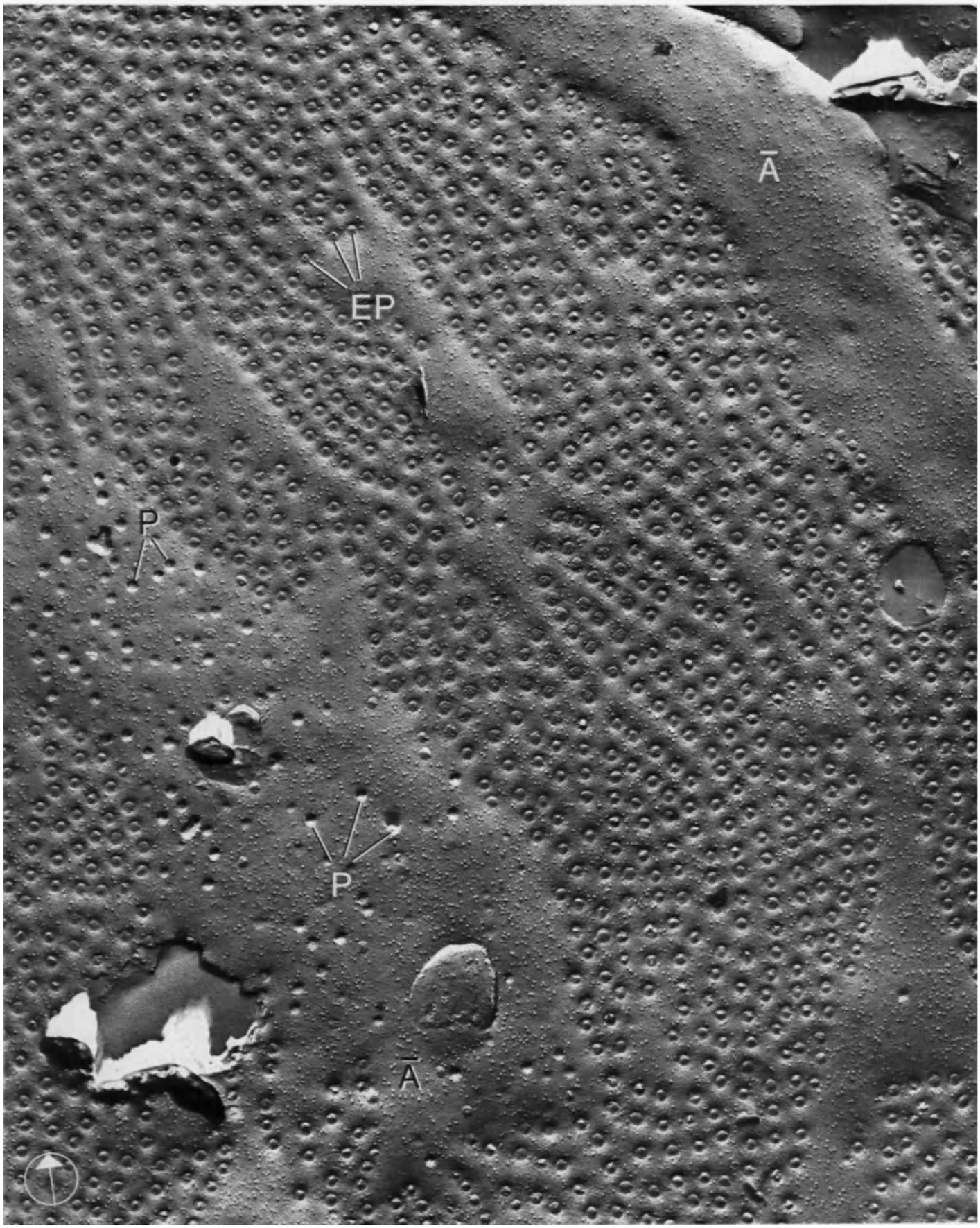

Plate 6

Plate 7 Capillary Endothelium from the Rat Kidney

This replica offers the possibility to examine pores on both A- and B-faces of the same cell. In the upper left-hand corner of the figure, one recognizes the familiar appearance of pores (EP) as seen in the A-face, that is circular depressions with a flat, shallow floor (see Plates 5 and 6). By contrast, pores appear entirely different in the membrane face exposed in the remainder of the picture. In this face, a B-face according to the low number of membrane-associated particles present on it, each pore appears as a circular rim slightly raised above the fracture face of the membrane. That rims are raised on the fracture face is indicated by the fact that they project faint shadows oriented in the same direction as those of membrane-associated particles. The floor in the rims is again shallow and flat. The low ridge (→) separating the A-face from the B-face represents the fracture across the cytoplasm of the endothelial cell which is extremely attenuated in the region pierced by pores. In the area of the ridge, one can see the entire extension of the pore structure bridging the two faces of the endothelial cell membrane.

Magnification × 115,000

Selected References

FRIEDERICI, H.H.R.: The tridimensional ultrastructure of fenestrated capillaries. J. Ultrastruct. Res. **23**, 444–456 (1968).

FRIEDERICI, H.H.R.: On the diaphragm across fenestrae of capillary endothelium. J. Ultrastruct. Res. **27**, 373–375 (1969).

SIMIONESCU, M., SIMIONESCU, N., PALADE, G.E.: Morphometric data on blood capillaries. J. Cell Biol. **60**, 128–152 (1974).

SMITH, U., RYAN, J.W., SMITH, D.S.: Freeze-etch studies of the plasma membrane of pulmonary endothelial cells. J. Cell Biol. **56**, 492–499 (1973).

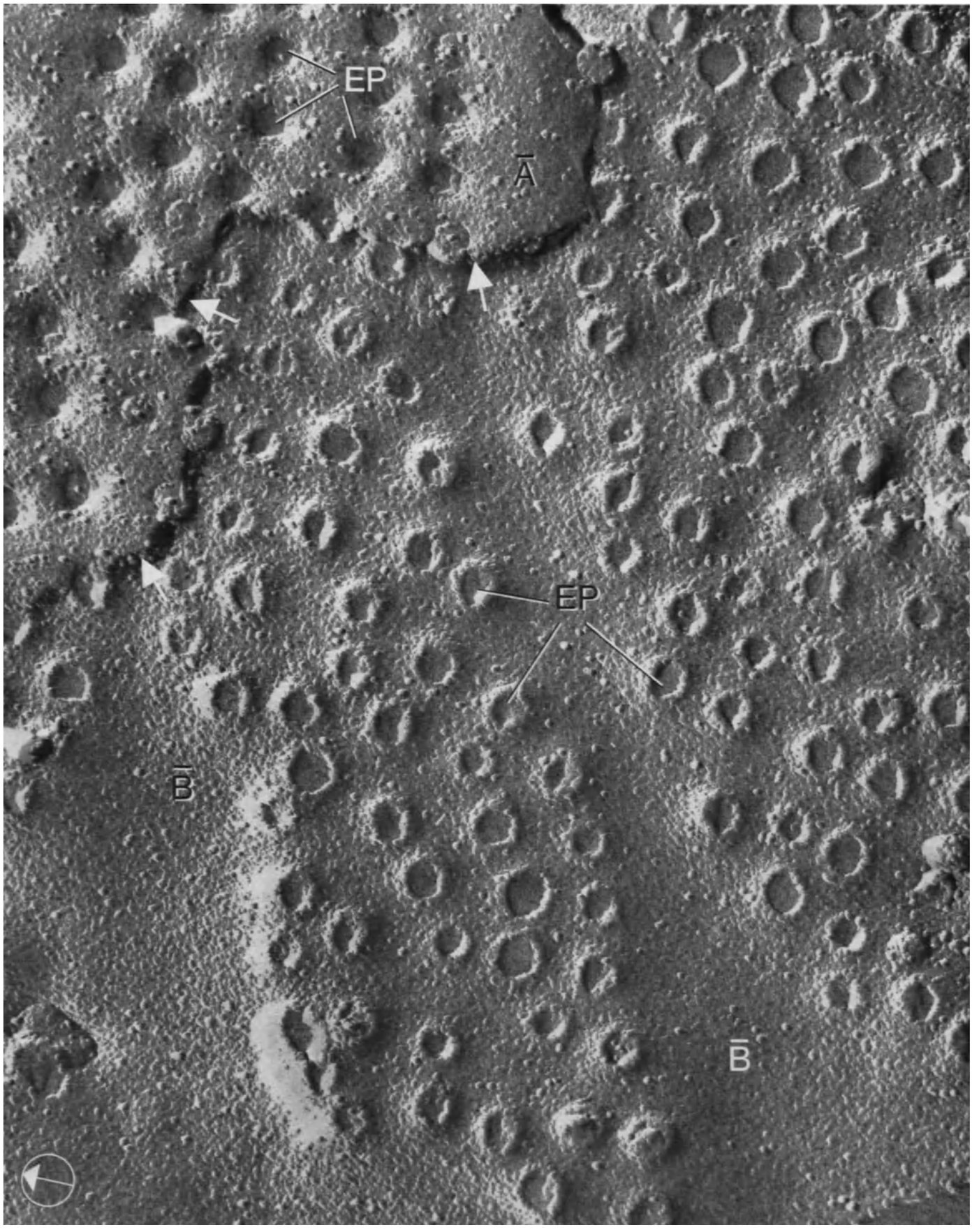
EP
Ā
EP
B̄
B̄

Plate 8 Capillary Endothelium from the Rat Kidney (Renal Corpuscle)

The diameter of endothelial pores can vary to a fairly large extent. Here are shown the large pores of the endothelium of the renal corpuscle. The pores (EP) have a rim structure, thus indicating that they are exposed on the B-face of the endothelial membrane. Only in the bottom of the picture, the endothelium A-face can be seen. In this face, accordingly, the pores appear as circular or ovoid depressions. Moreover, some of them are situated at the level of the ridge (→) separating the A- from the B-face and thus present the two characteristic morphological appearances described in Plate 7. Two endocytotic pits (P) can be seen in the endothelium A-face. See Plates 53 to 56 for further details on the renal corpuscle.

Magnification × 94,000

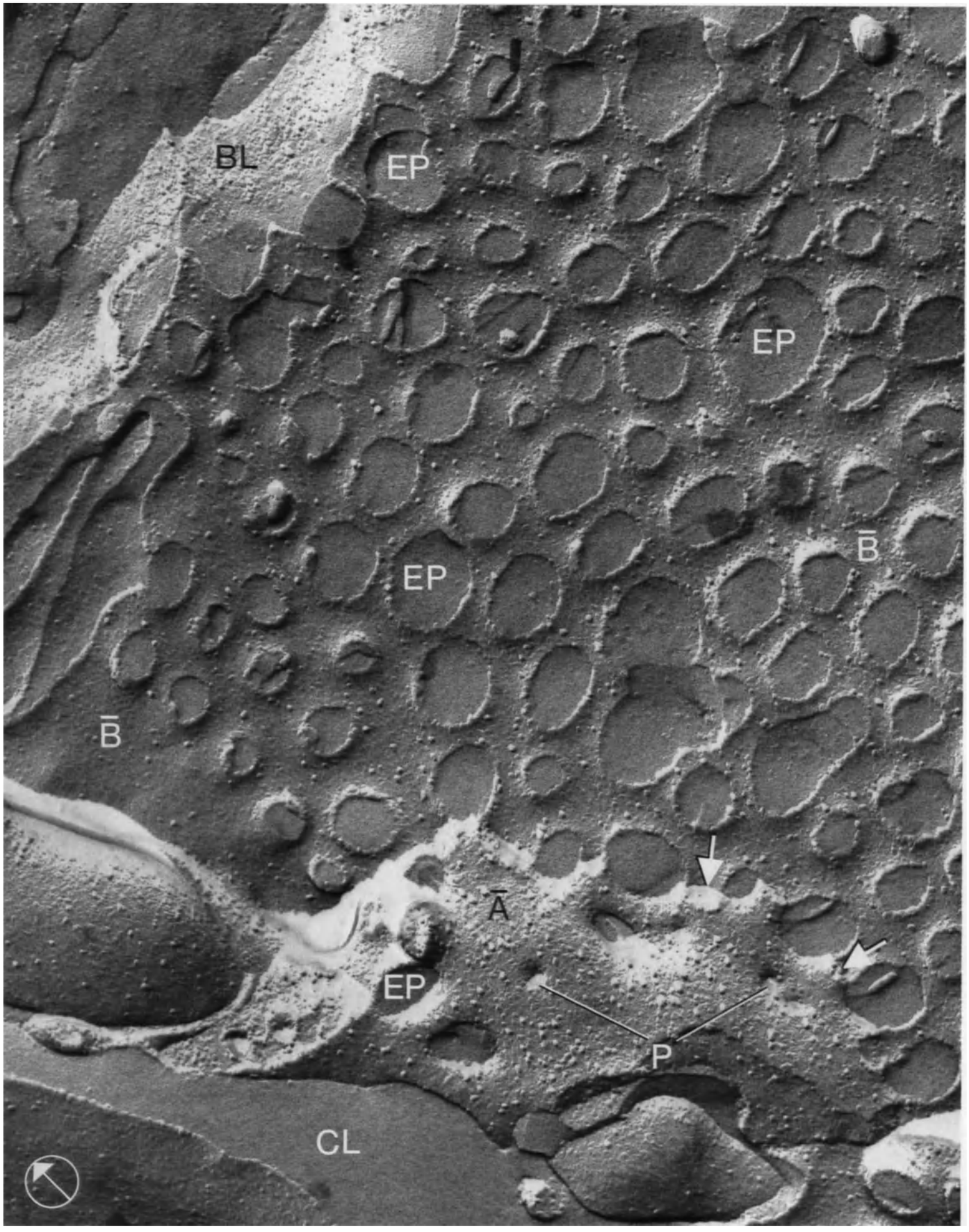
BL
EP
EP
EP
B̄
B̄
Ā
EP
P
CL

Plate 9 Endothelial Cell from the Sinusoids of the Mouse Liver

A last example of pores is shown in endothelial cells of the liver sinusoids. In these cells, the pores (EP) are of variable shape and size; they are also irregularly clustered on the cell surface. Pores appear here in the A-face of the endothelial cell membrane and the circular areas (→) deprived of particles might represent specific zones in which new pores are to be formed. In the lower right-hand corner of the picture, parts of the vascular pole of an hepatocyte (H) can be seen separated from the endothelial cell by the space of Disse (D).

Magnification × 89,000

Selected References

ORCI, L., MATTER, A., ROUILLER, CH.: A comparative study of freeze-etch replicas and thin-sections of rat liver. J. Ultrastruct. Res. **35**, 1–19 (1971).

WISSE, E.: An electron microscopic study of the fenestrated endothelial lining of rat liver sinusoids. J. Ultrastruct. Res. **31**, 125–150 (1970).

WISSE, E.: An ultrastructural characterization of the endothelial cell in the rat liver sinusoid under normal and various experimental conditions, as a contribution to the distinction between endothelial and Kupffer cells. J. Ultrastruct. Res. **38**, 528–562 (1972).


Ā
EP
EP
EP
D
H

Plate 10 Endothelial Cell from the Mouse Liver

As already pointed out in Plate 6, endocytosis is readily differentiated from the endothelial pores. Essentially, endocytosis is indicated on membrane A-faces by the openings of the microvesicles which appear as small hemispherical pits (P). The bottom of the pits, in contradistinction to that of pores, is never flat. As well as showing the openings of the endocytotic vesicles in the A-face of the membrane, this figure reveals also several endocytotic vesicles (EV) within the cell cytoplasm (Cy). Most of them are still abutting to the membrane and clearly demonstrate the relationship between the pits and the vesicles.

Magnification $\times 82{,}000$

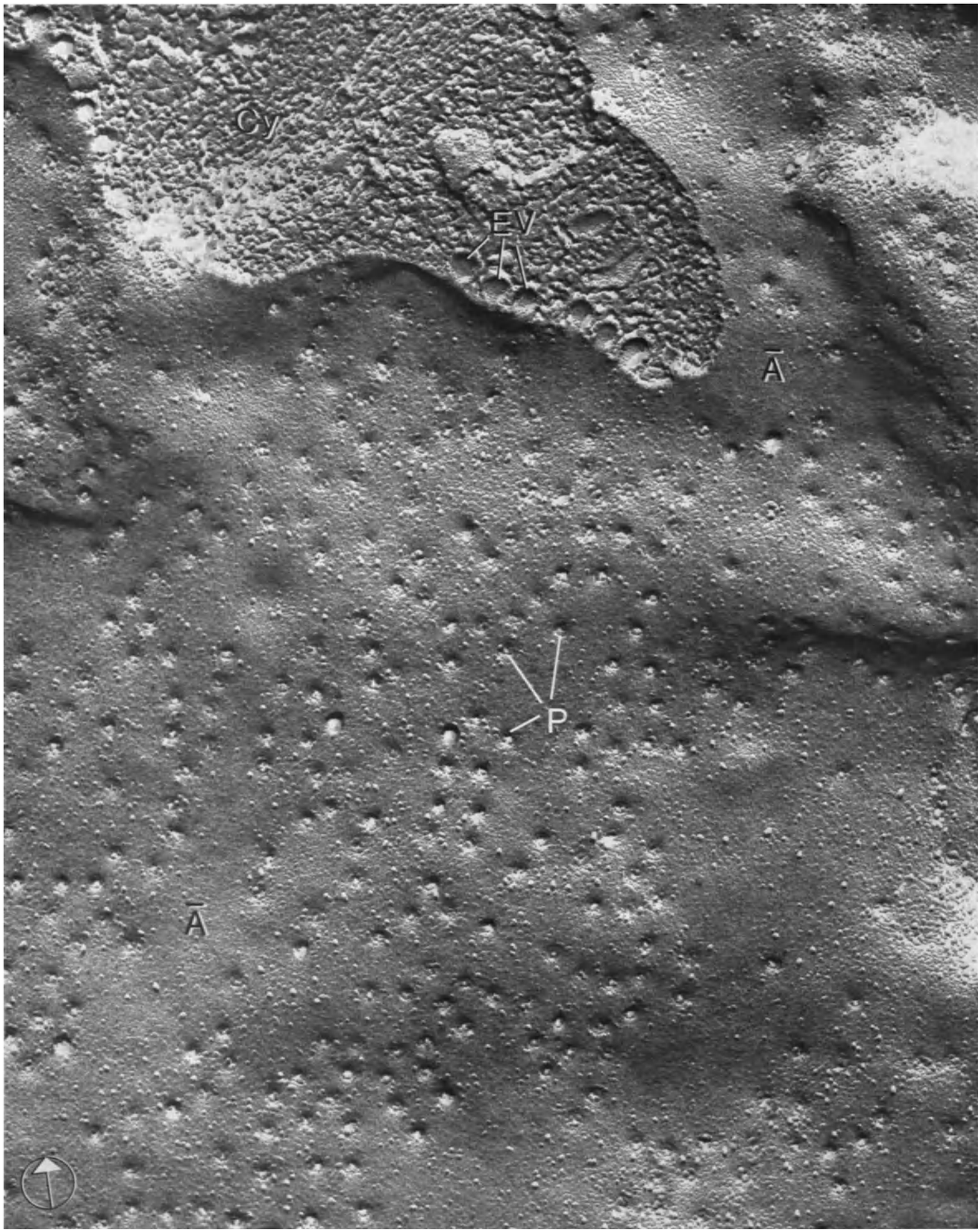
Cy
EV
Ā
P
Ā

Plate 11 Capillary Endothelium from the Chinese Hamster Kidney

In membrane B-faces, endocytosis takes also a characteristic appearance. Since in this case the observer is situated inside the cell looking at the outer leaflet of the plasma membrane, most endocytotic vesicles will be seen as small hemispheres (EV) bulging from the membrane face. In other instances, the fracture process has taken away the entire vesicle, leaving only the trace of its neck (or opening) in the membrane which appears as a circular rim (→).

Magnification × 74,000

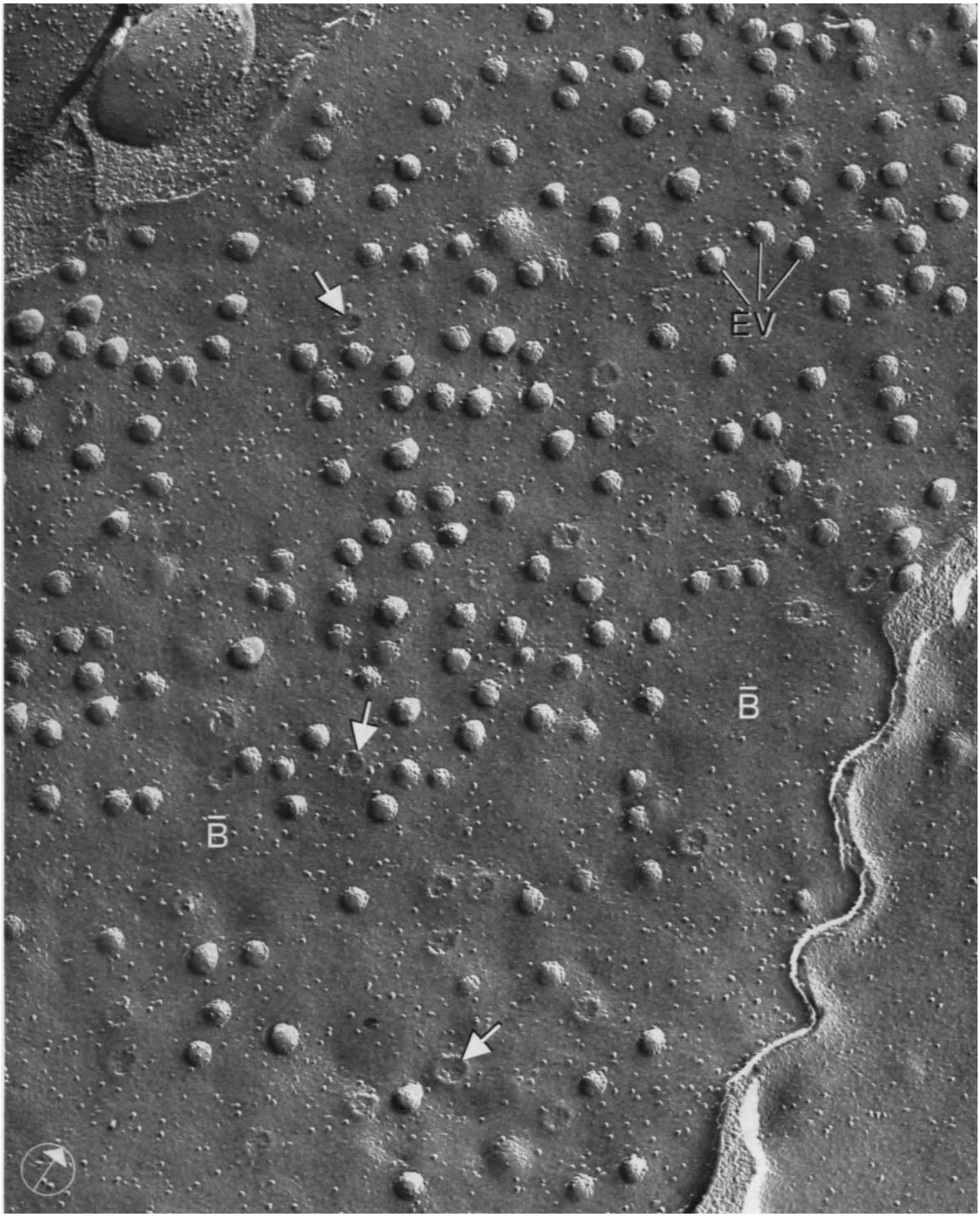
EV
B
B

Plate 12 Endocrine Cell from the Rat Pancreas (Isolated Islet of Langerhans)

Still differing in appearance from the pores and the endocytosis is the process of exocytosis (or emiocytosis). This process, detectable in secretory cells, is the mechanism by which the content of a secretory granule is liberated in the extracellular space. This occurs when the membrane of the secretory granule fuses with the cell membrane, the coalescence of these two membranes creating an opening through which the granule's content – or granule-core – is released. As a surface phenomenon, such a process is accordingly clearly revealed in freeze-etch replicas. As seen in this image, the typical appearance of an exocytotic event is that of a discontinuity (→) in the membrane fracture face in which a rounded mass – presumably the granule-core – protrudes. Since the granule's membrane has usually fewer membrane-associated particles (about $200/\mu^2$ in the A-face) than the cell membrane (about $2000/\mu^2$ in the A-face), one is tempted to interpret the two smooth areas indicated by stars on the membrane face as late events in the exocytosis. At this stage, the granule's membrane would have been completely incorporated into the plasma membrane creating the areas with few particles*. Such altered areas are transient and will disappear owing to redistribution of the particles in the plane of the membrane (see reference in Plate 23: SINGER and NICOLSON, 1972).

Magnification × 78,000. From L. ORCI, Diabetologia **10**, 1–25 (1974).

Selected References

ORCI, L., AMHERDT, M., MALAISSE-LAGAE, F., ROUILLER, CH., RENOLD, A.E.: Insulin release by emiocytosis: demonstration with freeze-etching technique. Science **179**, 82–84 (1973).

SMITH, U., SMITH, D.S., WINKLER, H., RYAN, J.W.: Exocytosis in adrenal medulla demonstrated by freeze-etching. Science **179**, 79–82 (1973).

* However, it is not possible to exclude that the disappearance of particles is an event preceding or accompanying the fusion of the granule's membrane with the plasma membrane.

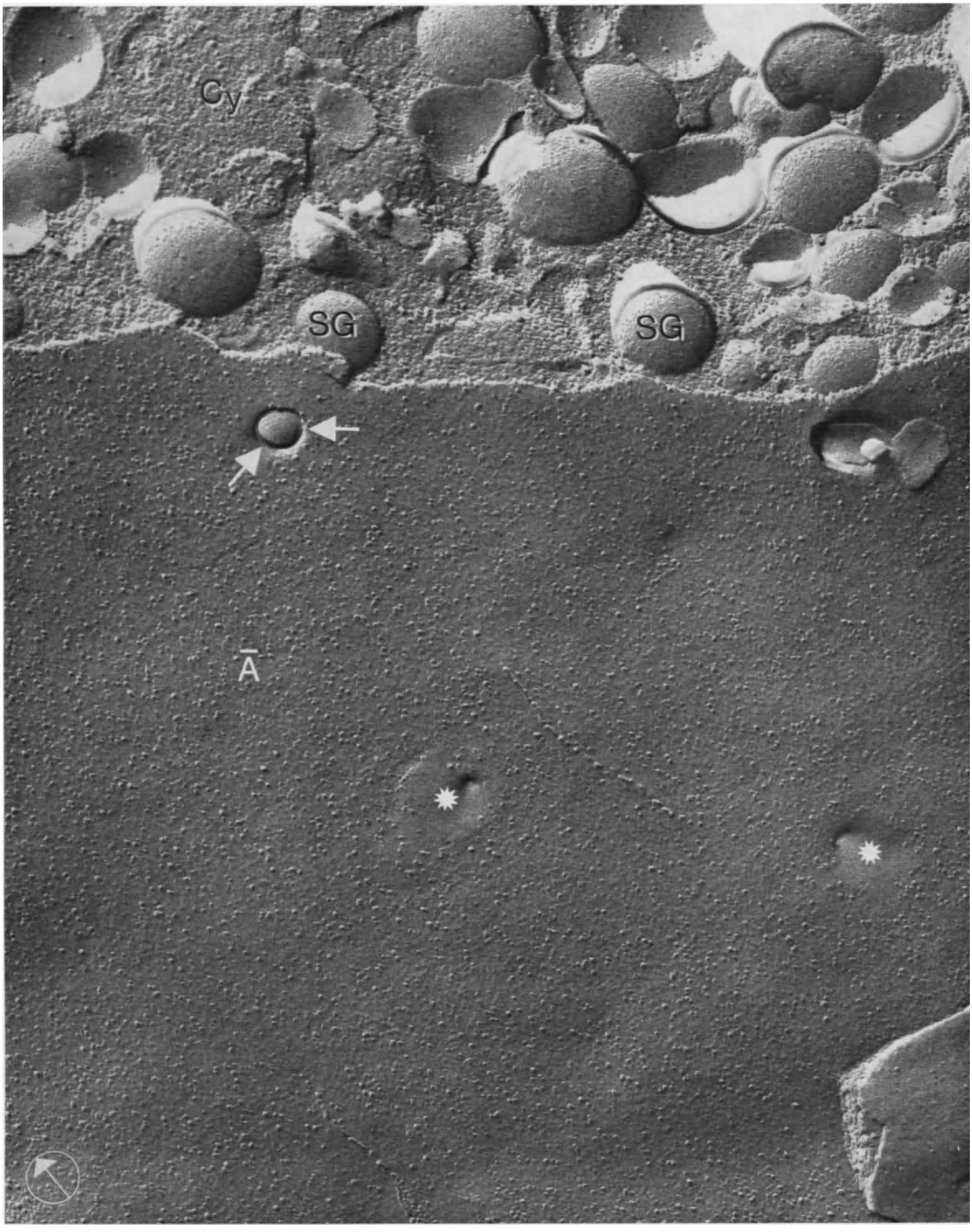
Cy
SG
SG
Ā

Plate 13 Epithelial Cells from the Distal Tubule of the Rat Kidney

Differentiations of the basal pole of the cell are represented mainly by invaginations or infoldings of the plasma membrane which are found in cells ensuring important movements of ions and water. The infoldings extend for variable length into the basal cytoplasm where they delimit narrow compartments containing mitochondria (M) (see also Plate 14). In suitable areas of this replica, one can see the invaginations of the membrane at the base of the cell, either in face-view (A-face) or in cross fracture (→). In addition, a part of the fenestrated peritubular capillary (EC) has been exposed. The tubular and the endothelial cells are both underlined by a band of tiny dots protruding above the fracture face and corresponding to the basal lamina (BL). In between the two basal laminae, notice the larger profiles of fractured collagen fibers (CF) which also protrude above the fracture face.

Magnification × 48,000

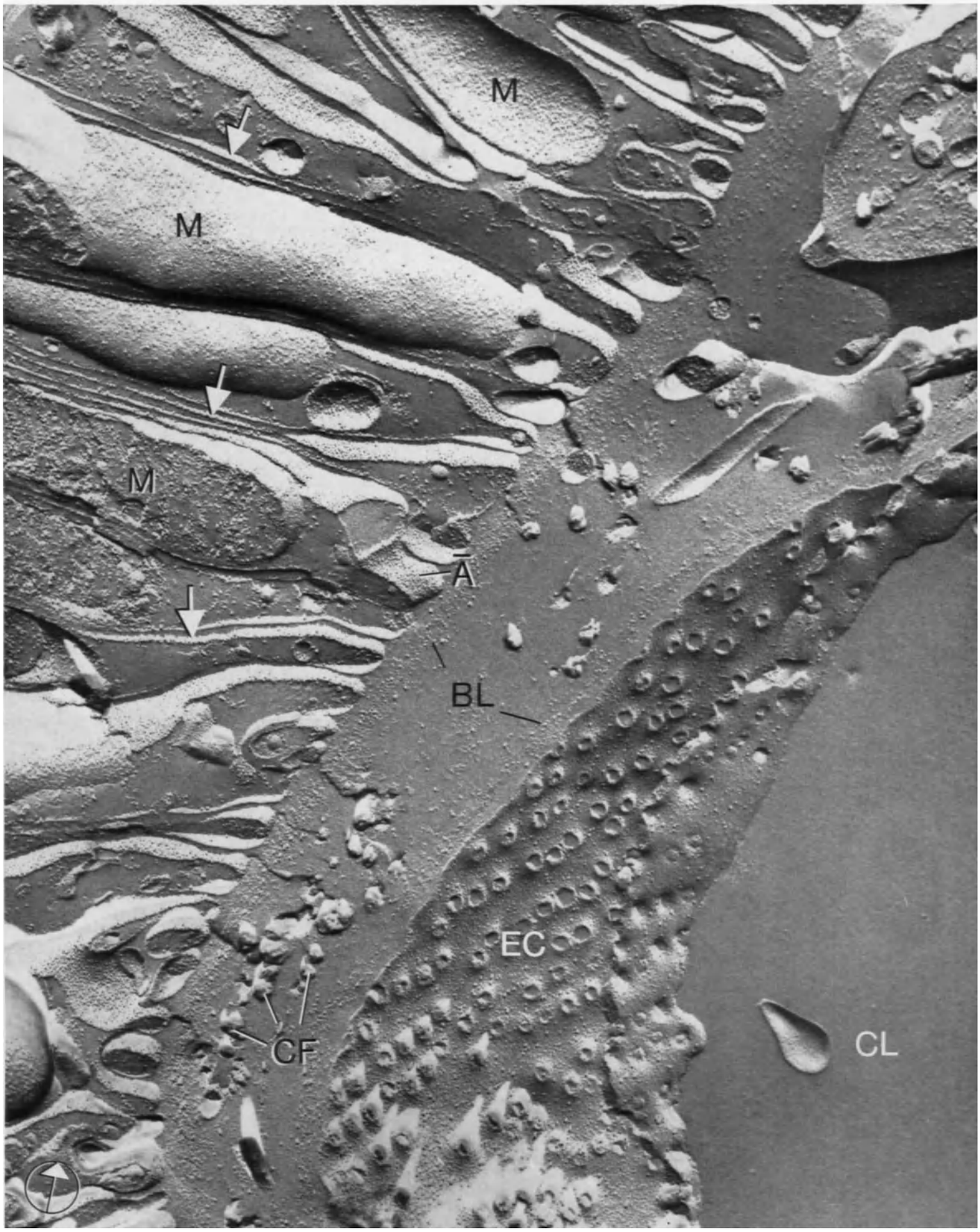
M
M
M
A
BL
EC
CF
CL

Plate 14 Distal Tubule from the Rat Kidney

The fracture of distal tubular cells allows one to study the freeze-etch appearance of mitochondria which are numerous in the cytoplasmic compartments delimited by the basal infoldings (BI). Mitochondria (M) have been exposed in various orientations, and fracture faces belonging to the outer and inner membranes can be recognized. The richly particulated bands visible in the mitochondrial matrix (→) represent transverse fractures of the cristae.

Magnification × 54,000

Selected References

MALHOTRA, S.K.: On the structure of membranes of mitochondria. Sub-Cell. Biochem. **1**, 171–177 (1972).

PACKER, L.: Functional organization of intramembrane particles of mitochondrial inner membranes. J. Bioenerg. **3**, 115–127 (1972).

Plate 14

Plate 15 Proximal Tubule of the Rat Kidney

Among the many differentiations of the cell surface, the microvilli are particularly conspicuous. When numerous, microvilli bring a sizable increase of the cellular surface and are thus found in absorptive epithelia, such as those of the small intestine and kidney proximal tubule. In this picture, practically the whole field is occupied by elongated cylindrical profiles. On each profile, two areas can be distinguished. One of these is convex and studded with membrane-associated particles, the other is concave and has only few particles. These two areas represent respectively the A- and the B-face of a single microvillus (Mv) and the white disc (→) interposed between these faces is the microvillar core which has received virtually no platinum. The fact that the plasma membrane limiting each microvillus is extremely rich in particles (about $3500/\mu^2$ in the A-face) indicates a high level of functional complexity. By comparison, Plate 16 will show microvilli from another tissue with very few particles. In the lower right-hand corner of the picture, a part of the tubular cell cytoplasm (Cy) with many organelles can be seen.

Magnification × 57,000

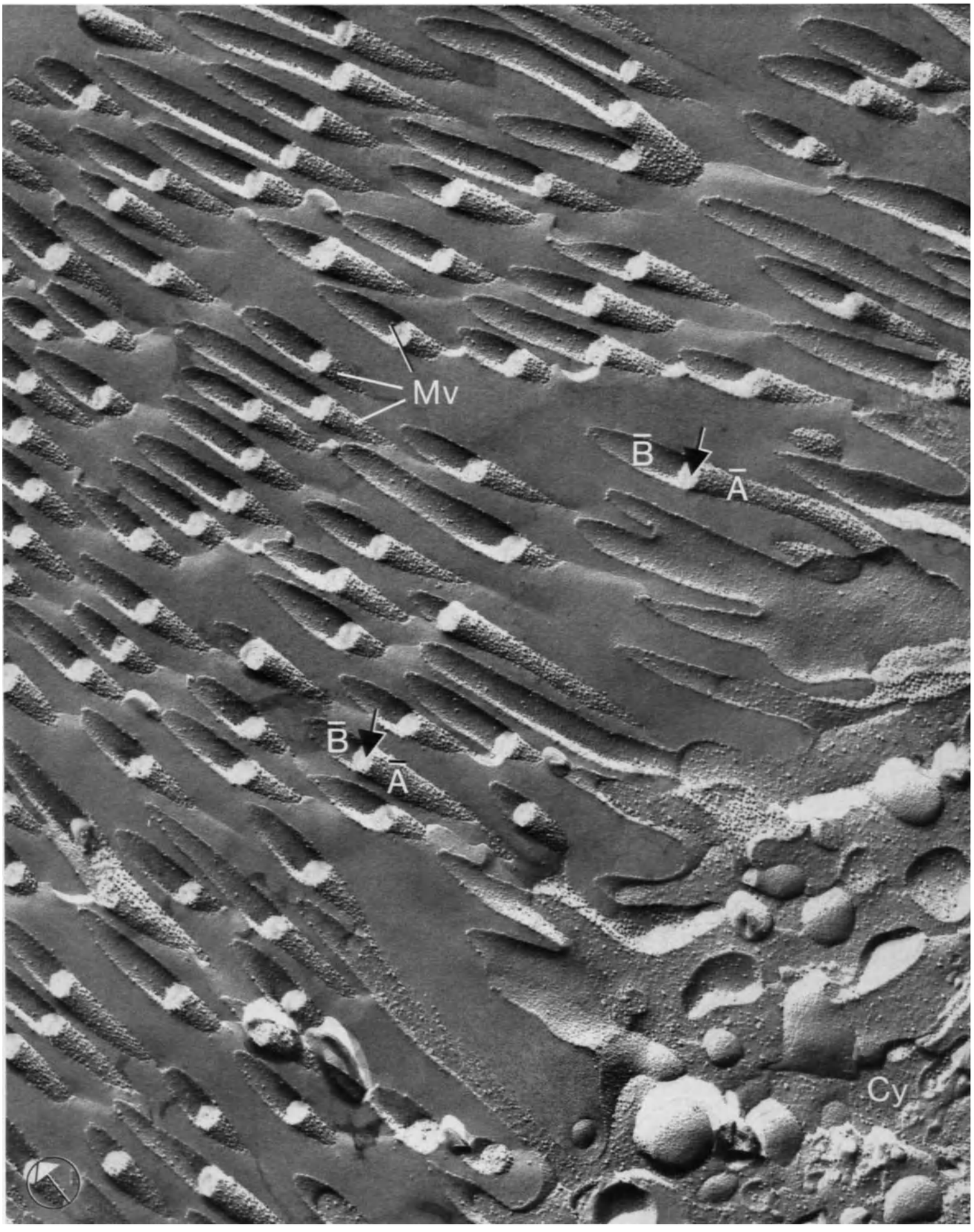
Mv
B̄
Ā
B̄
Ā
Cy

Plate 16 Follicular Cell from the Thyroid Gland of the Rat

In this epithelium, microvilli are rather short and plump. They are also not as numerous as in the brush border of the kidney proximal tubule or of the small intestine. The fracture has exposed a large area of the B-face of the follicular cell lateral plasma membrane, a part of the cell cytoplasm (Cy) as well as several microvilli (Mv) extending into the follicular lumen (*). The convex profiles represent the A-face, whereas the concave ones represent the B-face of the microvillar membrane. Notice that the A-face contains relatively few particles. Below the level of the microvilli, one recognizes a honeycomb pattern of ridges and grooves. These strands correspond to the tight junction (TJ) present at the juxtaluminal edge of the follicular cells (see also Plates 18–20).

Magnification $\times 99{,}000$

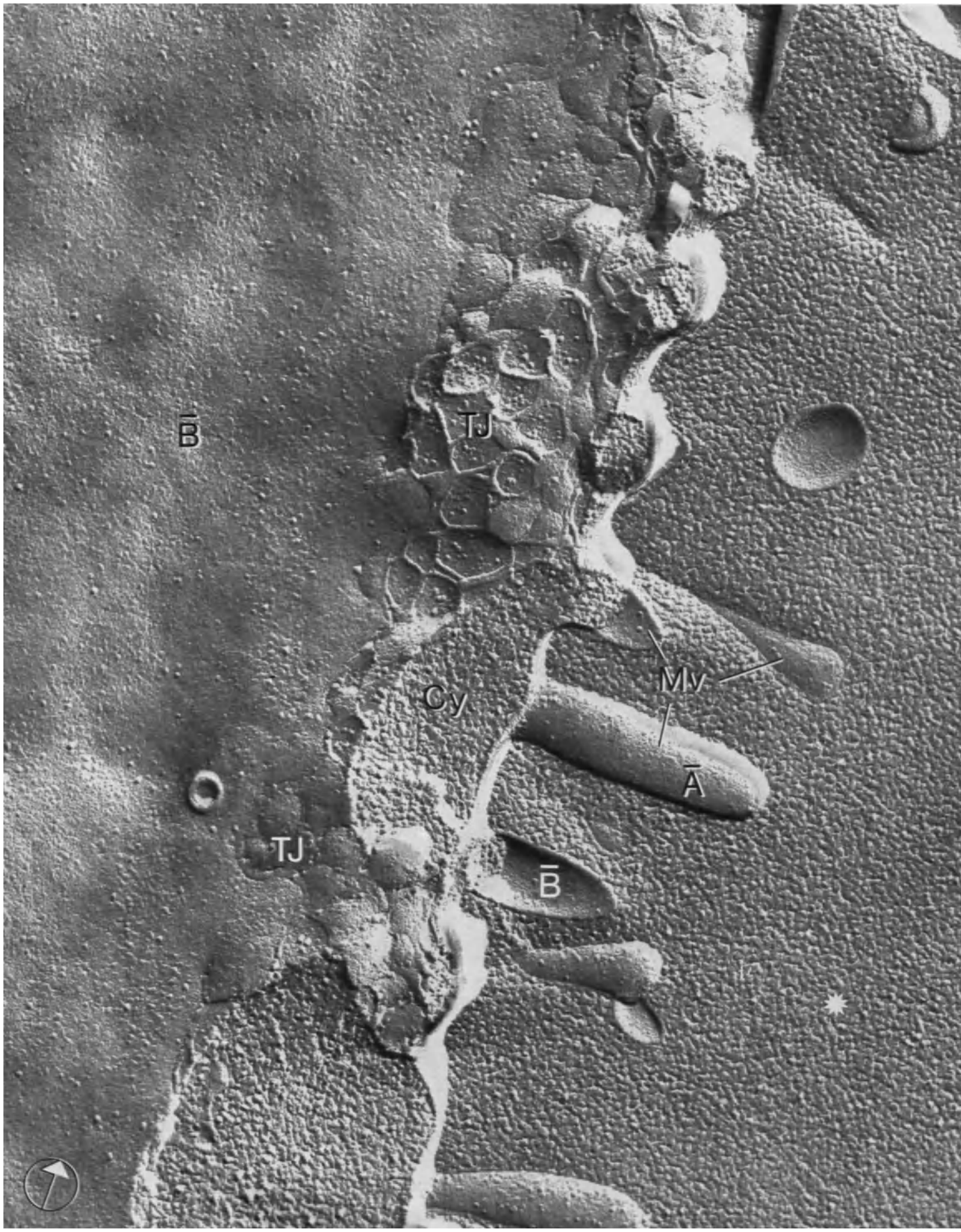
B̄
TJ
Cy
My
Ā
TJ
B̄

Plate 17 Follicular Cells from the Thyroid Gland of the Rat

The luminal membrane of two follicular cells (A-face) is seen from inside the follicular lumen, and during the fracturing process most of the microvilli (Mv) have broken away. What remains of them is only their bases which are slightly raised above the fracture face. The fractured bases of microvilli must be clearly distinguished from the endothelial pores described in Plates 5 to 9. The fact that the broken microvillar bases are raised above the A-face of the membrane and that they enclose the cytoplasmic matrix might be used as significant criteria for distinction. A large area of the follicular lumen (*) appears in the lower right-hand part of the picture. It contains several profiles of intact microvilli.

Magnification $\times$ 71,000

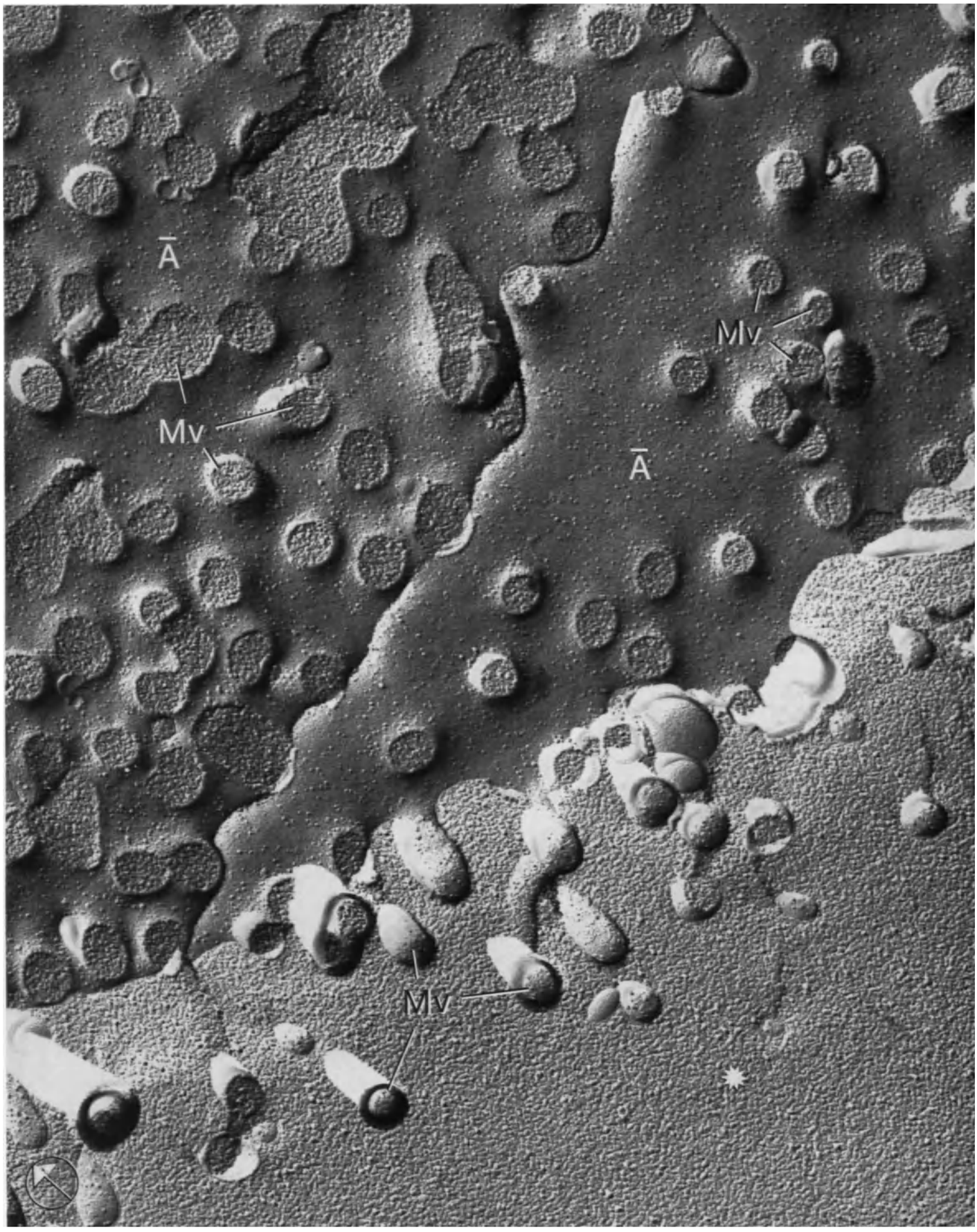

Plate 17

Plate 18 Human Small Intestine

In all tissues, cells share membrane and cytoplasmic differentiations involved in intercellular contacts. Among these differentiations, also called intercellular junctions, two are mainly cytoplasmic and are thought to be involved in cell to cell adhesion. These are the desmosome (macula adherens) and the intermediate junction (zonula adherens). Although desmosomes can be identified by freeze-etching (see references in Plate 23: McNUTT and WEINSTEIN, 1973), they will not be shown here. The two other junctional differentiations, namely the tight (zonula occludens) and the gap junction (nexus), occur at the plasma membrane and are, accordingly, most readily visualized in replicas. This figure presents the characteristic appearance of a tight junction in the membrane faces of absorptive cells of the small intestine. The tight junction (TJ) is situated at the apical part of the lateral plasma membranes, below the level of the microvilli (Mv) (broken here) and it has the function of sealing the intestinal lumen from the surrounding intercellular fluid. A tight junction is determined by the fusion of the outer leaflets of two adjacent plasma membranes. It appears in freeze-etch replicas as a system of anastomosing ridges in the A-face with corresponding grooves in the B-face.

Magnification $\times 80{,}000$

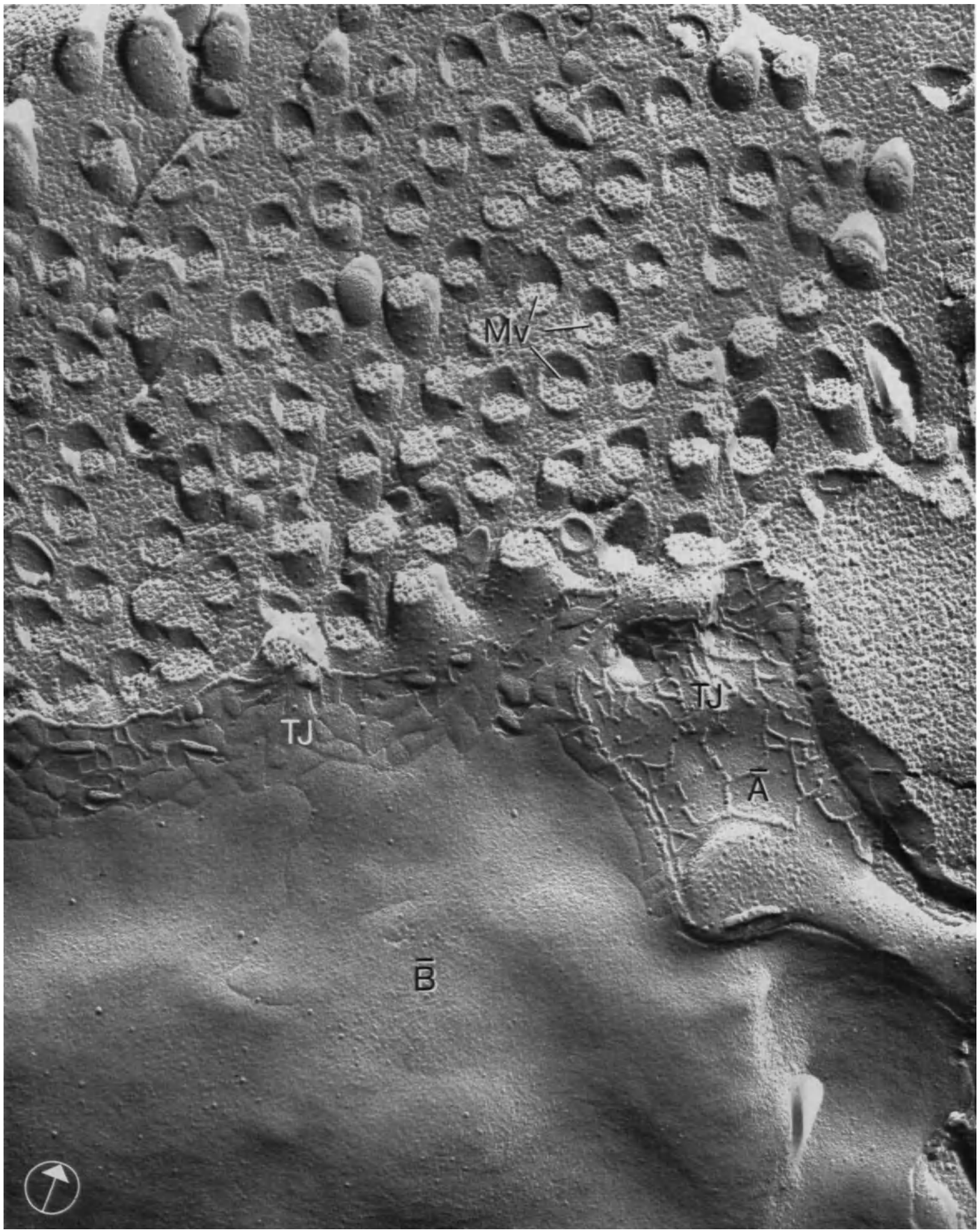

Plate 18

Plate 19 Acinus of the Rat Exocrine Pancreas

The number of tight junctional elements (ridges or grooves) present between individual cells may vary to a great extent, and recent studies have indicated that the permeability of a given epithelium to the paracellular flux of water and ions probably depends on the total number and disposition of these junctional elements on the lateral side of the cells. In this replica, a well-developed tight junctional network (TJ) has been exposed on both the A- and the B-face of the epithelial cells around the acinar lumen. As already seen (see Plate 18), each element appears as a ridge in the A-face or as a groove in the B-face of the cell membrane. See Plates 28–33 for further details on the acinar cells.

Magnification × 64,000

Selected References

CLAUDE, P., GOODENOUGH, D.A.: Fracture faces of zonulae occludentes from "tight" and "leaky" epithelia. J. Cell Biol. **58**, 390–400 (1973).

FRIEND, D.S., GILULA, N.B.: Variations in tight and gap junctions in mammalian tissues. J. Cell Biol. **53**, 758–776 (1972).

PRICAM, C., HUMBERT, F., PERRELET, A., ORCI, L.: A freeze-etch study of the tight junctions of the rat kidney tubules. Lab. Invest. **30**, 286–291 (1974).

Plate 19

Plate 20 Endocrine Cells from Human Pancreas (Isolated Islet of Langerhans)

In this highly magnified picture, the characteristic appearance of the tight junctional elements is emphasized. The fracture plane has exposed large areas of the A-face of a cell membrane. This face carries linear ridges (TJ) which are interrupted only by focal discontinuities. In the center of the picture, part of the B-face belonging to the plasma membrane of the adjacent cell involved in the tight junction can be seen. This face is slightly above the plane of the A-face and the step is situated at the level of a junctional ridge which is, accordingly, partially covered by the B-face. Tight junctional elements (TJ) entirely situated in the B-face appear as furrows or grooves. Grooves are complementary to ridges in the A-face. At certain points where individual ridges approach each other, one can see small clusters of aggregated particles (GJ). These represent gap junctions whose freeze-etch appearance is characterized in Plates 21–23. Notice that the membrane-associated particles are scarce within the tight junctional area.

Magnification × 156,000

Selected Reference

WADE, J.B., KARNOVSKY, M.J.: The structure of the zonula occludens. A single fibril model based on freeze-fracture. J. Cell Biol. **60**, 168–180 (1974).

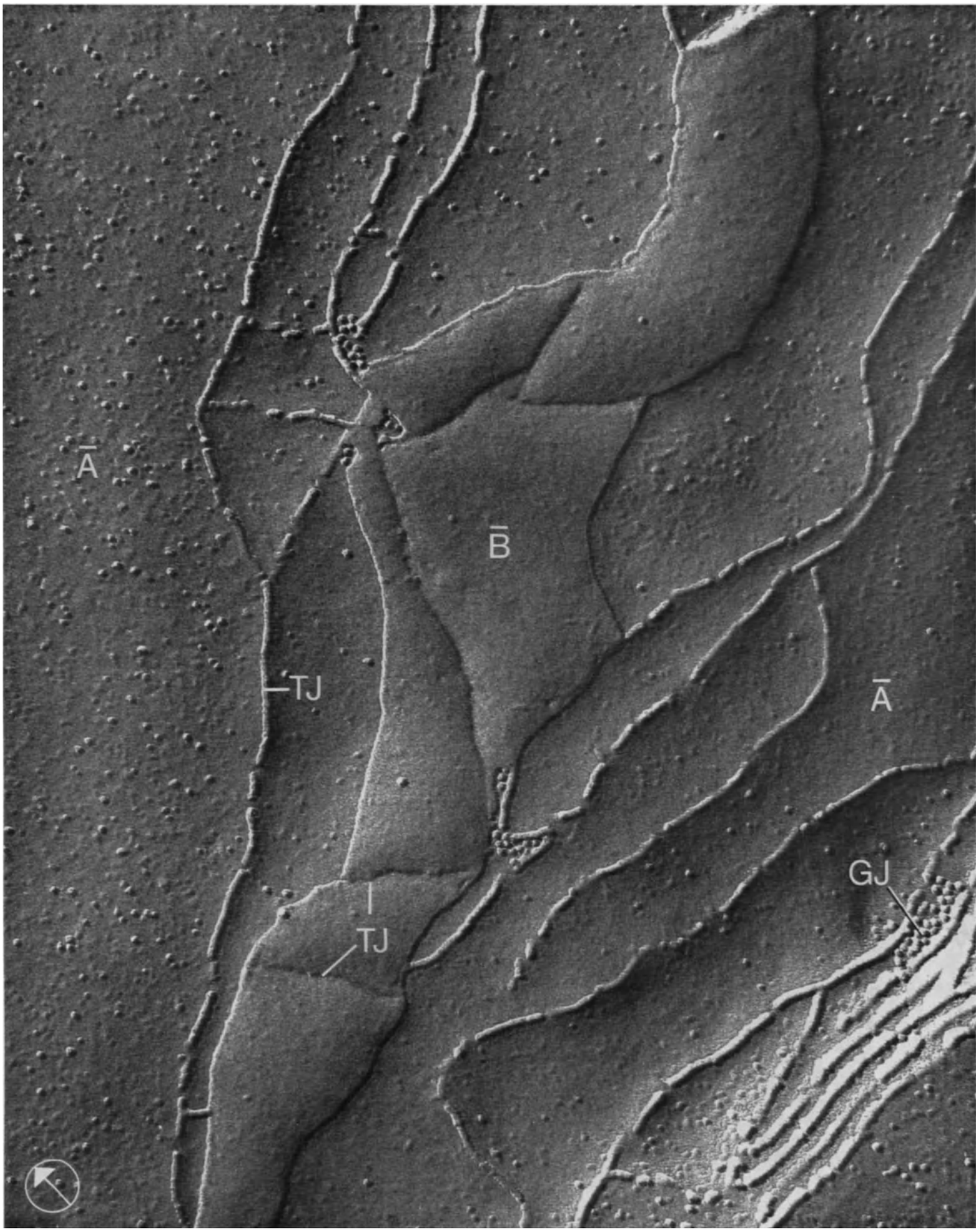

Plate 20

Plate 21 Liver Cells from the Mouse

This replica illustrates A- and B-faces of two adjacent cells. The non-junctional area of the A-face, visible in the upper and lower parts of the figure, shows randomly scattered membrane-associated particles. By contrast, in a large zone in the center of the figure (GJ), membrane-associated particles are regularly and closely packed. The area where membrane-associated particles are closely packed is found where conventional electron microscopy reveals a narrowing of the extracellular space from the usual width of 150–200 Å down to a 20–30 Å gap, forming a so-called gap junction. The junction contains bridging elements which have been shown to provide a passage for small molecules (MW < 500) and ions between the two cells across the gap (ionic and metabolic coupling). The membrane B-face in the gap junction, also characteristic, is illustrated in Plate 22.

Magnification × 71,000

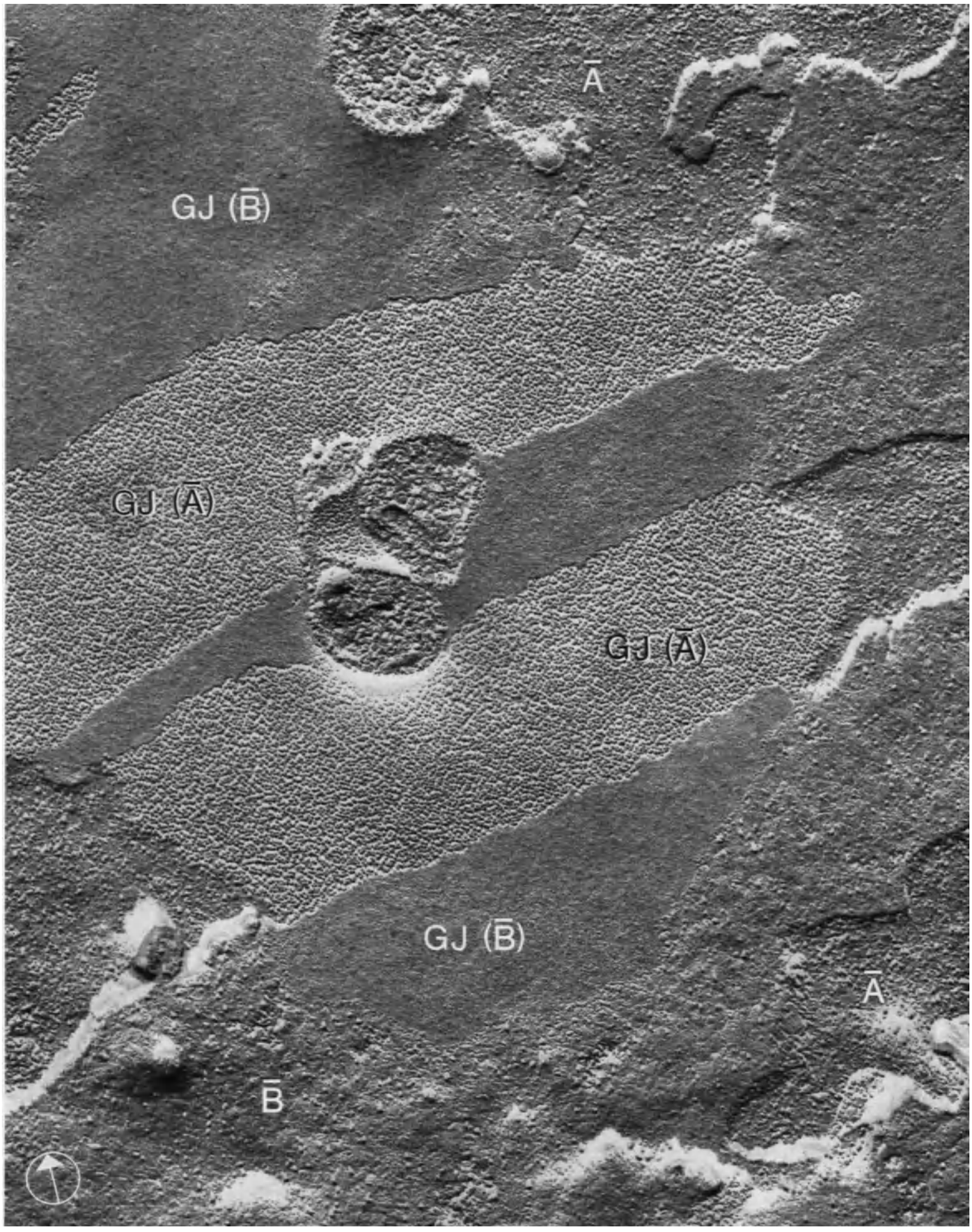
Ā
GJ (B̄)
GJ (Ā)
GJ (Ā)
GJ (B̄)
Ā
B̄

Plate 22 Liver Cells from the Mouse

As in Plate 21, fracture faces in the region of a gap junction (GJ) are illustrated here. The junctional A-face shows the regular array of membrane-associated particles and is partially covered by large pieces of B-face belonging to the plasma membrane of the other cell involved in the junction. The B-face in the gap junction is devoid of globular particles and contains only closely packed pits whose spacing is identical to that of the particles in the A-face. The pitted junctional B-face merges sharply with the B-face outside the junction which shows scattered globular particles. The complementarity observed between A- and B-faces in the gap junction indicates that the specific array extends across the whole width of the junctional membrane.

Magnification × 129,000

Selected Reference

SPYCHER, M.A.: Intercellular adhesions: an electron microscope study of freeze-etched rat hepatocytes. Z. Zellforsch. **111**, 64–74 (1970).

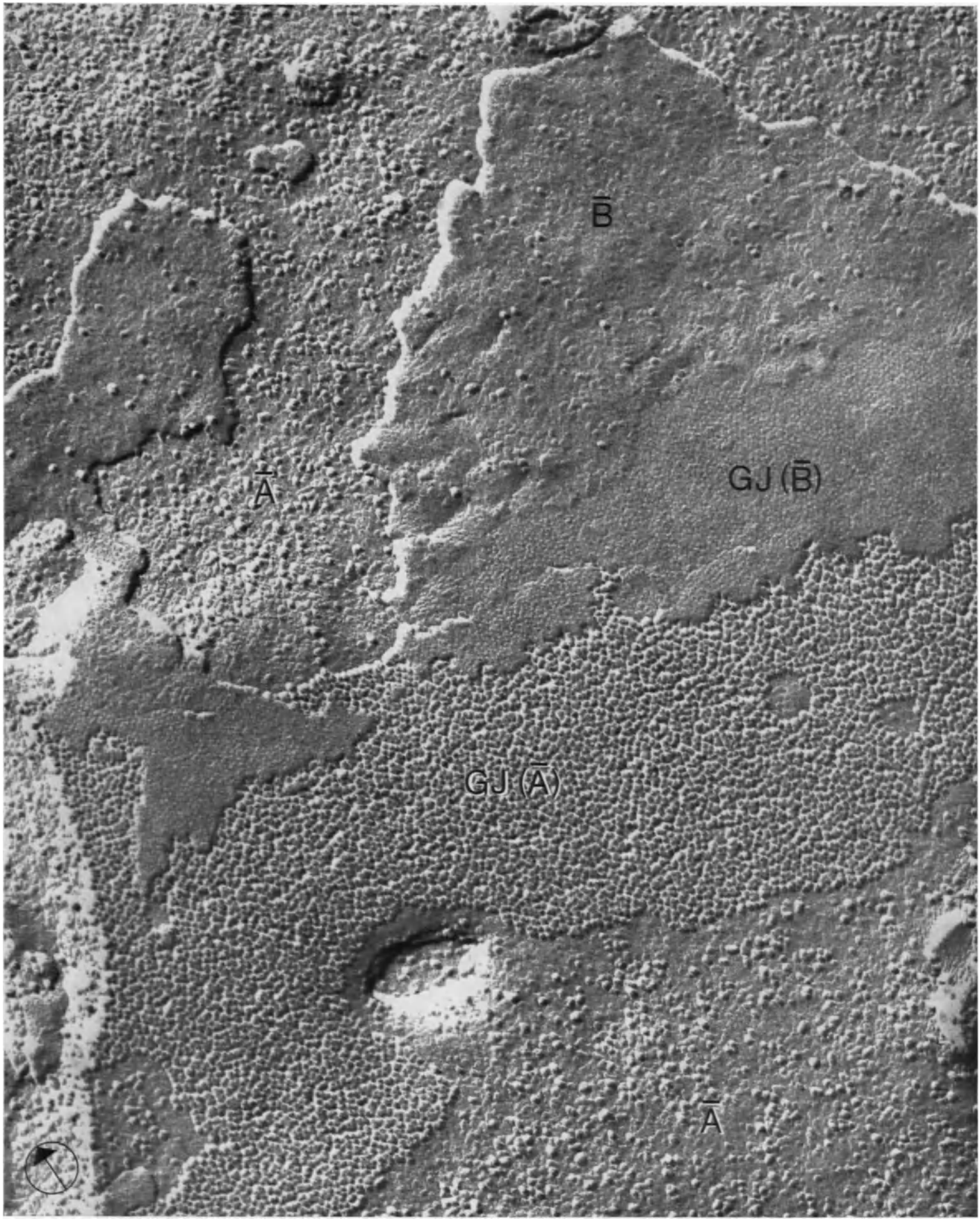
B̄
Ā
GJ (B̄)
GJ (Ā)
Ā

Plate 23 Endocrine Cell from the Rat Pancreas (Isolated Islet of Langerhans)

Membrane differentiations representing gap and tight junctions are frequently associated. In this high-magnification picture, a cell membrane A-face shows several aggregates of membrane-associated particles (GJ) as well as linear ridges (TJ). Notice that particles forming the gap junction have a very regular size, whereas the randomly scattered particles outside the junctional area show varying diameters.

Magnification $\times 200{,}000$

Selected References

CHALCROFT, J.P., BULLIVANT, S.: An interpretation of liver cell membrane and junction structure based on observation of freeze-fracture replicas of both sides of the fracture. J. Cell Biol. **47**, 49–60 (1970).

FRIEND, D.S., GILULA, N.B.: Variations in tight and gap junctions in mammalian tissues. J. Cell Biol. **53**, 758–776 (1972).

GOODENOUGH, D.A., REVEL, J.P.: A fine structural analysis of intercellular junctions in the mouse liver. J. Cell Biol. **45**, 272–290 (1970).

MCNUTT, N.S., WEINSTEIN, R.S.: The ultrastructure of the nexus: a correlated thin-section and freeze-cleave study. J. Cell Biol. **47**, 666–688 (1970).

MCNUTT, N.S., WEINSTEIN, R.S.: Membrane ultrastructure at mammalian intercellular junctions. In: Progr. Biophys. molec. Biol. **26**, 45–102 (1973).

ORCI, L., UNGER, R.H., RENOLD, A.E.: Structural coupling between pancreatic islet cells. Experientia (Basel) **29**, 1015–1018 (1973).

REVEL, J.P., KARNOVSKY, M.J.: Hexagonal array of subunits in intercellular junctions of the mouse heart and liver. J. Cell Biol. **33**, $C_7 - C_{12}$ (1967).

REVEL, J.P., YEE, A.G., HUDSPETH, A.J.: Gap junctions between electrotonically coupled cells in tissue culture and in brown fat. Proc. nat. Acad. Sci. (Wash.) **68**, 2924–2927 (1971).

SINGER, S.J., NICOLSON, G.L.: The fluid mosaic model of the structure of cell membranes. Science **175**, 720–731 (1972).

STAEHELIN, L.A., MUKHERJEE, T.M., WILLIAMS, A.W.: Freeze-etch appearance of the tight junctions in the epithelium of small and large intestine of mice. Protoplasma **67**, 165–184 (1969).


TJ
GJ
A
TJ
GJ

Nucleus

Plate 24 Liver Cell from the Mouse

This section across the nucleus reveals mainly the respective areas occupied by euchromatin (eu) and heterochromatin (he), and the nucleolus (nu). The peripheral band of heterochromatin is interrupted at the level of the nuclear pores (NP).

Magnification × 26,000

Plate 25 Epithelial Cell from the Rat Kidney (Proximal Tubule)

Instead of going across the nucleus, the freeze-fracture exposed fully the nuclear envelope. Areas of this envelope which have fewer particles are parts of the B-face of the outer membrane. Areas richly particulated represent the A-face of the inner membrane. On both these faces, which are separated by distinct ridges (→) representing the height of the cisternal space delimited by the two membranes, the nuclear pores (NP) are conspicuous and their number can be easily assessed.

Magnification × 31,000

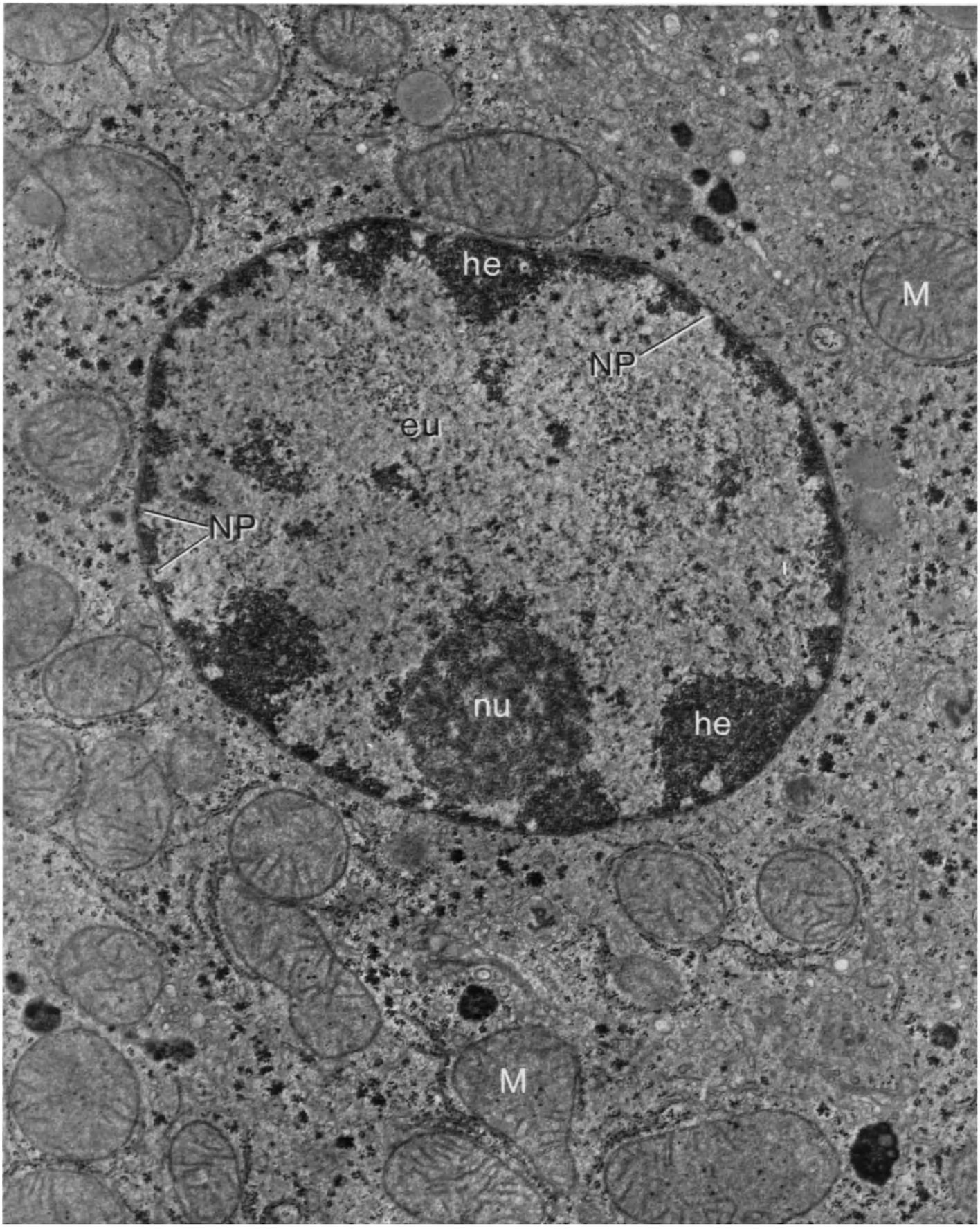
he
M
NP
eu
NP
nu
he
M

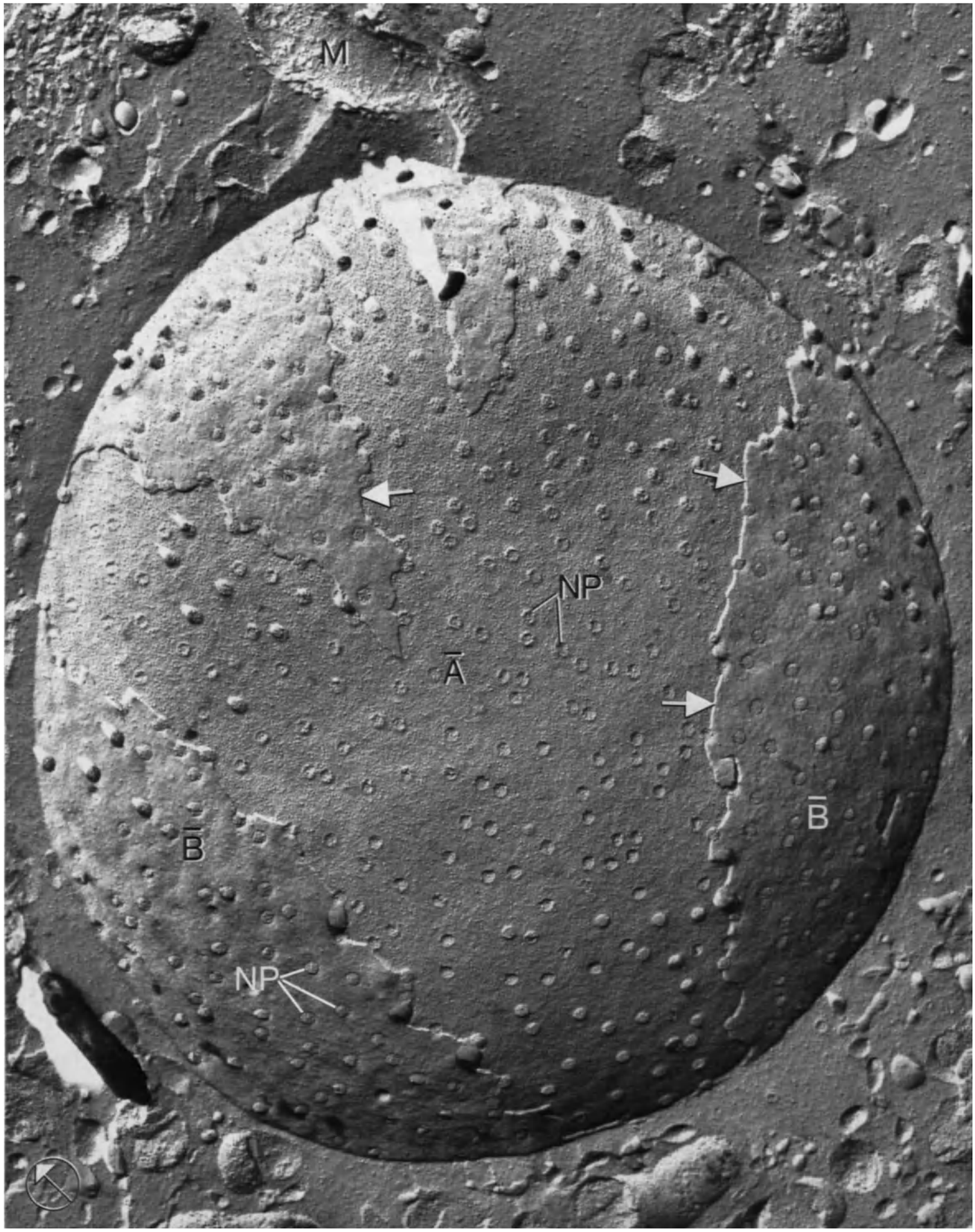

Plate 25

Plate 26 Liver Cell from the Rat

The form and the disposition of nuclear pores (NP) is seen only in a grazing section of the nuclear envelope. This means that very few pores from the total number are offered for examination.

Magnification × 38,000

Plate 27 Endocrine Cell from the Rat Pancreas (Isolated Islet of Langerhans)

Both a large area of the nuclear envelope and a part of the nucleoplasm (*) have been exposed. Notice that pores (NP) tend to be clustered in discrete zones of the nuclear envelope.

Magnification × 44,000

Selected References

KARTENBECK, J., ZENTGRAF, H., SCHEER, U., FRANKE, W.W.: The nuclear envelope in freeze-etching. Ergebn. Anat. **45**, 1–55 (1971).

MAUL, G.G.: On the octagonality of the nuclear pore complex. J. Cell Biol. **51**, 558–563 (1971).

MAUL, G.G., PRICE, J.W., LIEBERMAN, M.W.: Formation and distribution of nuclear pore complexes in interphase. J. Cell Biol. **51**, 405–418 (1971).

MONNERON, A., BLOBEL, G., PALADE, G.E.: Fractionation of the nucleus by divalent cations. J. Cell Biol. **55**, 104–125 (1972).

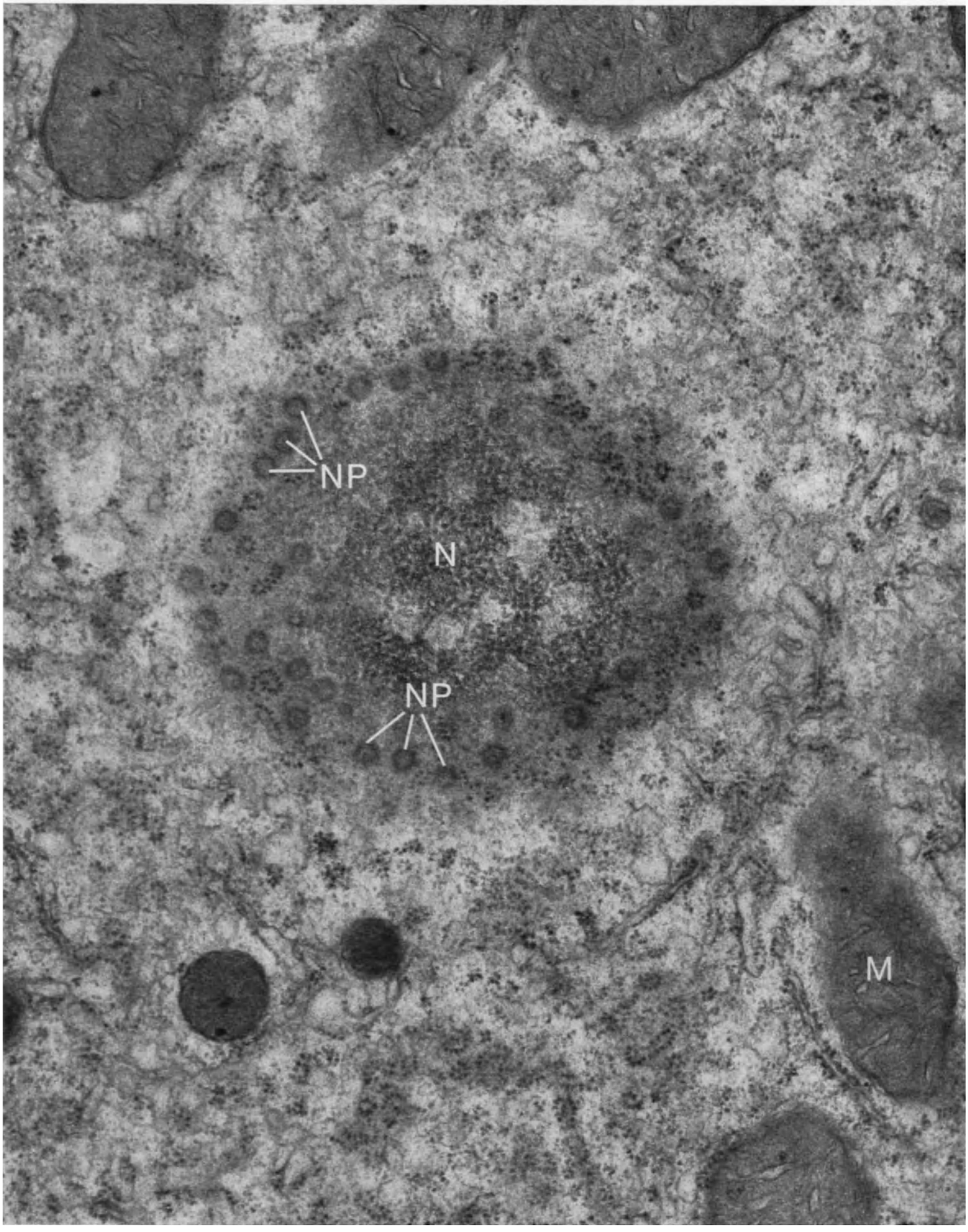
NP
N
NP
M

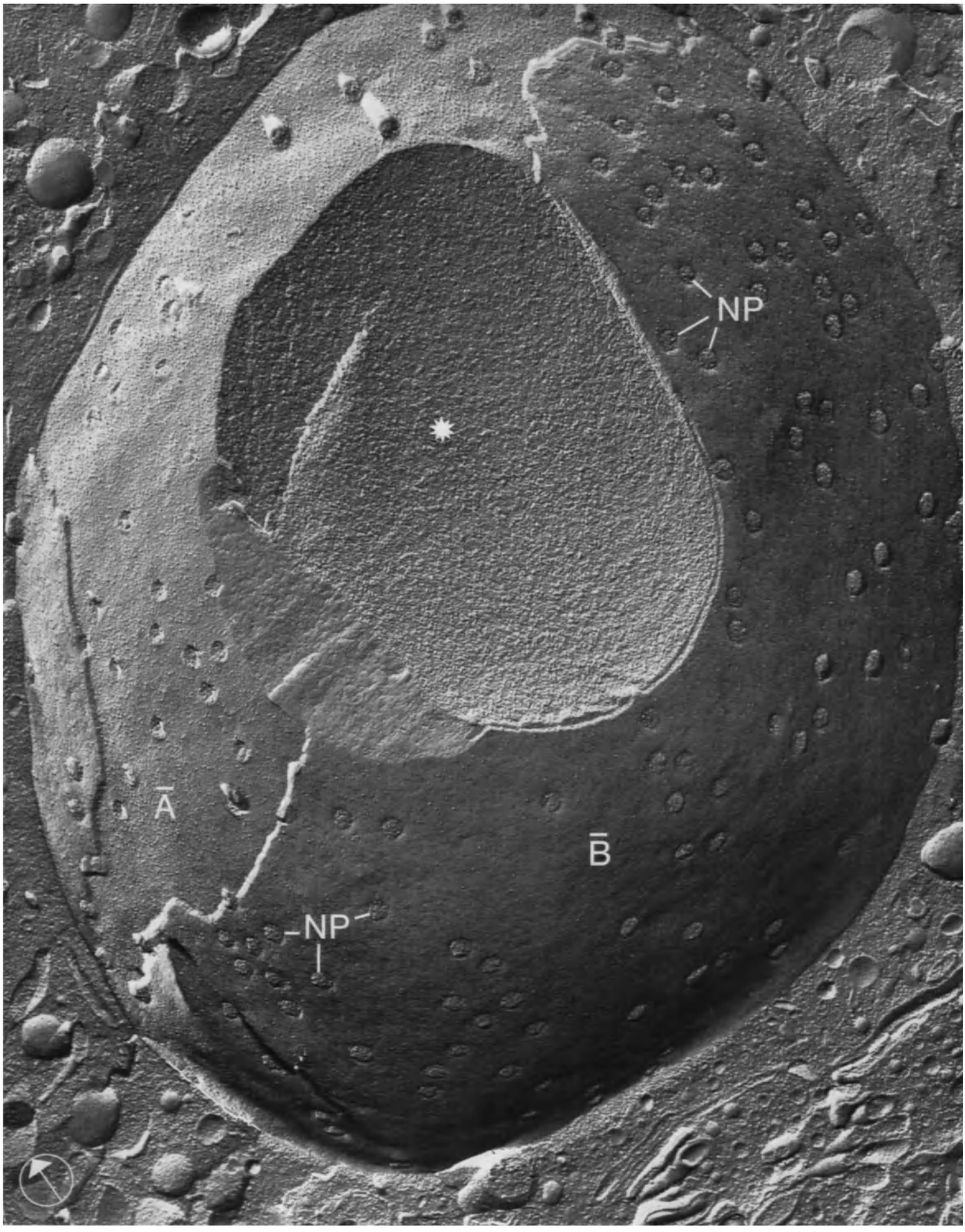

Plate 27

Exocrine Pancreas

Plate 28 Exocrine Pancreas from the Rat

The organelles of the acinar cell are disposed in a characteristic pattern. Zymogen granules (ZG) are usually packed between the Golgi complexes (G) and the plasma membrane delimiting the acinar lumen (*), whereas stacked rough endoplasmic cisternae (RER) occupy the opposite pole of the cell.

Magnification × 17,000

Plate 29 Exocrine Pancreas from the Rat

A fracture across acinar cells gives a good insight into the spatial distribution of the various organelles. Even at this relatively low magnification, the tight junctional elements (TJ) sealing the acinar lumen can be distinguished (see Plates 32–33 for further details).

Magnification × 14,000

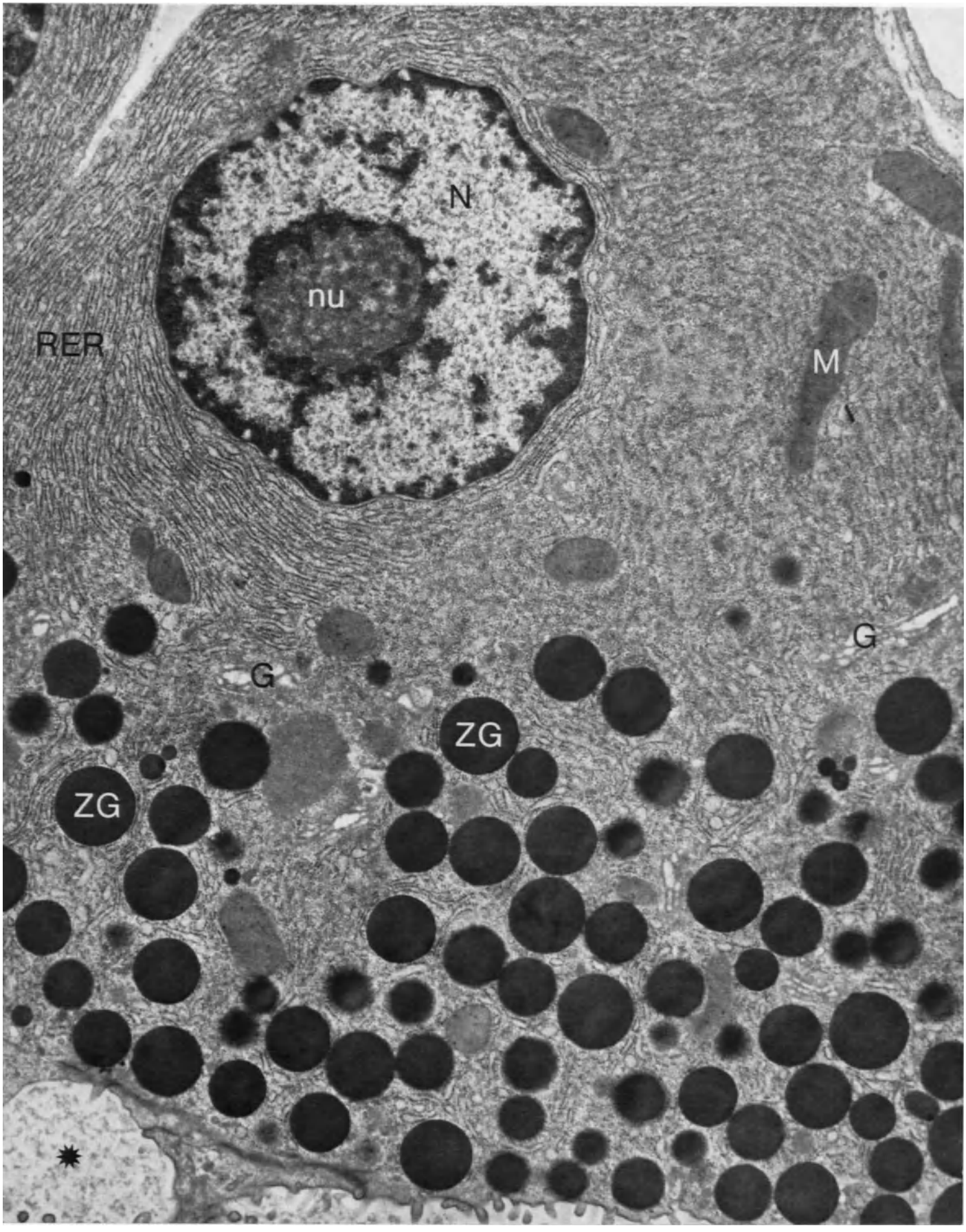

Plate 28

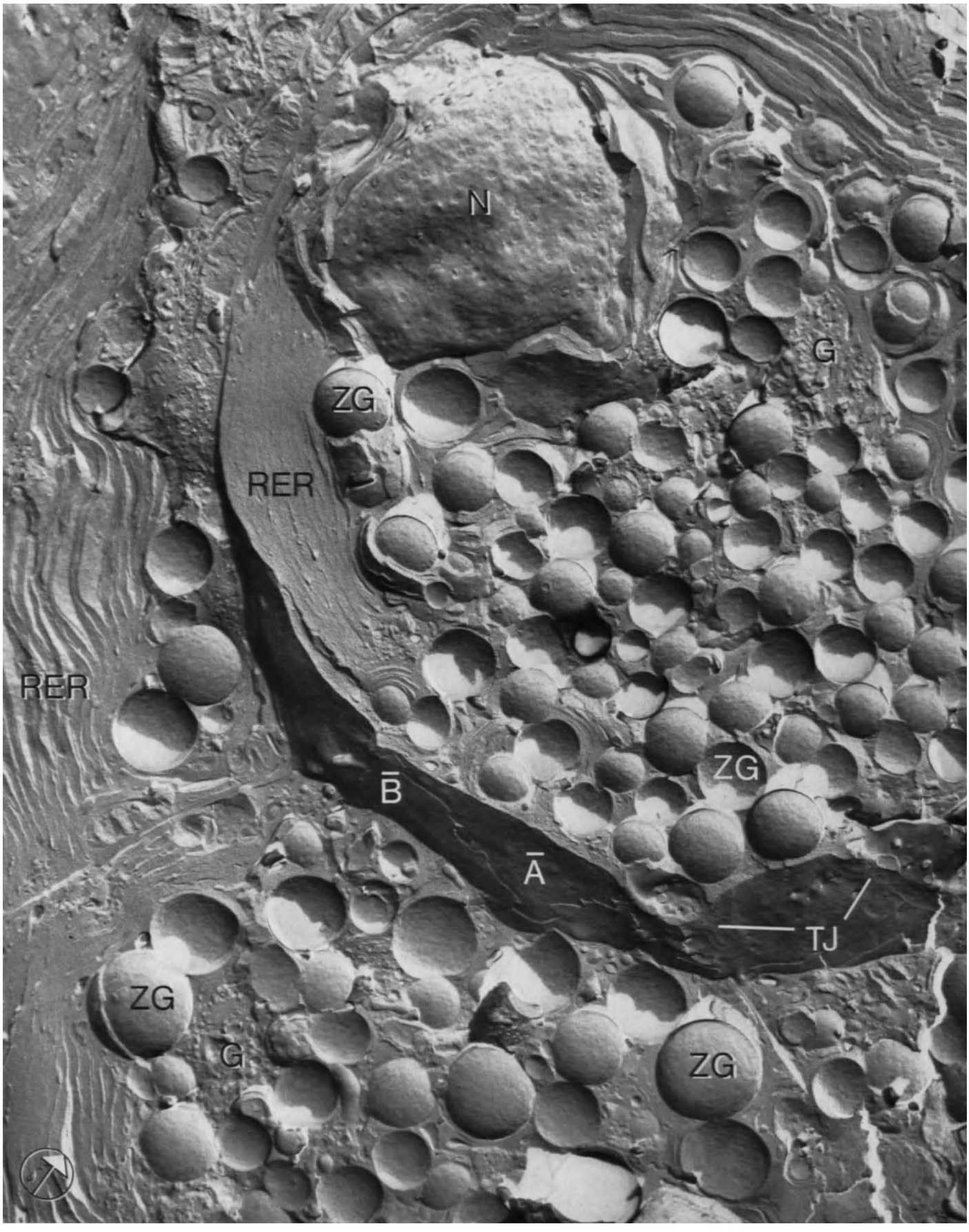
N
G
ZG
RER
RER
ZG
B̄
Ā
TJ
ZG
G
ZG

Plate 30 Exocrine Cell from the Dog Pancreas

The flat and parallel cisternae of the rough endoplasmic reticulum (RER), whose membranes are richly studded with ribosomes (R), are particularly conspicuous in exocrine cells.

Magnification × 51,000

Plate 31 Exocrine Cell from the Spiny Mouse Pancreas

Freeze-fracturing reveals the sheet-like form of the rough endoplasmic reticulum cisternae (RER). Moreover, it shows that cisternae are provided with pores (→) which are particularly numerous in this animal species. In contrast with thin section, however, the fact that the freeze-fracturing process exposes the inside of membranes makes the ribosomes attached on the outer (true) surface of the rough endoplasmic reticulum invisible.

Magnification × 45,000

Selected Reference

Orci, L., Perrelet, A., Like, A.A.: Fenestrae in the rough endoplasmic reticulum of the exocrine pancreatic cells. J. Cell Biol. **55**, 245–249 (1972).

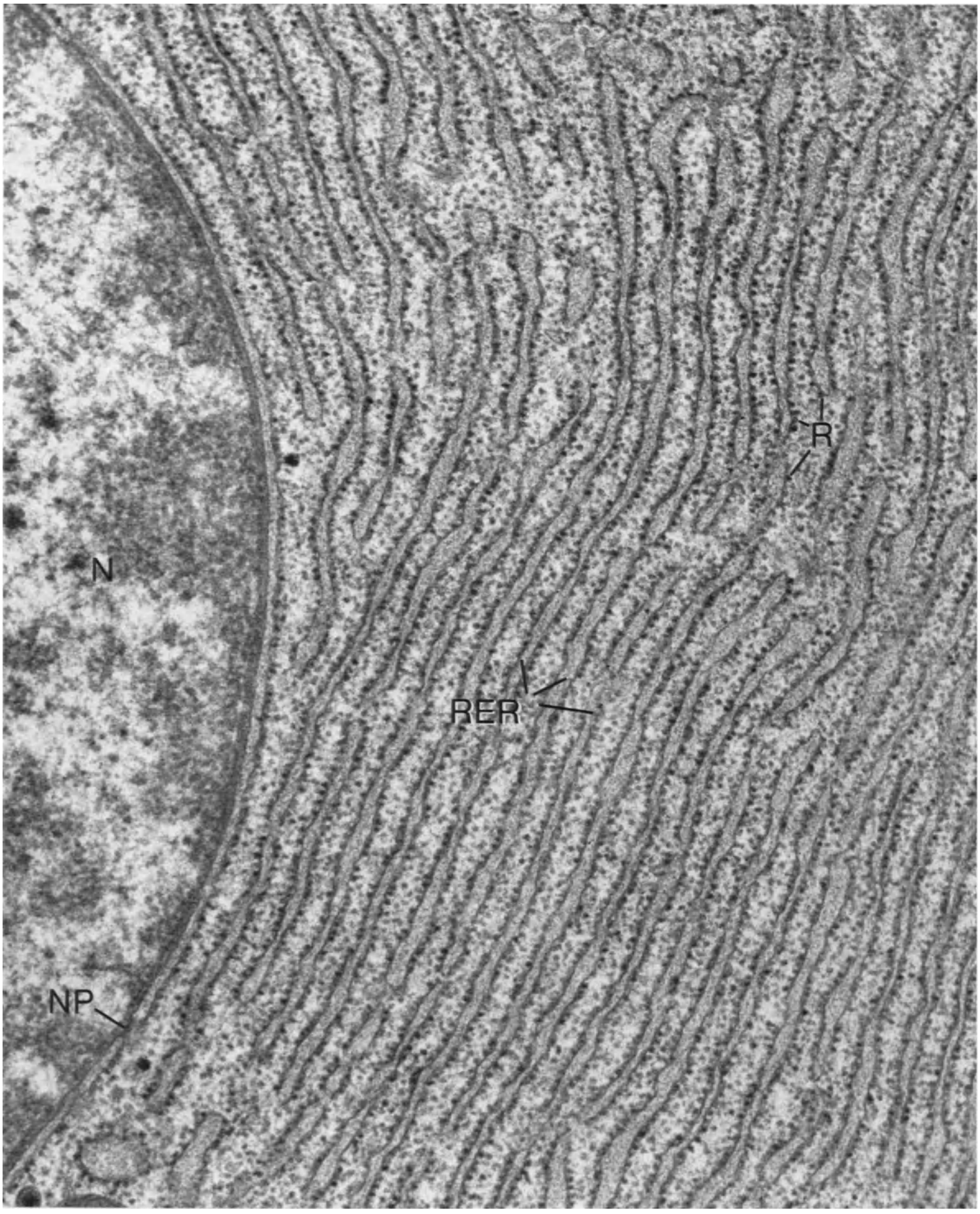
R
N
RER
NP

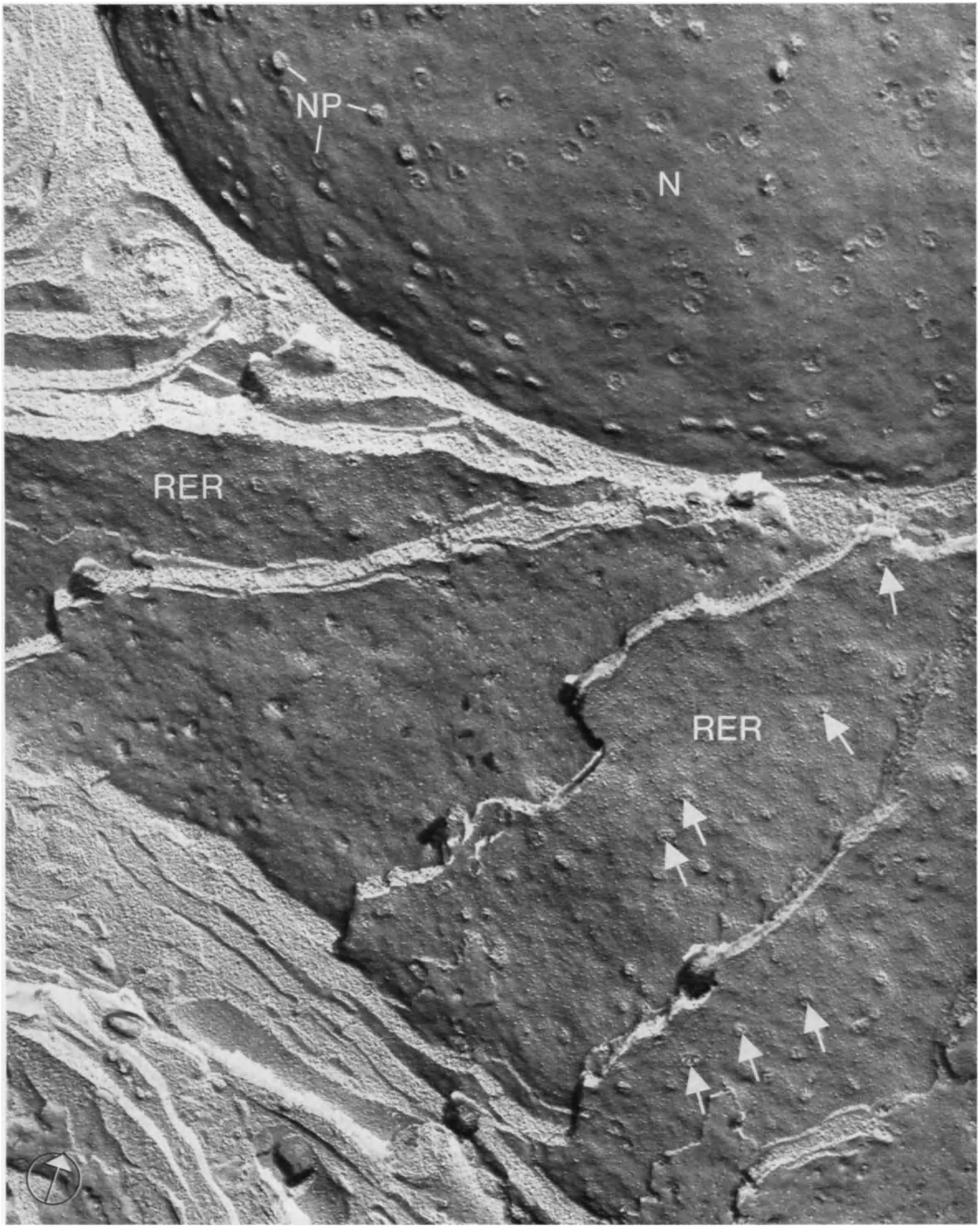
NP
N
RER
RER

Plate 32 Exocrine Pancreas from the Rat

Three exocrine cells outline the acinar lumen (*) which is isolated from the intercellular space (ICS) by tight junctions (TJ). Short microvilli (Mv) in longitudinal or transverse section can be seen in the lumen.

Magnification × 46,000

Plate 33 Exocrine Pancreas from the Rat

This higher magnification of Plate 29 shows cytoplasmic fractures exposing the membrane of the zymogen granules (ZG). Concave and convex profiles represent respectively the A- and the B-face of this membrane. On the faces of the lateral plasma membrane notice the network of tight junctional ridges (TJ) forming a belt around the acinar lumen. The membrane in this latter region has distinctly fewer particles than the lateral membrane.

Magnification × 44,000

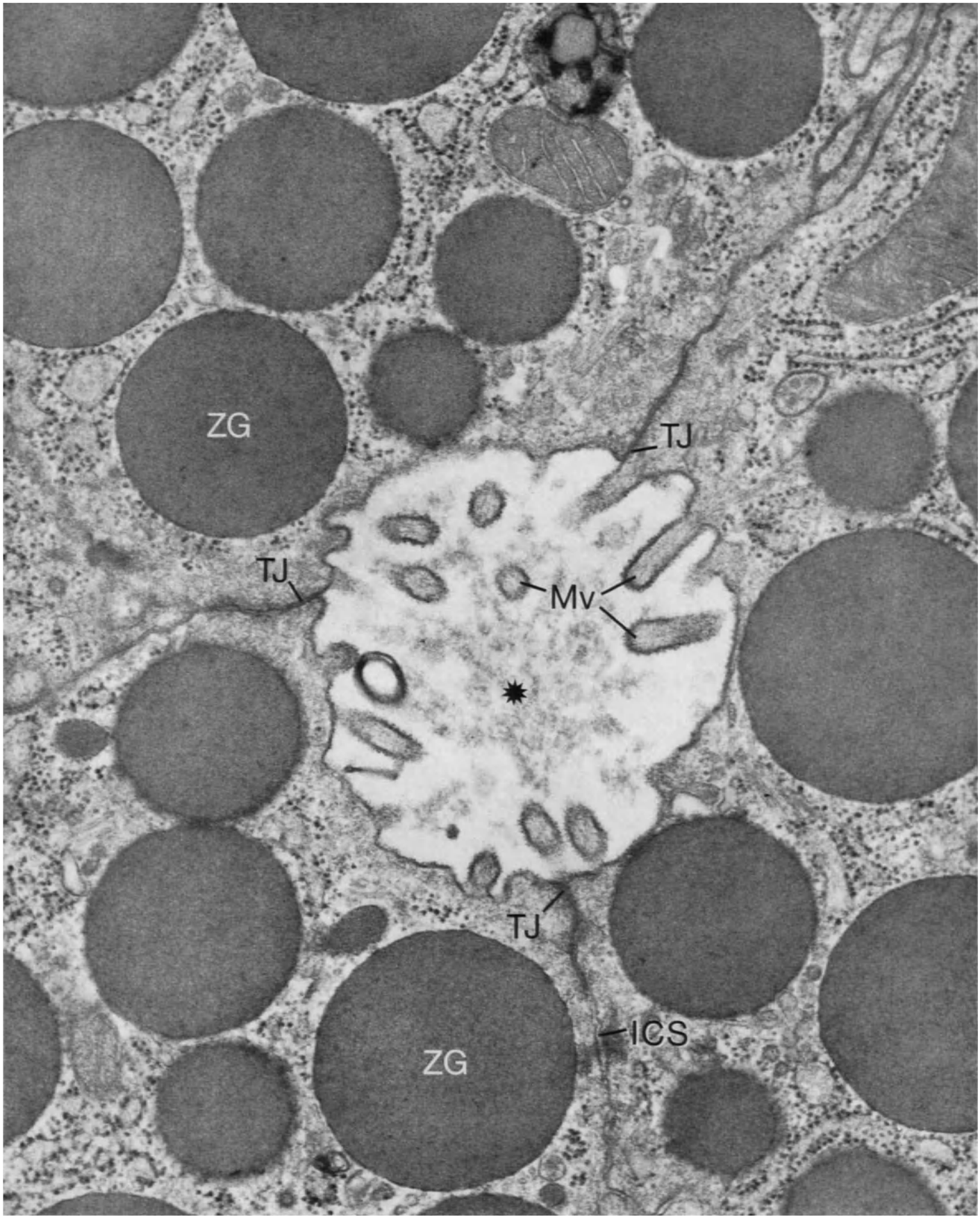
ZG
TJ
TJ
Mv
TJ
ICS
ZG

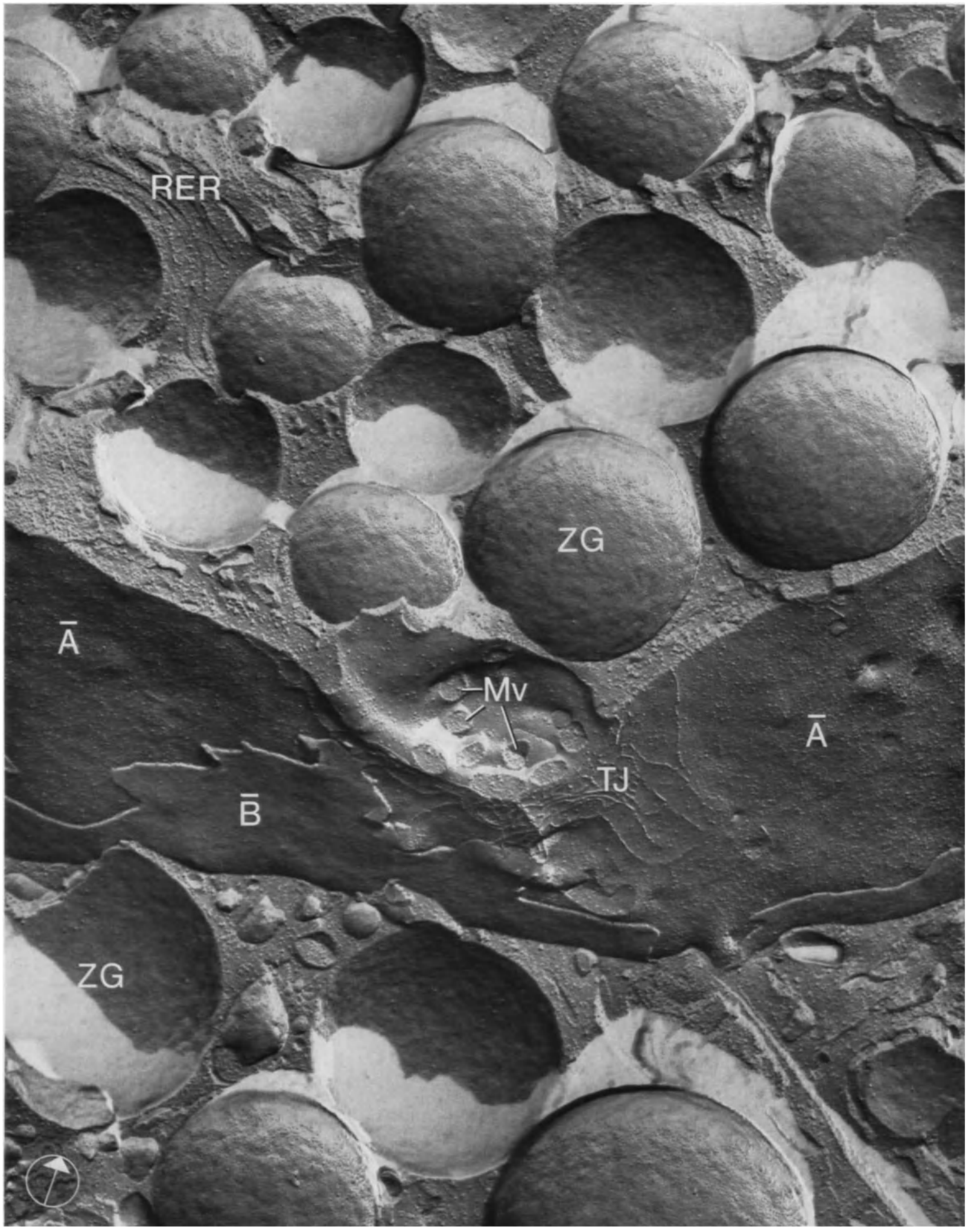
RER
ZG
Ā
Mv
Ā
TJ
B̄
ZG

Plate 34 Intralobular Duct of the Rat Exocrine Pancreas

The cells forming the wall of the duct are separated by a narrow intercellular space (ICS) which is obliterated at the level of the tight junction (TJ). Cells are provided with sparse microvilli (Mv).

Magnification × 30,000

Plate 35 Intralobular Duct of the Rat Exocrine Pancreas

Large areas of the luminal and lateral plasma membrane of the epithelial cells have been exposed. The luminal plasma membrane (A-face) is identified by many profiles of microvilli (Mv), whereas the lateral faces (A- and B-faces) are characterized by the presence of tight junctional elements (TJ). Notice that the luminal A-face has fewer particles that the lateral A-face of the same cell.

Magnification × 21,000

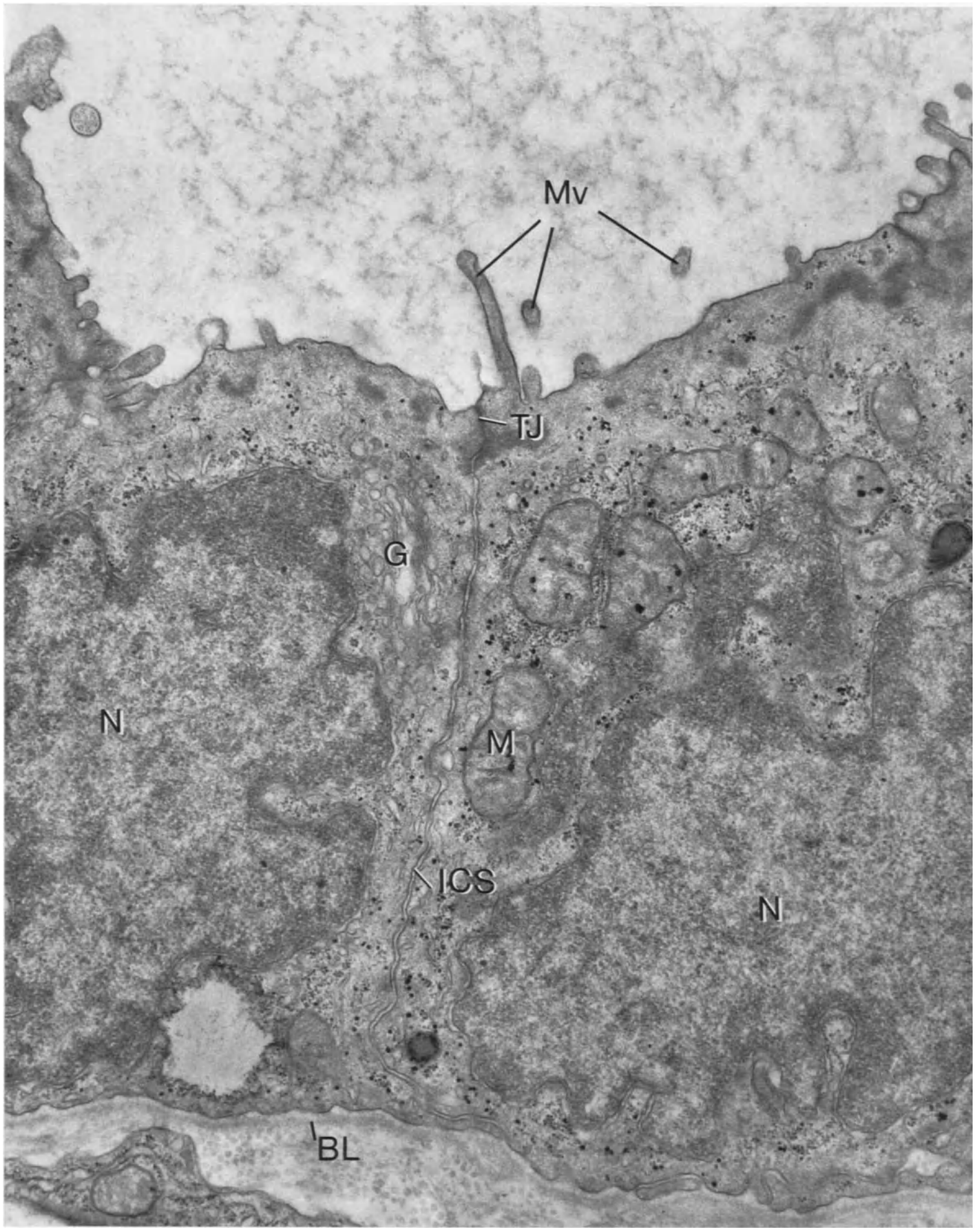
Mv
TJ
G
N
M
ICS
N
BL

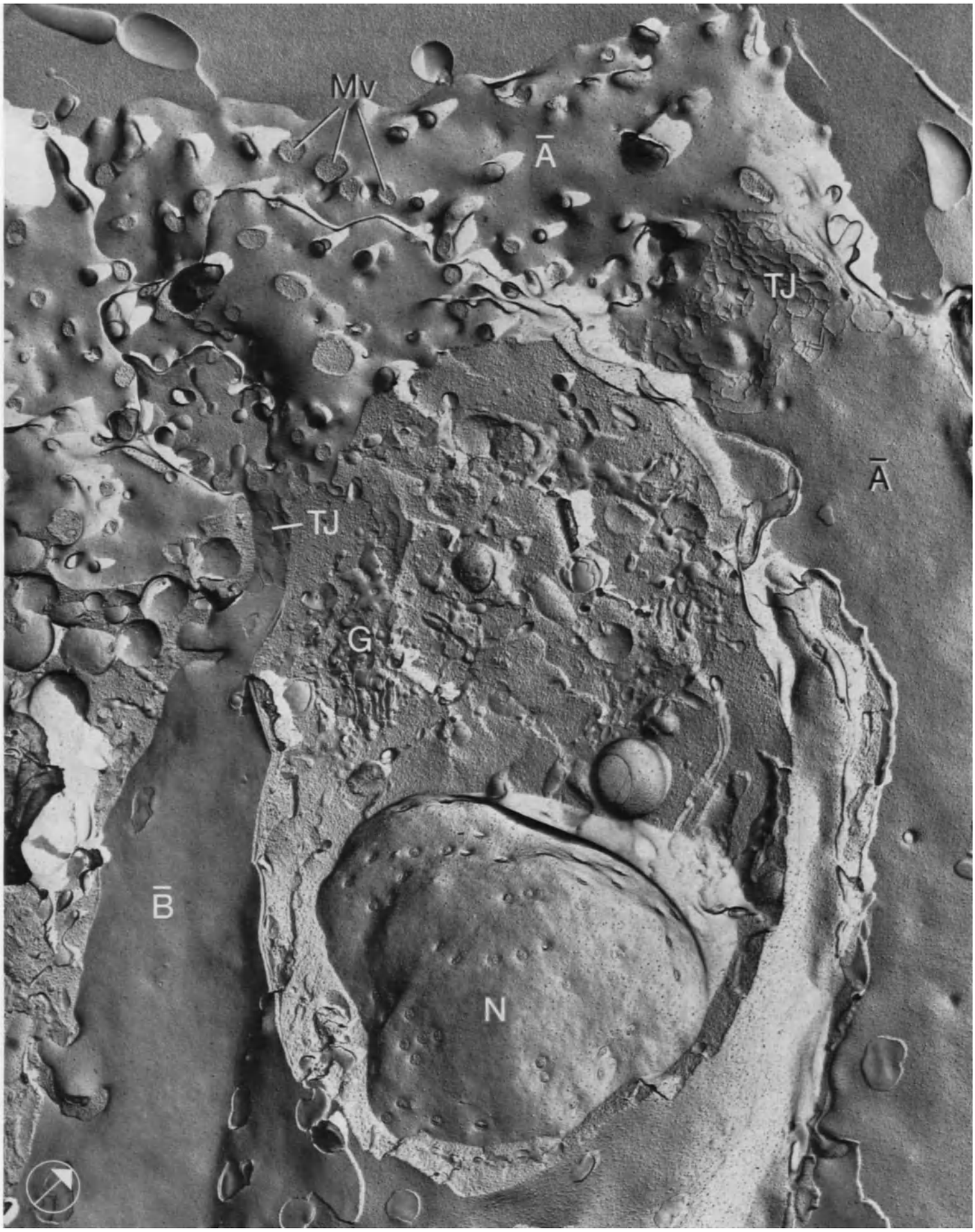
Mv
Ā
TJ
Ā
TJ
G
B̄
N

Endocrine Pancreas

Plate 36 Insulin-Producing Cell (Isolated B-Cell from the Islet of Langerhans of the Rat)

Endocrine cells secreting polypeptidic hormones store their product in characteristic membrane-bound organelles (secretory granules) (SG). In this cell type, the content of the granule – or granule core – is of irregular shape and separated from the limiting membrane by a wide halo.

Magnification × 15,000

Plate 37 Insulin-Producing Cell (Isolated B-Cell from the Islet of Langerhans of the Rat)

The endocrine cell has been fractured along a plane similar to that of the thin section. The nuclear envelope (N) with its pores is easily recognizable and most of the globular profiles in the cytoplasm represent membrane faces of the secretory granules (SG).

Magnification × 14,000

Plate 38 Insulin-Producing Cell (Isolated B-Cell from the Islet of Langerhans of the Rat)

In contrast with the preceding replica which revealed mostly the inside of the cell, this shows the plasma membrane and only a small part of the cytoplasm. The membrane face exposed is an A-face. The degree of clumping and loss of membrane-associated particles (→) is due to the fact that the preparation was exposed to proteolytic enzymes (Pronase) (see reference at the end of the Introduction: BRANTON, 1971).

Magnification × 35,000

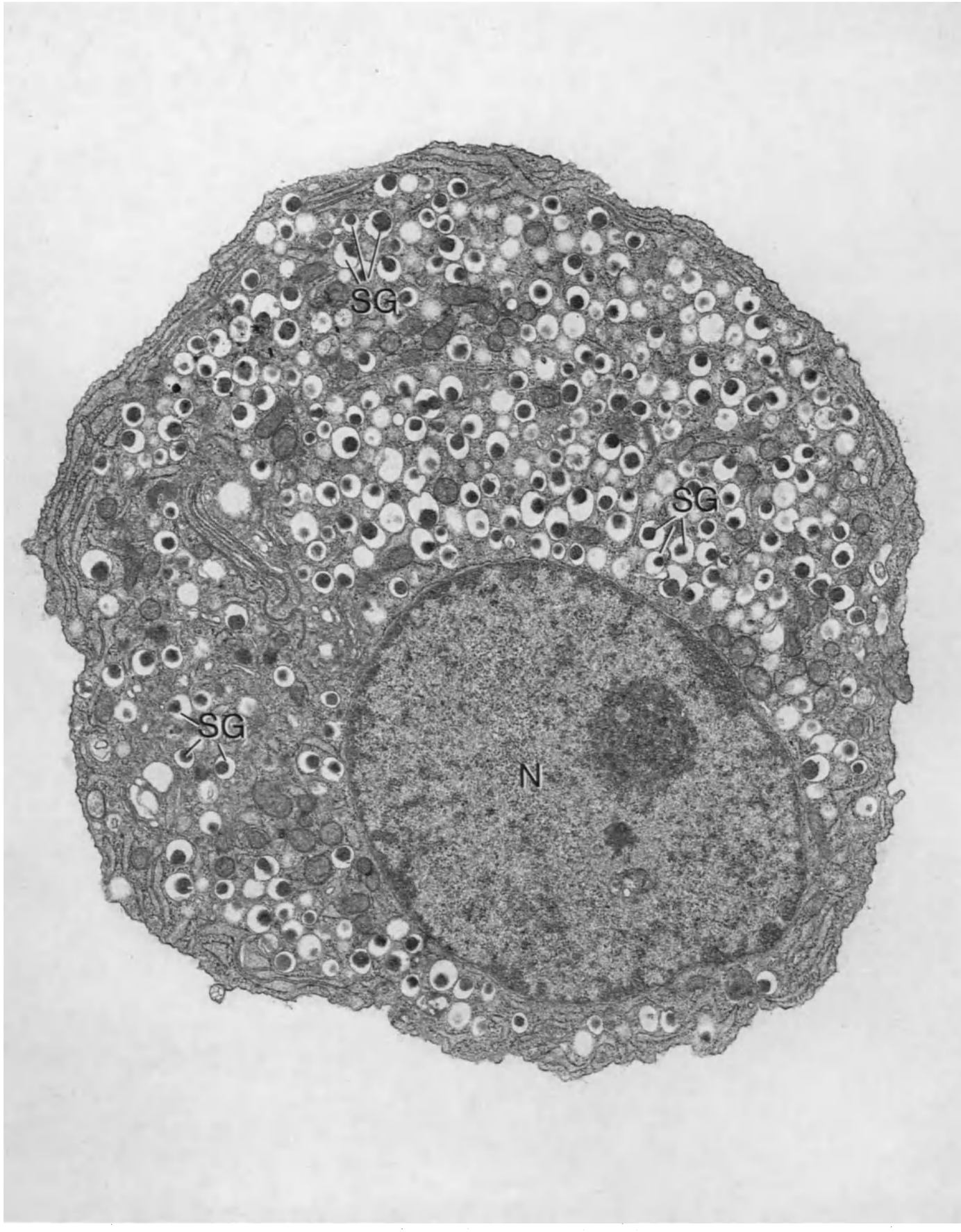

Plate 36

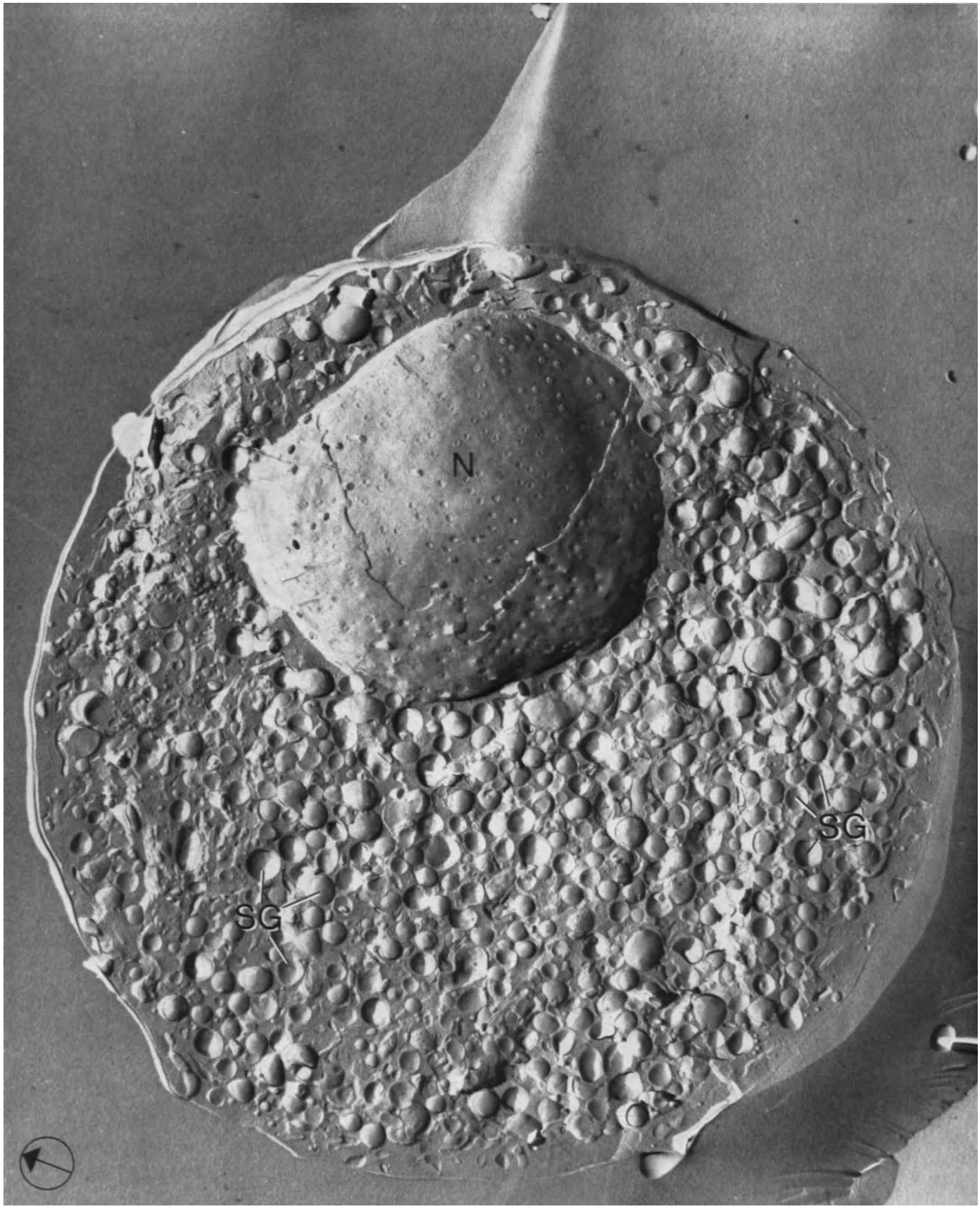
N
SG
SG

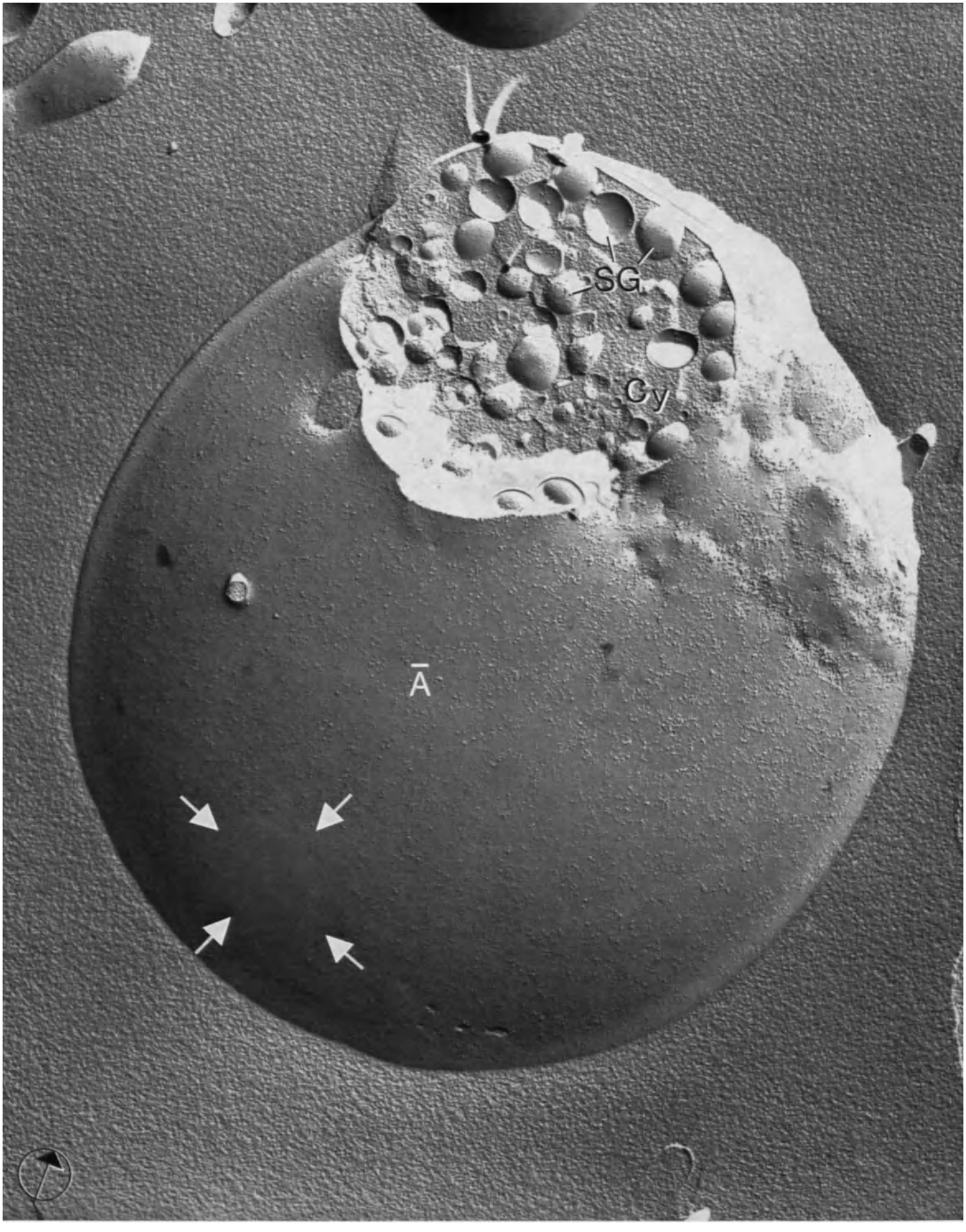

Plate 38

Plate 39 B-Cells from the Rat Pancreas (Isolated Islet of Langerhans)

This low power electron micrograph shows several B-cells and their relationships with each other in the tissue. At this magnification, the most apparent cytoplasmic organelles are the specific secretory granules (SG), the mitochondria (M) which are mainly rod-shaped and Golgi complexes (G).

Magnification × 10,000

Plate 40 Endocrine Cells from the Rat Pancreas (Isolated Islet of Langerhans)

In freeze-fracture one can recognize the membrane faces of secretory granules (SG), of mitochondria (M) and of the Golgi complex (G). In addition, the cell membranes (A- and B-faces) and the nuclear envelope (N) have been largely exposed.

Magnification × 16,000

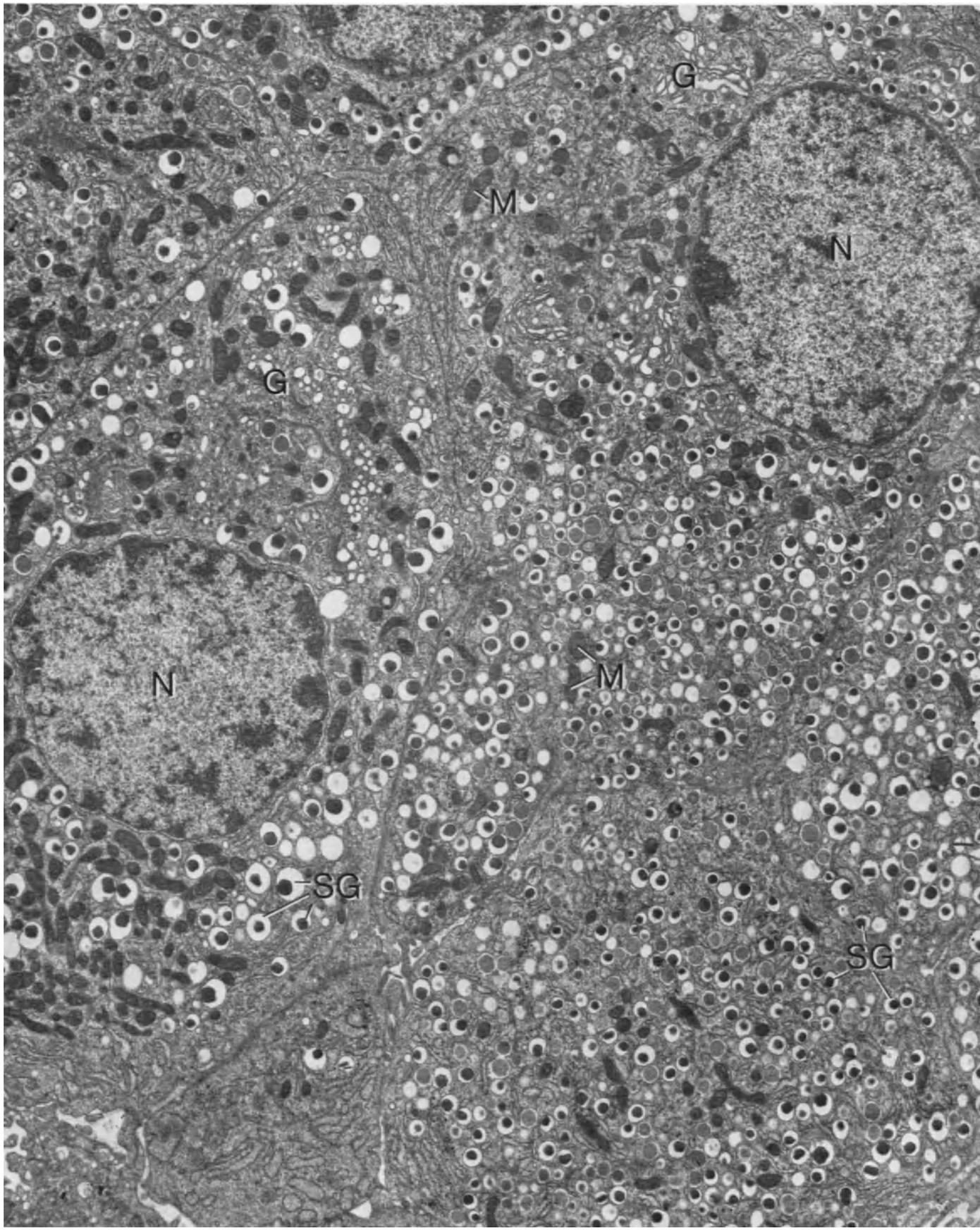
G
M
N
G
N
M
SG
SG

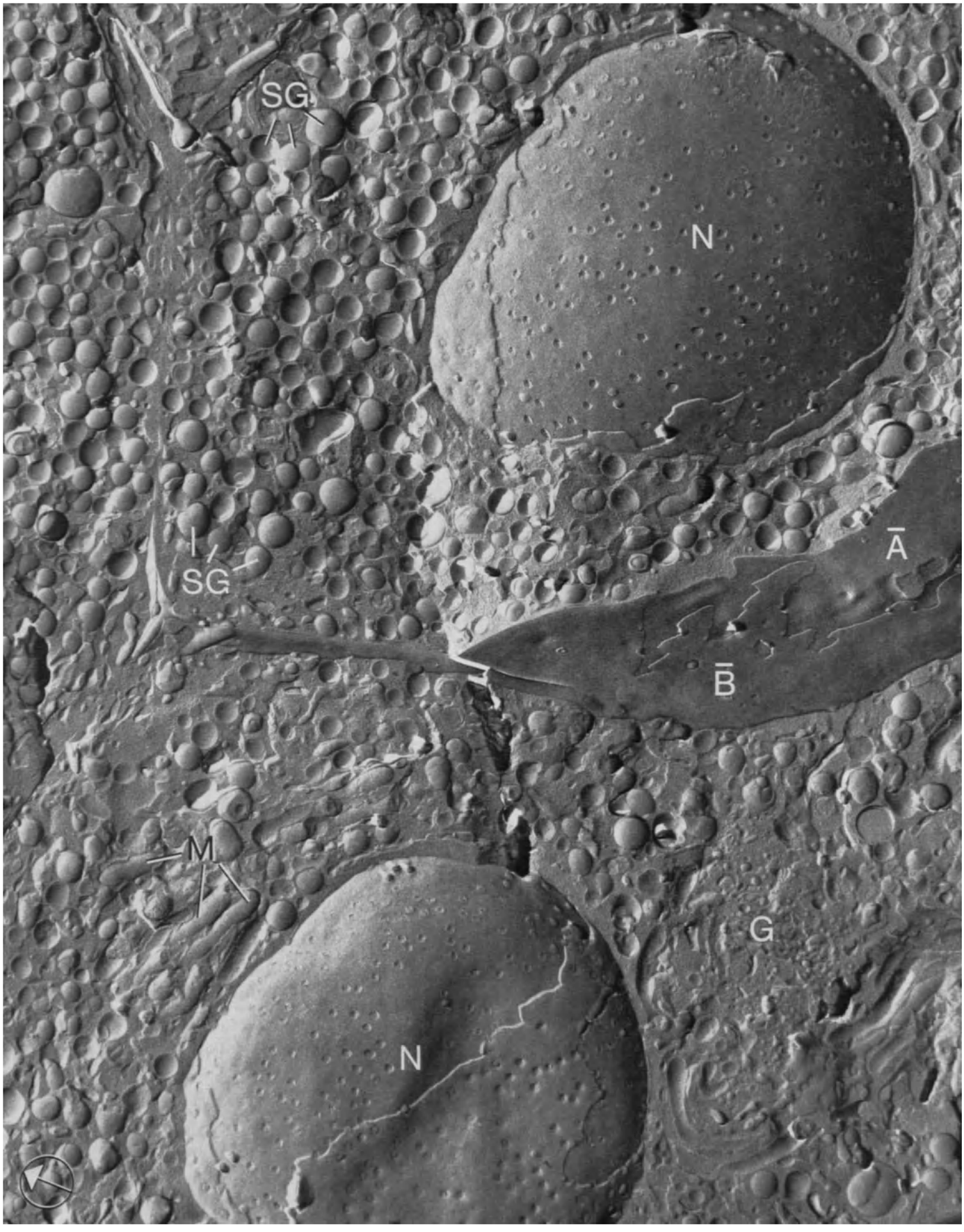
SG
N
I
SG
Ā
B̄
M
G
N

Intestine

Plate 41 Intestinal Epithelium of the Cat

Absorptive cells from the small intestine are characterized by a prominent microvillar border (Mv) covered by a thick cell coat (CC). The cell web (CW) is also conspicuous (see Plate 43).

Magnification 17,000

Plate 42 Intestinal Epithelium of the Mouse

The zone corresponding to the cell web (CW) is visible as a band devoid of large cytoplasmic organelles. It has a finely granular texture which extends into the microvillar cores. Small areas of lateral plasma membranes have been exposed near the apical pole of the cells and show the characteristic elements of tight junctions (TJ). Membrane faces of the microvilli (Mv) appear as convex and richly particulated, or as concave and poorly particulated profiles. The interpretation of such images is given in Plate 44.

Magnification × 30,000

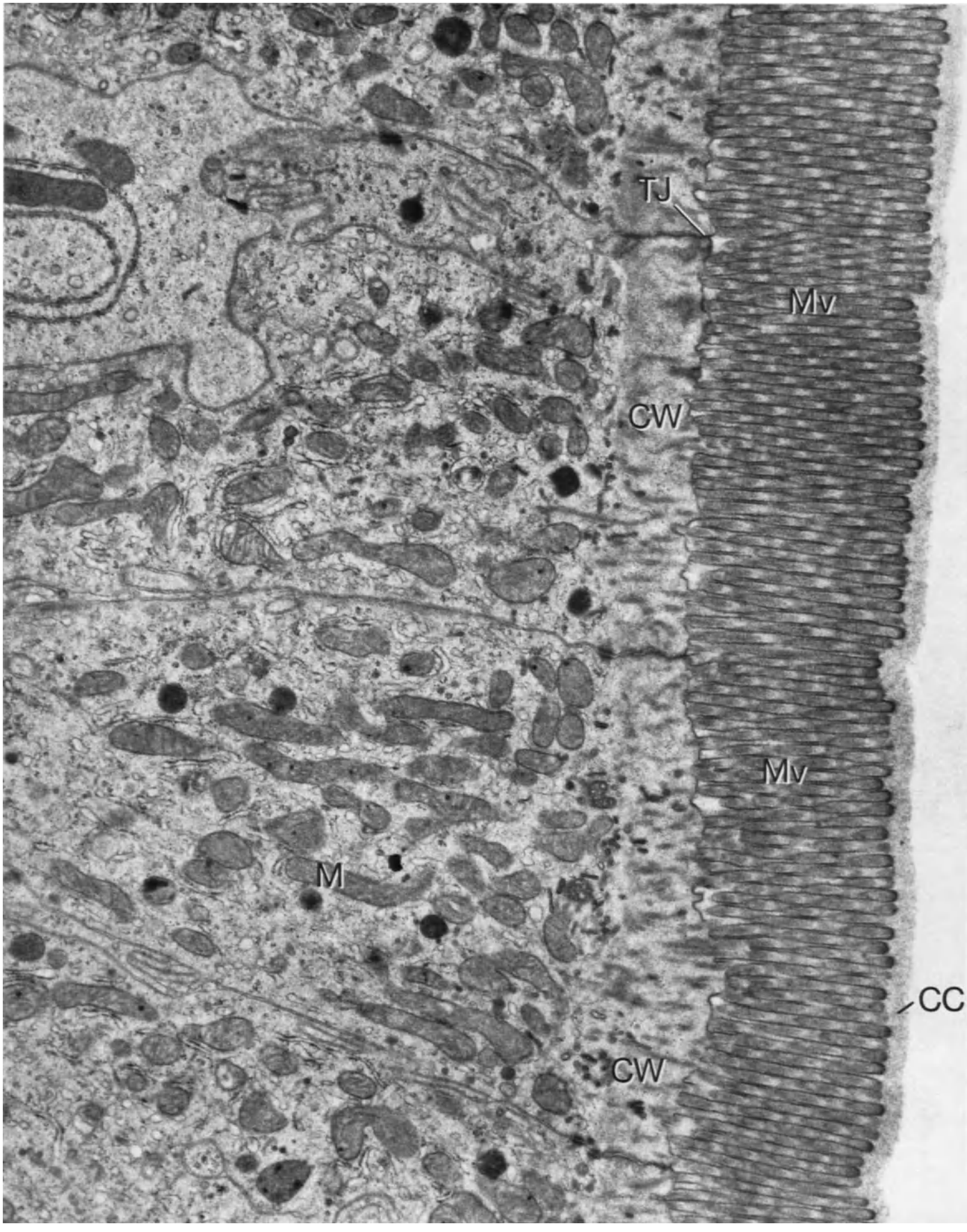
TJ
Mv
CW
Mv
M
CC
CW

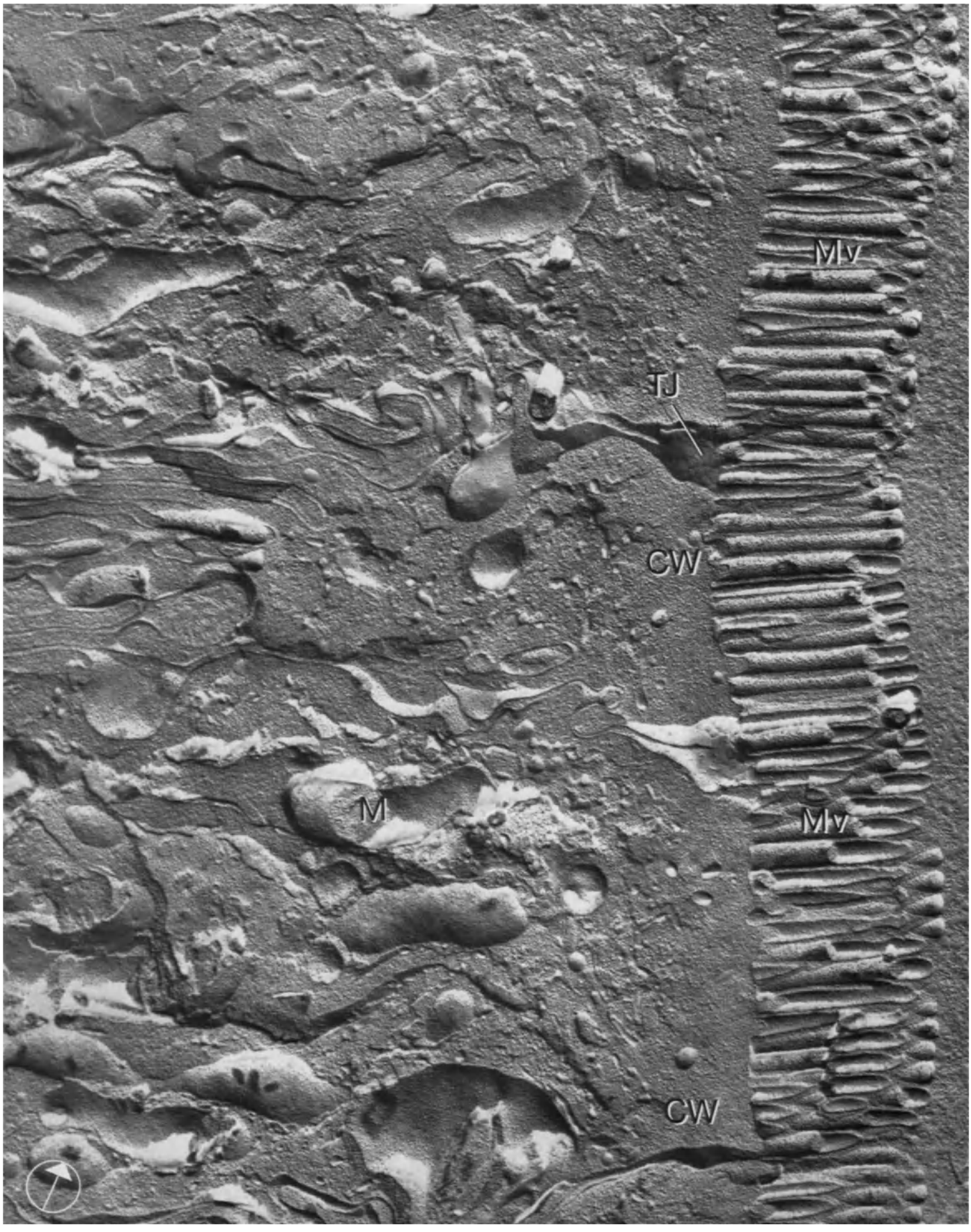
Mv
TJ
CW
M
Mv
CW

Plate 43 Intestinal Epithelium of the Cat

The fine structure of the microvilli (Mv) is clearly seen in a longitudinal section. Microvilli are long and regularly spaced cytoplasmic projections limited by the plasma membrane. They contain straight bundles of filaments (F) which anchor in the cell web (CW). A conspicuous tight junction (TJ) seals the intercellular space (ICS) near the apical pole of the cells.

Magnification $\times 55{,}000$

Plate 44 Intestinal Epithelium of the Rat

The splitting of the microvillar membrane produces two distinct faces. The B-faces are concave and have distinctly less membrane-associated particles (about $800/\mu^2$) than the complementary A-faces (about $2400/\mu^2$), which are convex. When A- and B-faces are exposed on the same microvillus, these faces are separated by a step ($\rightarrow$) representing the thickness of the fractured cytoplasmic core. Notice that both fracture faces at the tip of the microvilli have very few particles.

Magnification $\times 71{,}000$

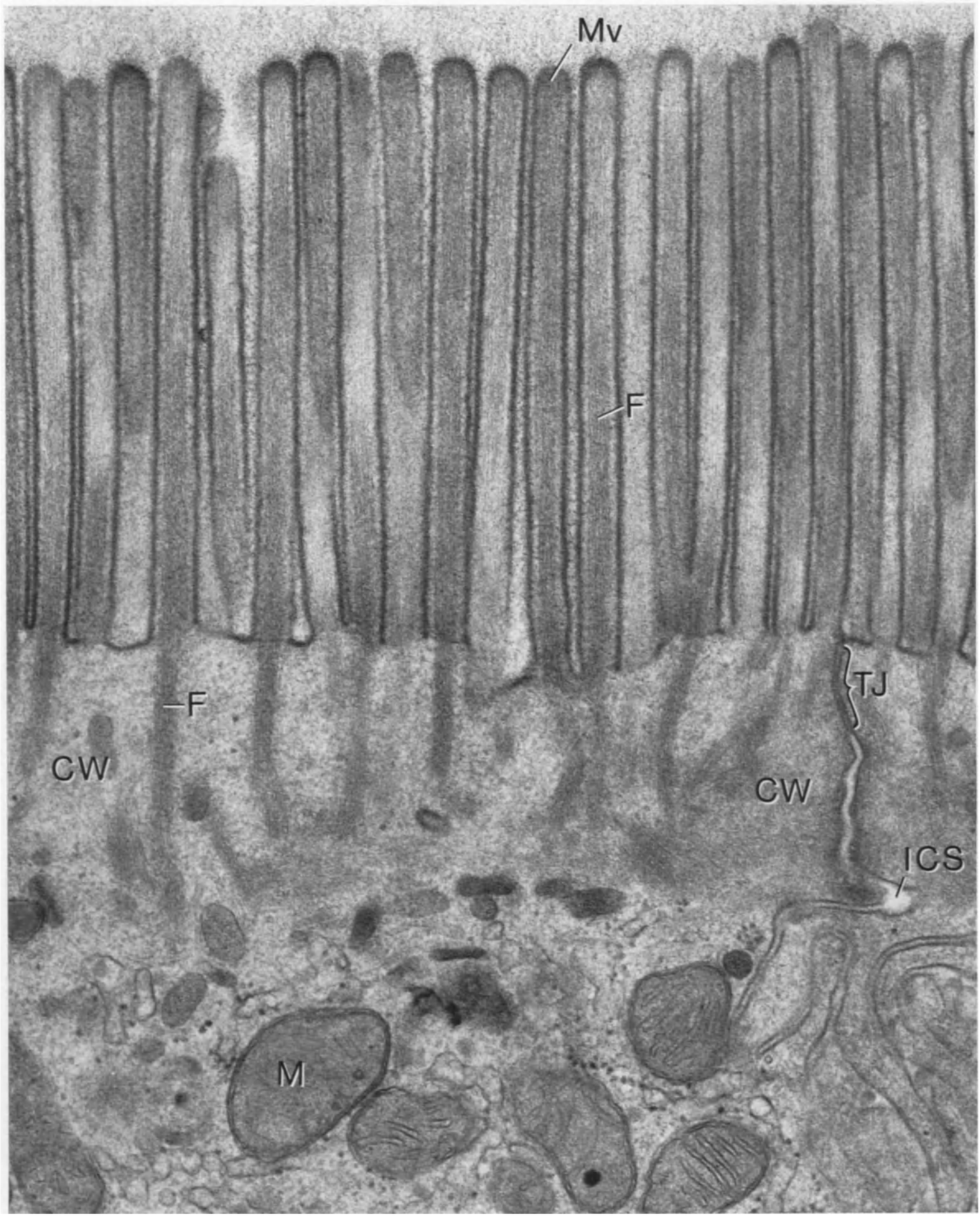
Mv
F
F
TJ
CW
CW
ICS
M

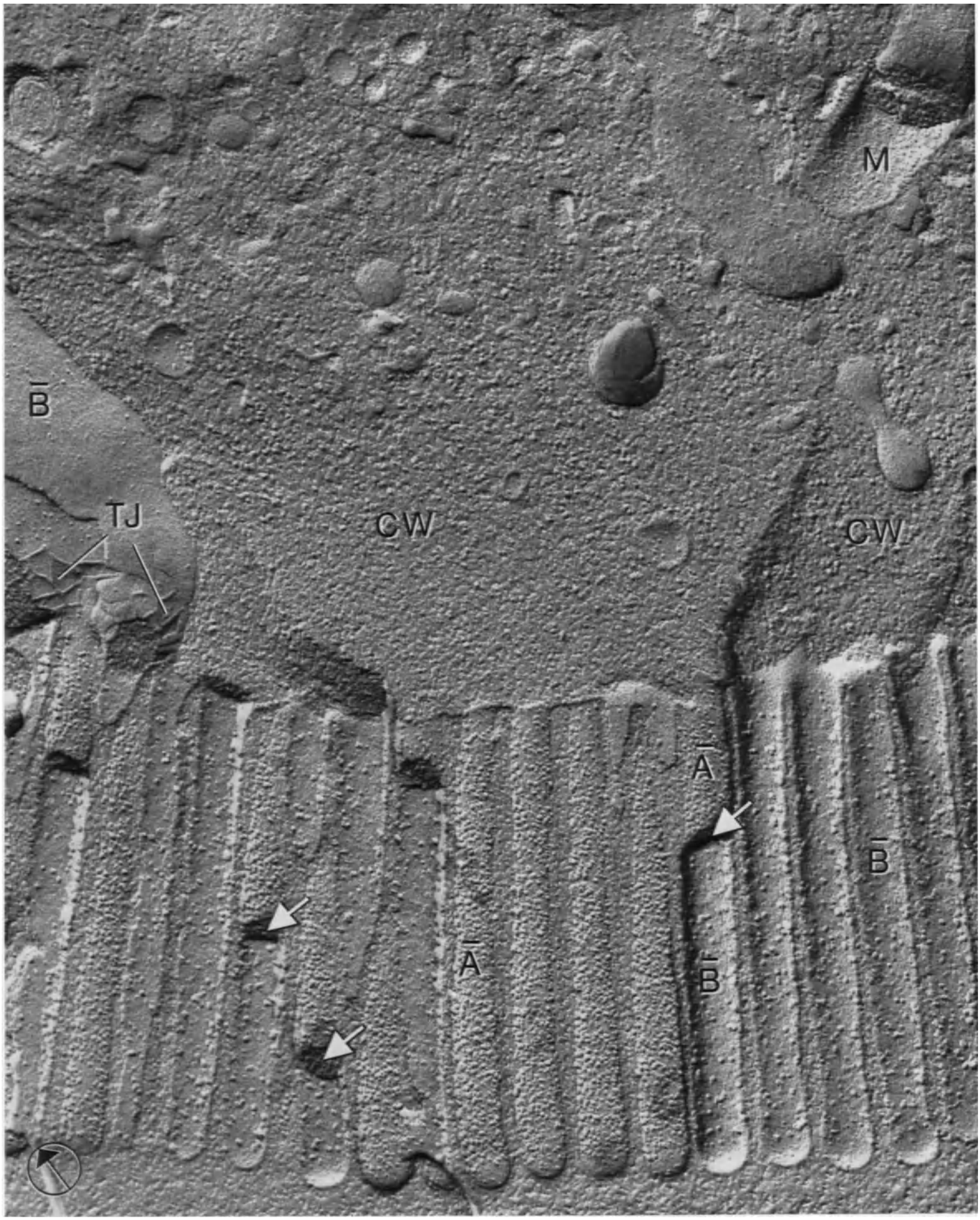
M
B
TJ
CW
CW
A
B
A
B
B

Plate 45 Intestinal Brush Border from the Chinese Hamster

The fine structure of the microvilli is presented here in cross section. Microvilli (Mv) appear as very regular profiles limited by a unit membrane (UM) and containing a central bundle of 10 to 20 thick filaments (F). The microvilli are themselves embedded in a dense cell coat (CC).

Magnification × 187,000

Plate 46 Intestinal Brush Border from the Mouse

This replica shows mainly face-views of the tips of the microvilli. These appear all convex, representing thus A-faces. The fact that this particular area of the membrane contains very few particles has already been noted in Plate 44.

Magnification × 101,000

Selected References

MAKITA, T., KHALESSI, A., GUTTMAN, F.M., SANDBORN, E.B.: The ultrastructure of small bowel epithelium during freezing. Cryobiol. **8**, 25–45 (1971).

MUKHERJEE, T.M., STAEHELIN, L.A.: The fine-structural organization of the brush border of intestinal epithelial cells. J. Cell Sci. **8**, 573–599 (1971).

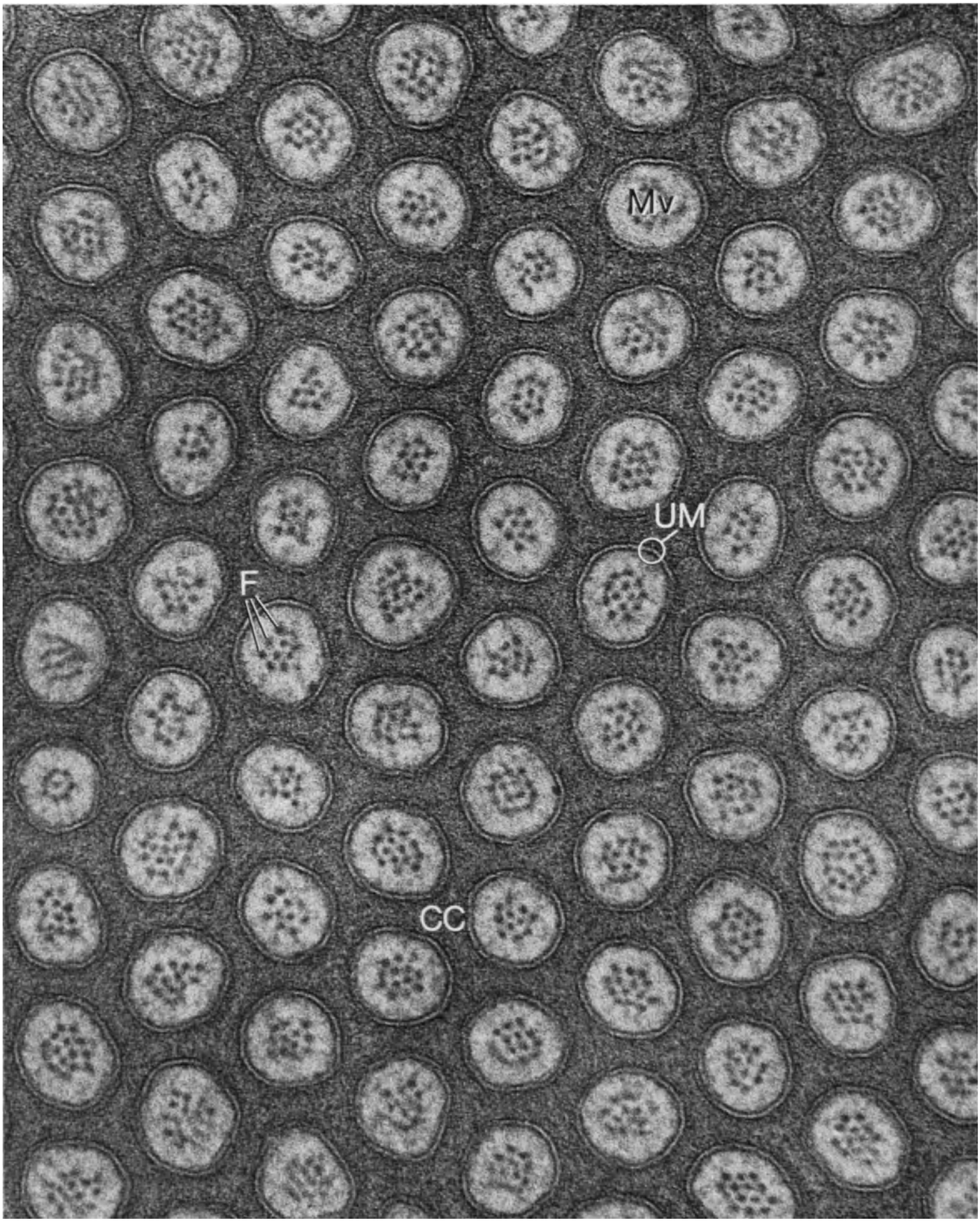
Mv
UM
F
CC

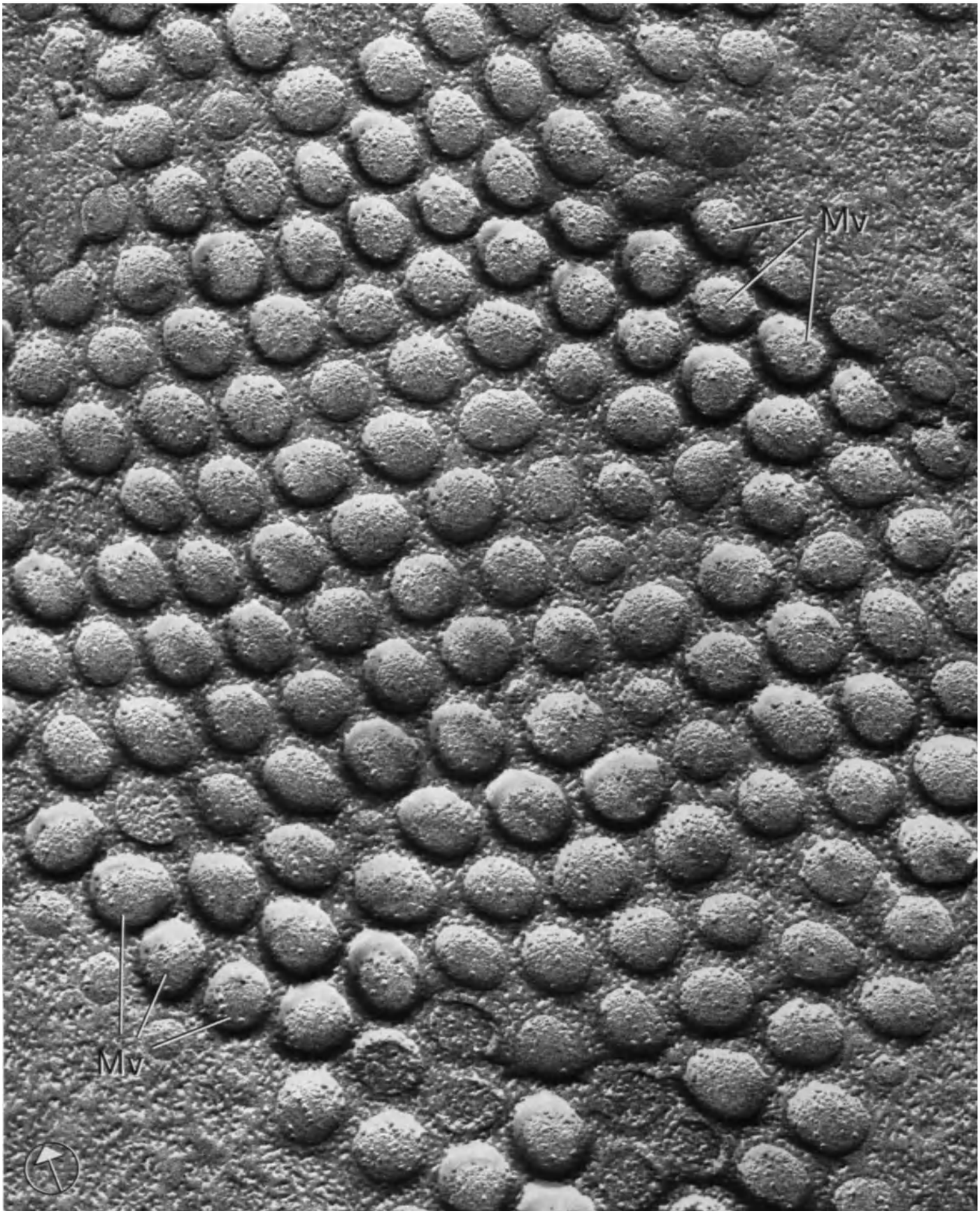
Mv
Mv

Plate 47 Goblet Cell from the Chinese Hamster Intestine

The apical pole of the goblet cell is packed with large polygonal mucous droplets (MD) around which the presence of a limiting membrane is dubious. The goblet cell is situated between two absorptive cells with brush borders (Mv).

Magnification × 40,000

Plate 48 Goblet Cell from the Human Intestine

Whereas the presence of a membrane around individual mucous droplets was not apparent in thin section, freeze-etching reveals both concave and convex fracture faces in the goblet cell cytoplasm. These correspond respectively to the A- and B-faces of the mucous droplet membrane. This membrane contains exceptionally few particles and reminds one of the aspect of myelin (see Plate 3). The droplet matrix (*) has a finely granular texture. Also seen is a part of the A-face of the goblet cell plasma membrane.

Magnification × 56,000

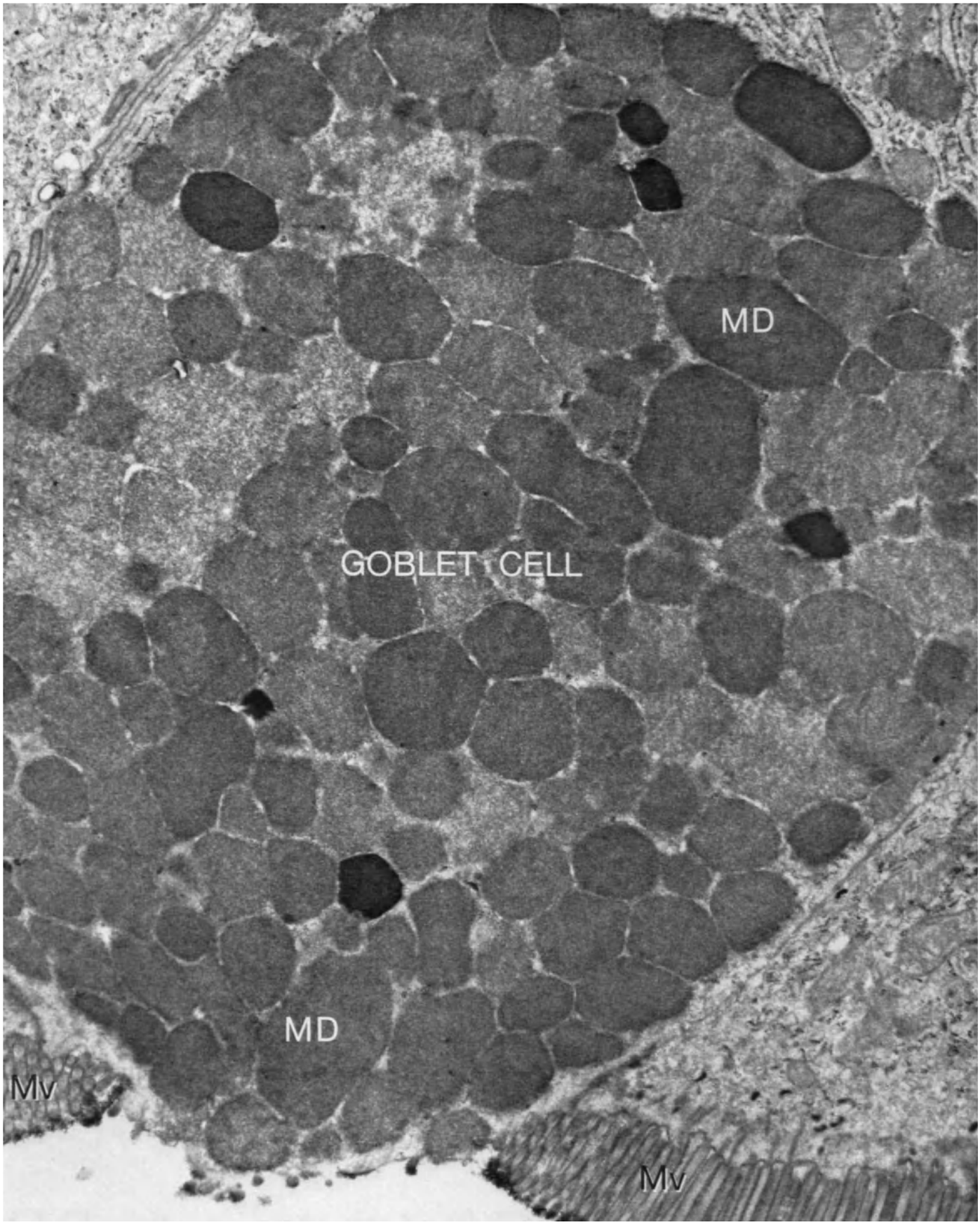

Plate 47

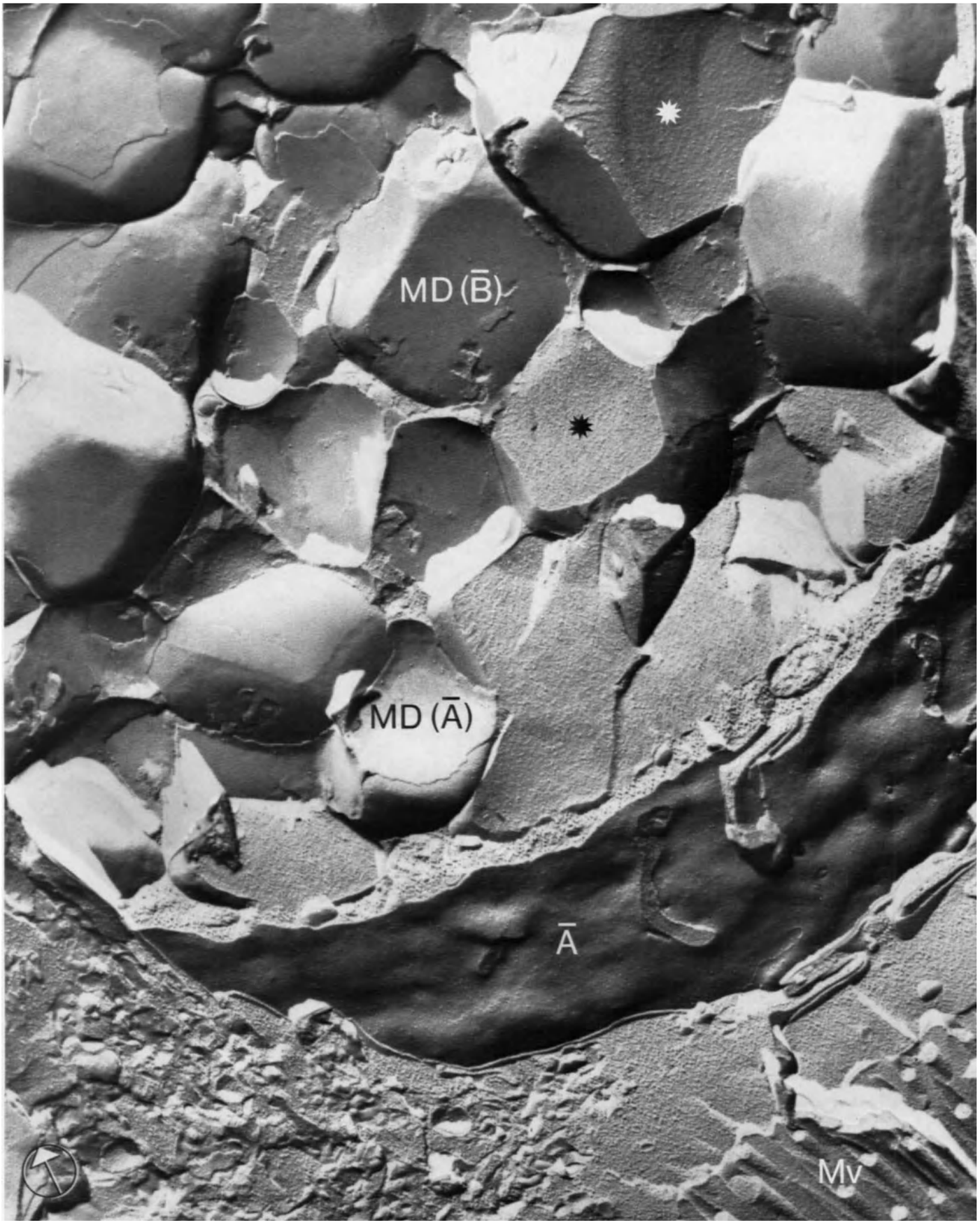
MD ($\bar{B}$)
MD ($\bar{A}$)
$\bar{A}$
Mv

Liver

Plate 49 Liver Cell of the Rat

In this section, one distinguishes many of the characteristic organelles of liver cells: cisternal elements of rough endoplasmic reticulum (RER), mitochondria (M), a microbody (Mb), Golgi complexes (G) in the vicinity of the bile canaliculus (BC) and deposits of glycogen (Gl).

Magnification $\times 20{,}000$

Plate 50 Liver Cell of the Rat

The identification of most organelles within the cell is fairly easy by freeze-etching, although in less detail than in a thin-section. For example, a small rounded organelle such as a microbody or a dense body cannot be identified unambiguously. The smooth, organelle-free areas are interpreted as glycogen deposits.

Magnification $\times 21{,}000$. From L. Orci *et al.* J. Ultrastruct. Res. **35**, 1–19 (1971).

Selected Reference

Orci, L., Matter, A., Rouiller, Ch.: A comparative study of freeze-etch replicas and thin sections of rat liver. J. Ultrastruct. Res. **35**, 1–19 (1971).

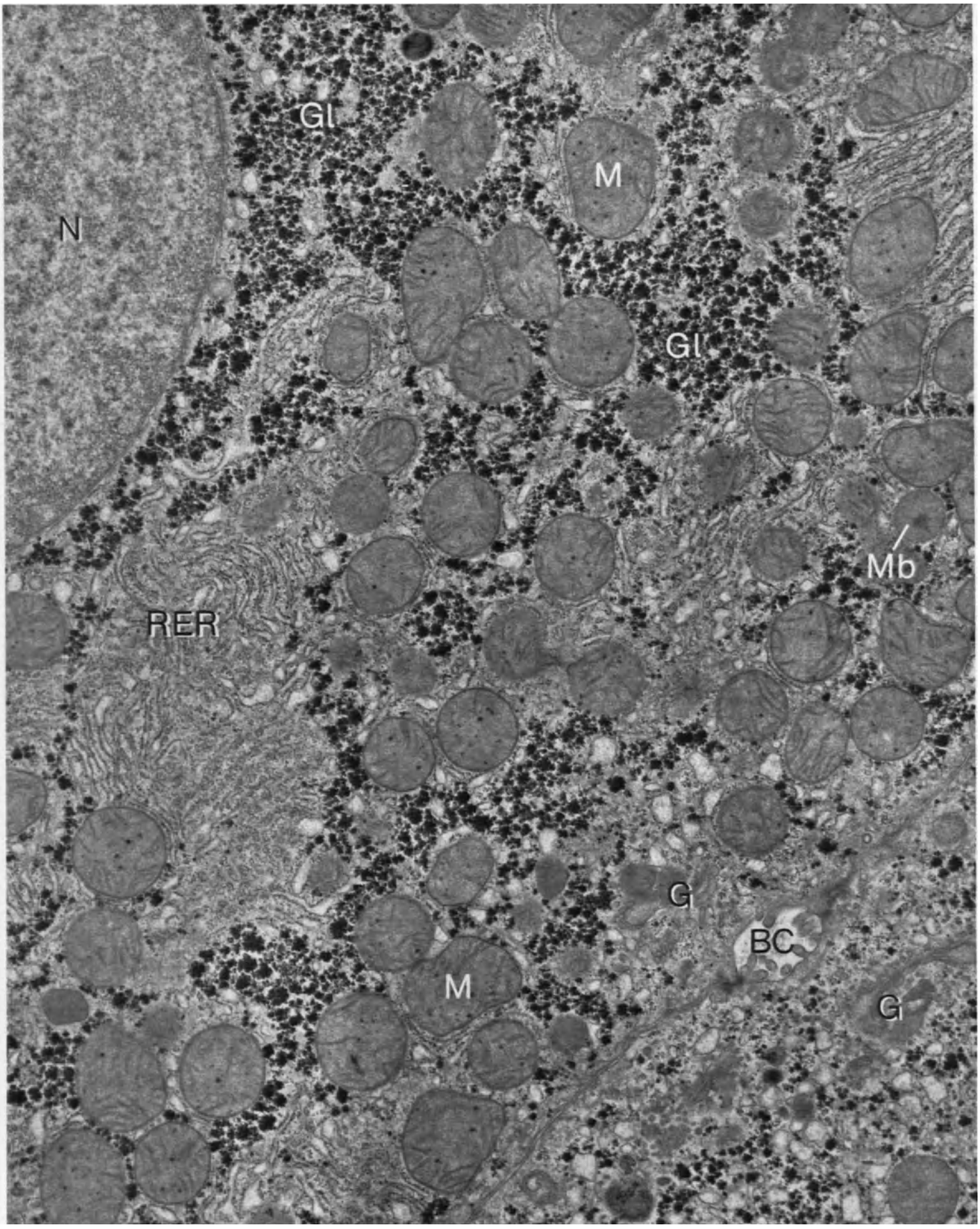
Gl
M
N
Gl
Mb
RER
G
BC
M
G

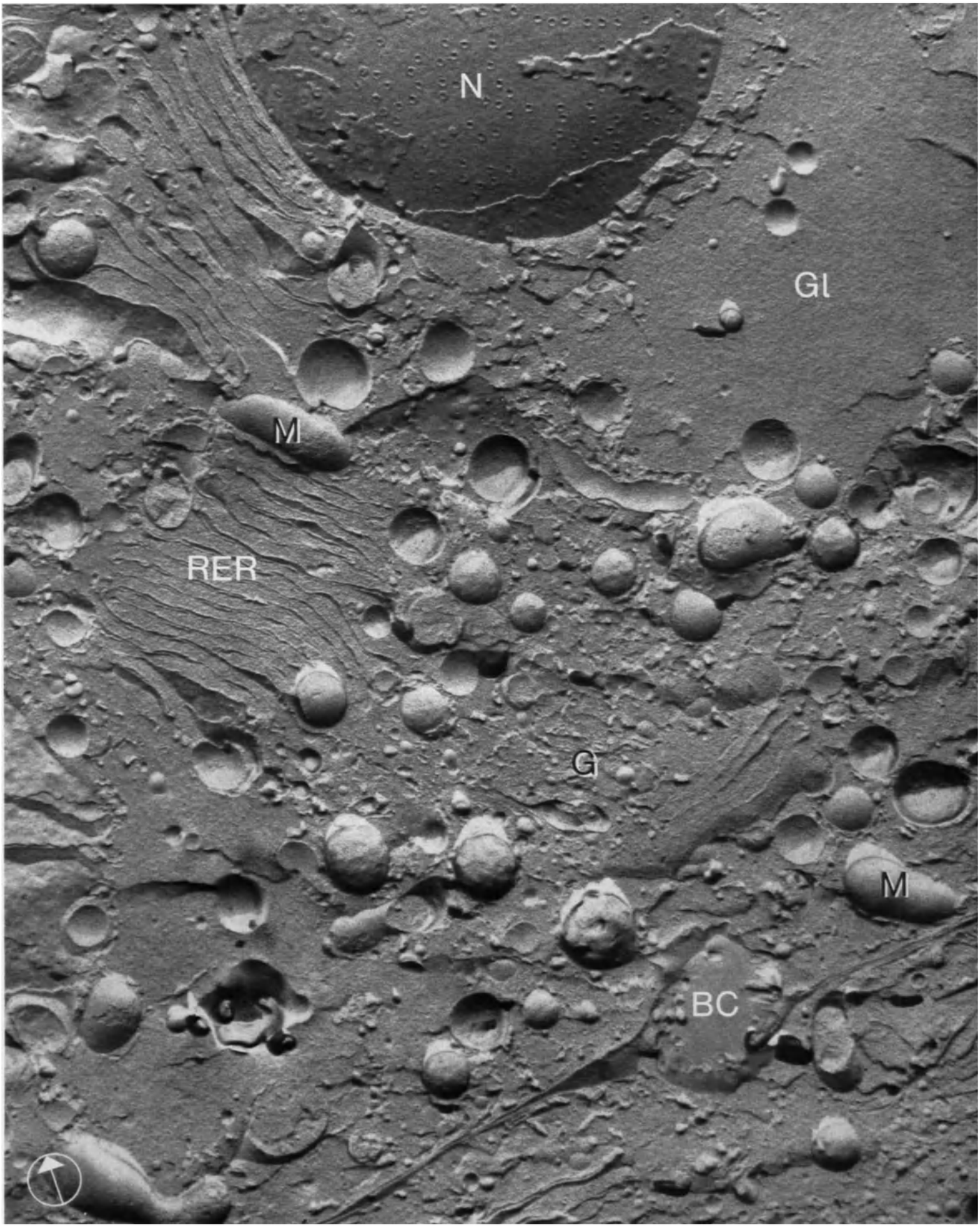
N
Gl
M
RER
G
M
BC

Plate 51 Endothelium of the Liver Sinusoids of the Rat

A tangential section through an endothelial cell reveals the presence of endothelial pores (EP) reaching variable sizes (see Plate 9). Endocytotic vesicles (EV), which are numerous in this cell type, can be differentiated from the pores by their thick coat lining. Short microvilli (Mv) of the hepatocytes are seen in the space of Disse (D).

Magnification × 37,000

Plate 52 Endothelium of the Liver Sinusoids of the Rat

In the A-face of the endothelial plasma membrane, one can distinguish the large and irregular depressions corresponding to the pores (EP) and the small circular pits (P) representing endocytotic events. Pores are clustered in discrete regions of the cell membrane. For comparison of the different types of endothelial pores, see Plates 5 to 9.

Magnification × 66,000

Plate 51


EP
CYTOPLASM
Ā
EP
Ā
ICS
P

Plate 53 Capillary Loop from the Rat Renal Corpuscle

The filtration barrier in the renal corpuscle is constituted by three characteristic elements, namely the fenestrated endothelium (EC), the basal lamina (BL) and the foot processes (FP) of the podocytes. Endothelial pores (EP) appear here mainly in face-view.

Magnification ×27,000

Plate 54 Capillary Loop from the Rat Renal Corpuscle

The three elements described in Plate 53 are easily recognizable in the freeze-etch replica. The plasma membrane (A-face) of the podocyte has been largely exposed and shows several endocytotic pits (P).

Magnification ×32,000

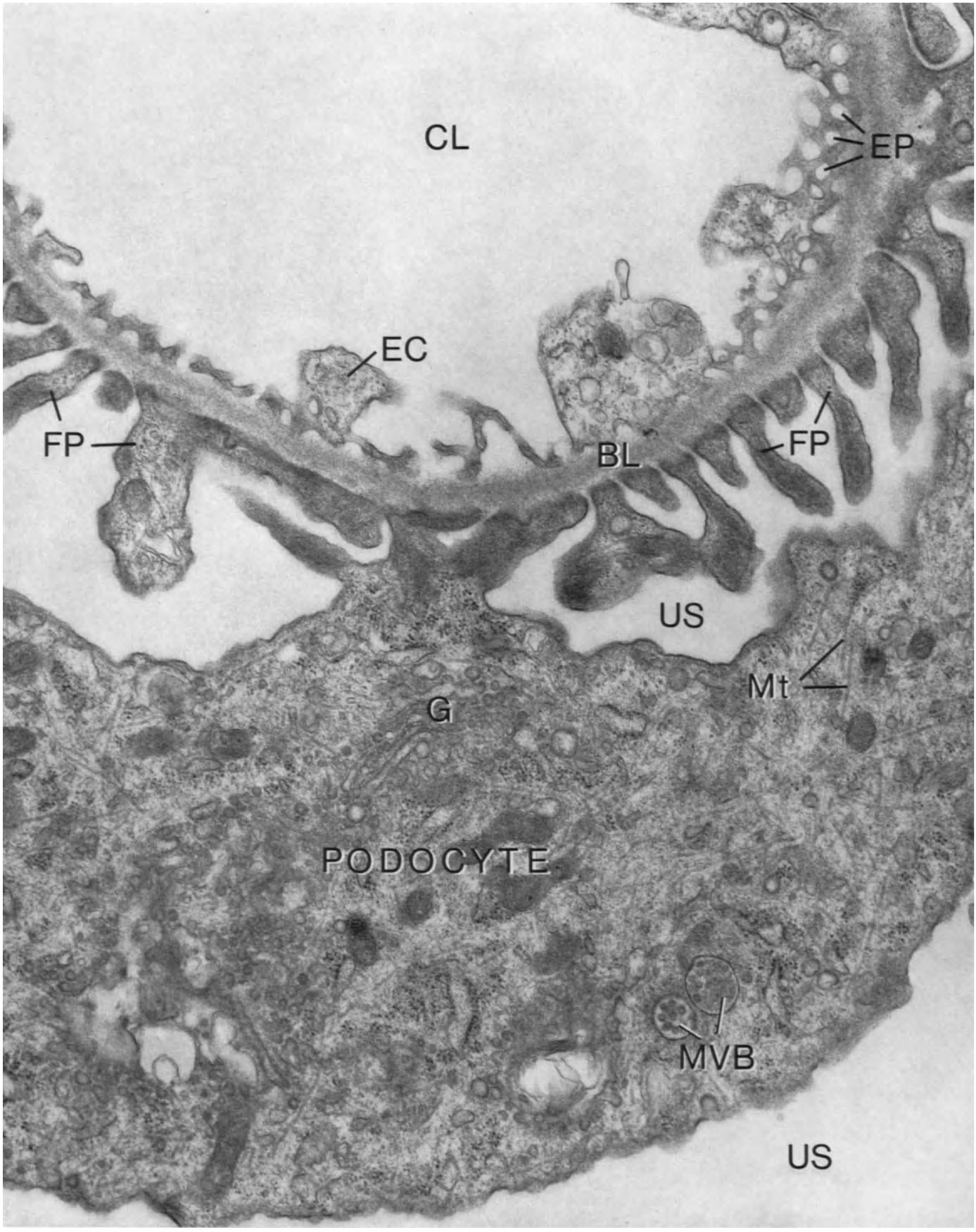
CL
EP
EC
FP
FP
BL
US
Mt
G
PODOCYTE
MVB
US


CL
EC
BL
US
FP
Ā
Ā
P
US

Plate 55 Capillary Loop from the Rat Renal Corpuscle

The fenestrated endothelium is shown here in greater detail. The observer is situated in the capillary lumen, the cell cytoplasm has been removed and accordingly the membrane face exposed is the endothelial B-face. The fairly large pores in the membrane thus appear as rims (see Plate 8). The granular texture of the basal lamina (BL) is particularly accentuated in the central region known in conventional electron microscopy as lamina densa. Between two foot processes (FP) one can see a tiny ridge (→) which could correspond to the slit membrane.

Magnification × 75,000

Plate 56 Foot Processes of the Podocyte (Rat Renal Corpuscle)

The fracture plane has exposed largely the foot processes (FP) B-face. The intermingled fracture faces form a continuous sheet interrupted only by the regular spaces of the urinary slit (*). The circular elevations (EV) visible on the B-faces represent the bulging membrane of endocytotic vesicles seen from the inside of the cell. From the outside of the foot processes, that is, in the A-face, such endocytotic events would appear as pits (see Plate 10).

Magnification × 63,000

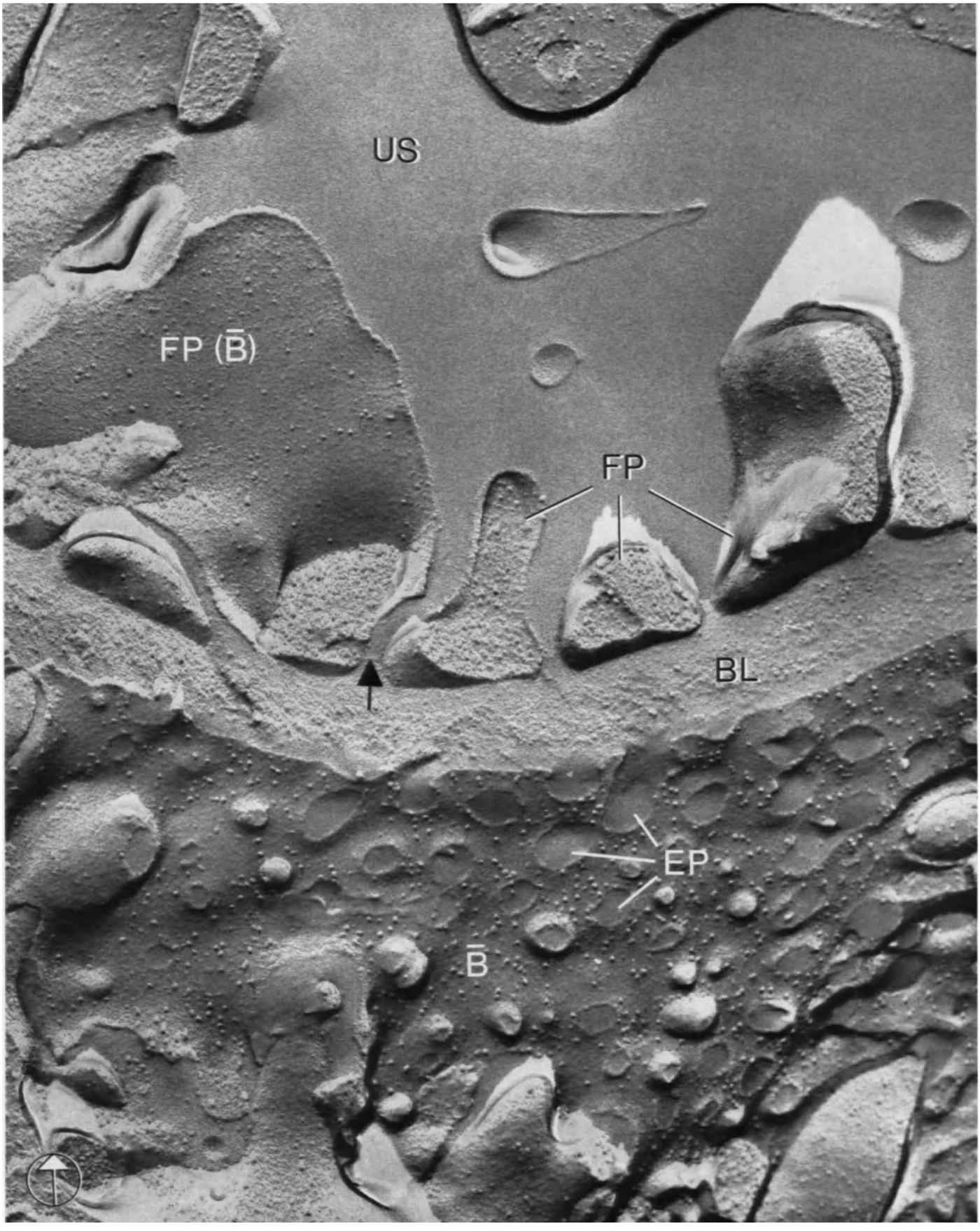

Plate 55

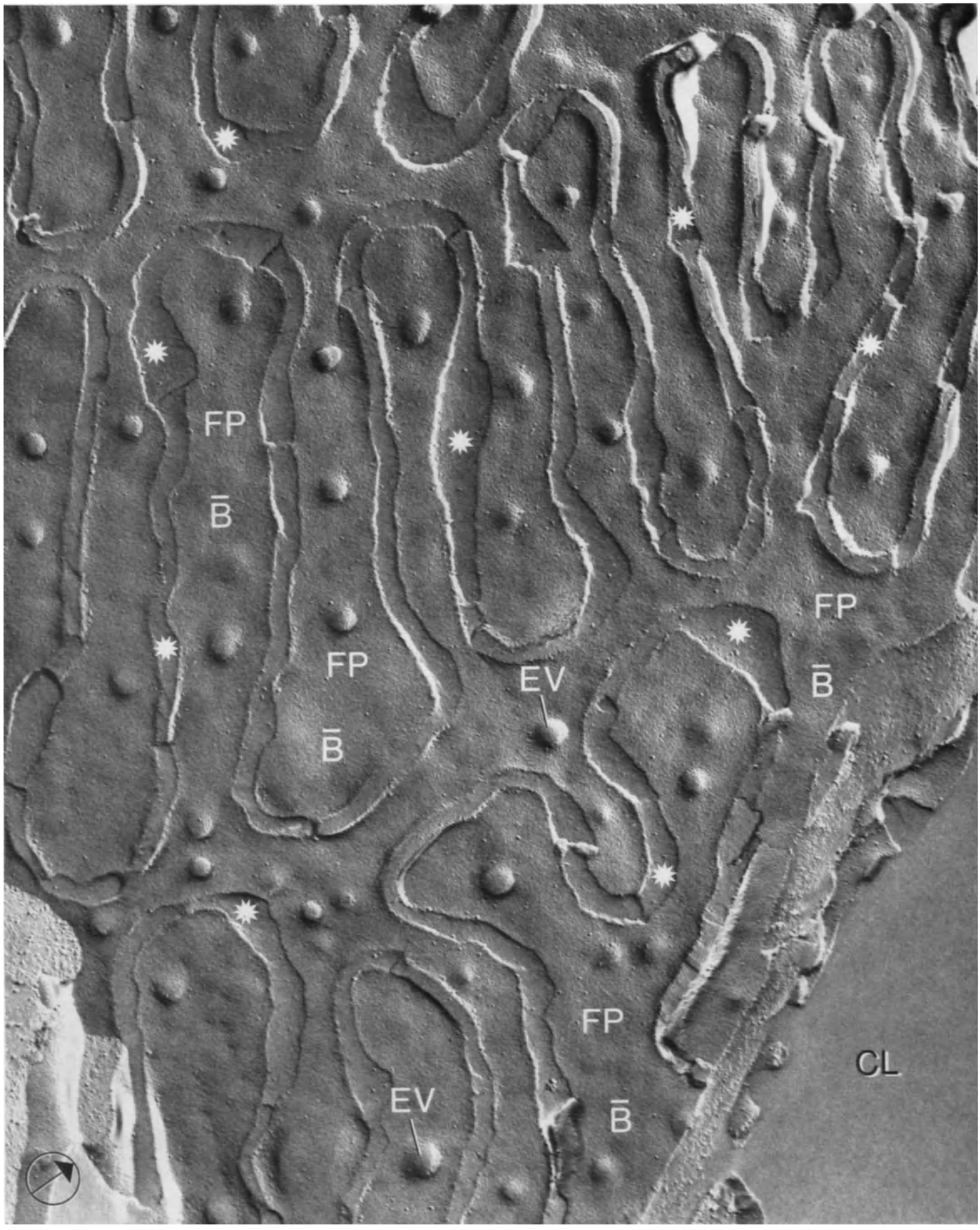
FP
B̄
FP
B̄
EV
FP
B̄
FP
EV
B̄
CL

Plate 57 Proximal Tubule of the Rat Kidney

The cells of the proximal tubule have a well-developed brush border. The basal pole is indented by a few infoldings (BI) underlined by a thick basal lamina (BL). The tissue was stained with Alcian blue seen here as a dense material in the intercellular space (ICS).

Magnification $\times 21{,}000$

Plate 58 Proximal Tubule of the Rat Kidney

In a replica of the tubular epithelium, one recognizes easily the microvillar profiles of the brush border. The cytoplasm of the epithelial cells contains numerous membrane faces belonging to cellular organelles, as well as a part of the nuclear envelope (N). The lateral plasma membrane and the membrane at the base of the cells have also been exposed.

Magnification $\times 18{,}000$

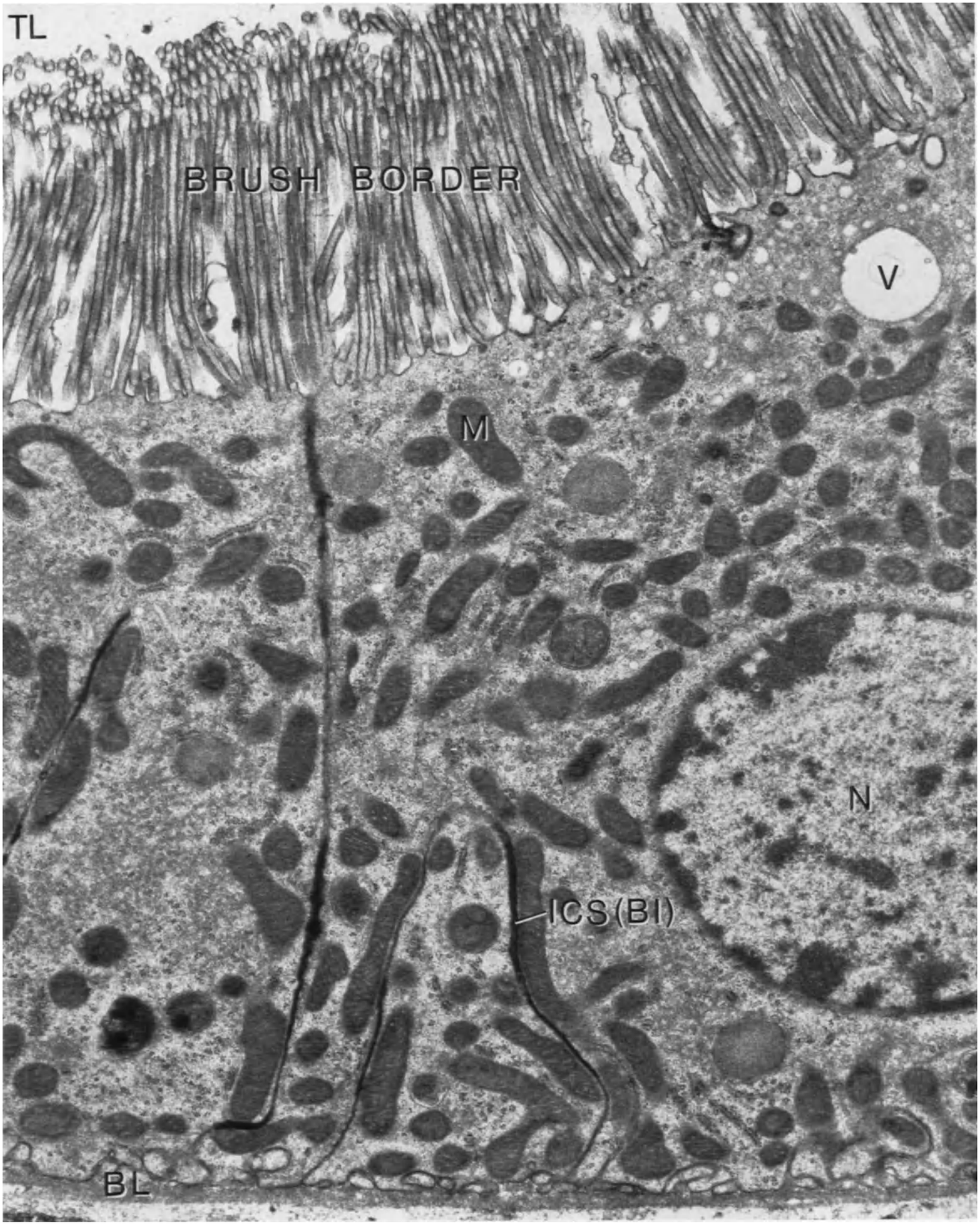
TL
BRUSH BORDER
V
M
N
ICS(BI)
BL

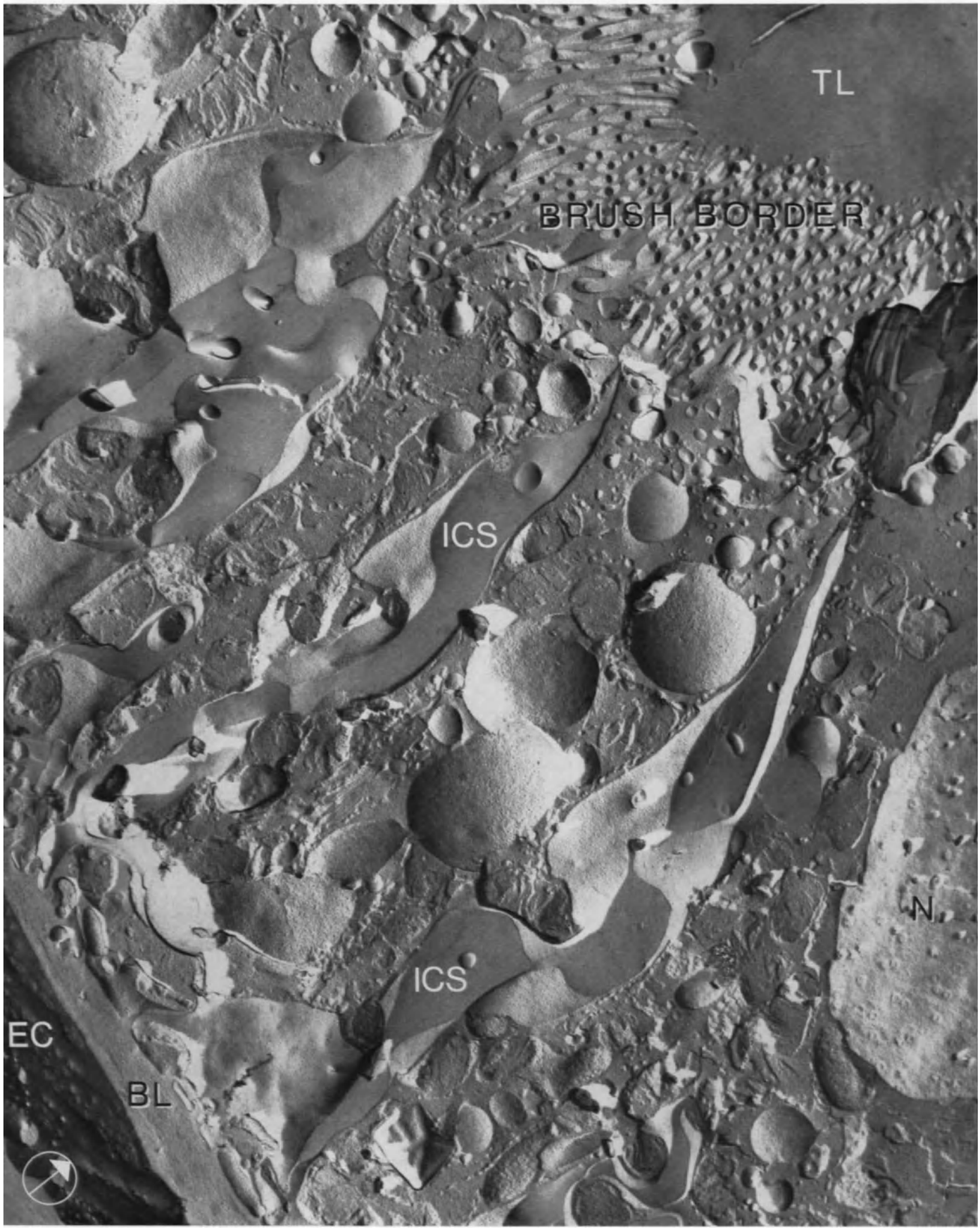

Plate 58

Plate 59 Distal Tubule of the Rat Kidney

In contrast with the cells of the proximal tubule, those of the distal tubule have only short and plump microvilli (none of them are seen in this picture), but very deep infoldings (BI) of the membrane at the basal pole. These infoldings delimit cytoplasmic compartments which contain large mitochondria (M) (see also Plates 13–14).

Magnification × 48,000

Plate 60 Distal Tubule of the Rat Kidney

The cytoplasm and also large areas of the luminal and lateral plasma membranes of tubular cells have been exposed. The faces of the plasma membrane are either richly particulated A-faces or smoother B-faces. Notice the short and plump microvillar profiles (Mv), as well as the narrowing of the intercellular space at the level of the tight junctions (TJ). The cytoplasm between the infoldings contains cross-fractured profiles of mitochondria (M).

Magnification × 33,000

Selected References

CLAUDE, P., GOODENOUGH, D.A.: Fracture faces of zonulae occludentes from "tight" and "leaky" epithelia. J. Cell Biol. **58**, 390–400 (1973).

FRIEDERICI, H.H.R.: The surface structure of some renal cell membranes. Lab. Invest. **21**, 459–471 (1969).

PRICAM, C., HUMBERT, F., PERRELET, A., ORCI, L.: A freeze-etch study of the tight junctions of the rat kidney tubules. Lab. Invest. **30**, 286–291 (1974).


TL
TJ
M
BI
BI
M
BI
BL


TJ
B
A
M
A
Mv
TJ
M
TL
ICS
A
A

Trachea

Plate 61 Tracheal Epithelium of the Rat

Most epithelial cells lining the trachea are provided at their apical pole with motile cilia (kinocilia). Each cilium originates from a basal body (BB) which can be seen here as a dense ring-like structure in the apical cytoplasm. Cilia (Ki) extend in the tracheal lumen and each displays the characteristic 9+1 microtubular doublets. Slender microvilli (Mv) are present in between cilia. Notice the dense boundary limits between the epithelial cells at the level at which one can find tight junctions (TJ). Tracheal epithelium contains also goblet cells.

Magnification × 15,000

Plate 62 Tracheal Epithelium of the Rat

The area of the tracheal epithelium is comparable to that seen in Plate 61. The membrane limiting the cilia (Ki) has been exposed at several places and numerous tight junctional grooves (TJ) can be seen in the B-face of the lateral plasma membrane of the ciliated cells.

Magnification × 24,000

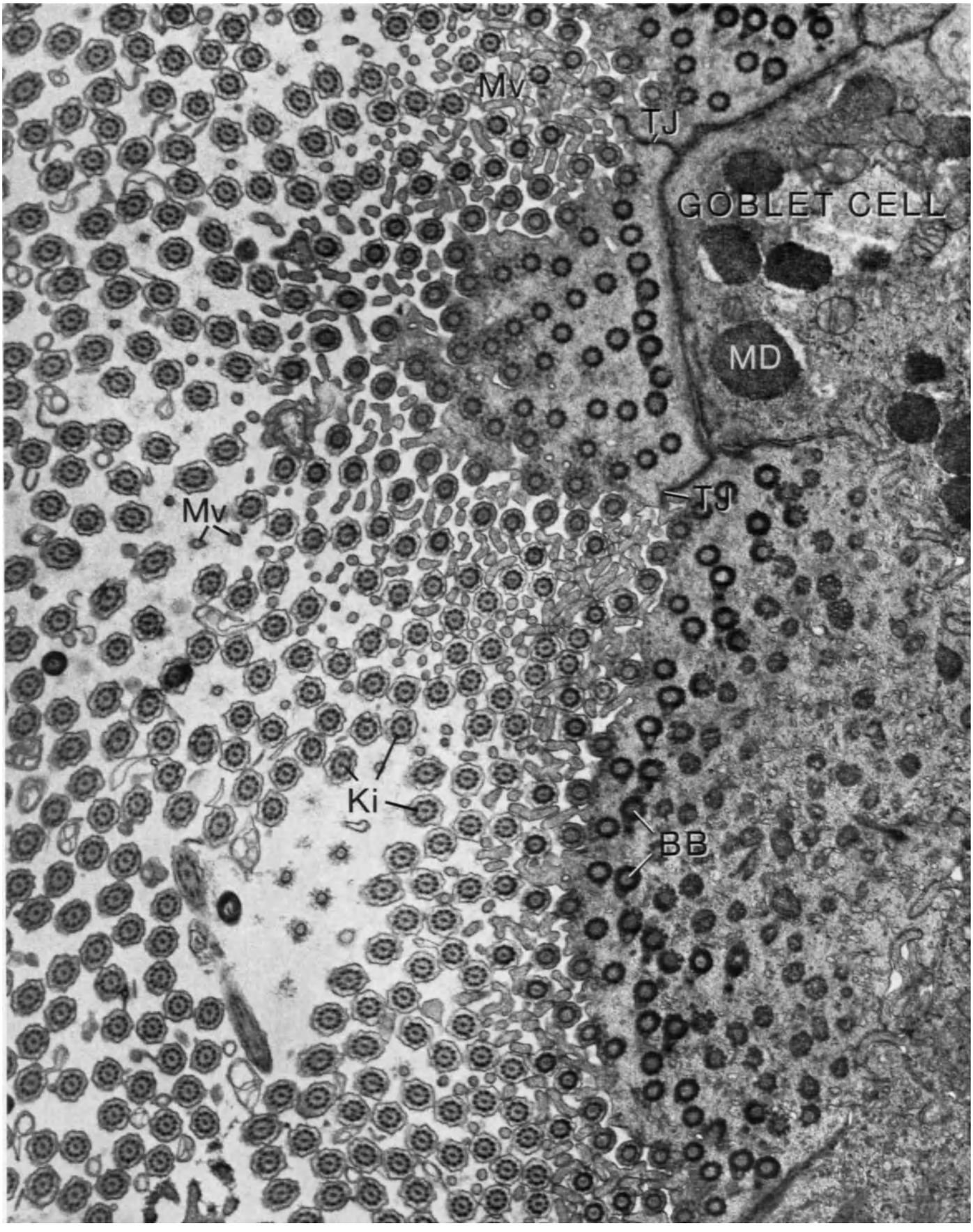

Plate 61


Cy
Ki
Mv
TJ
Ki
Cy

Plate 63 Kinocilia from the Tracheal Epithelium of the Rat

In a longitudinal orientation, one distinguishes clearly the continuity of the ciliary membrane with the apical membrane of the epithelial cell. The basal body (BB) present at the base of each cilium, as well as the microtubular apparatus (Mt) extending into the cilium core, can also be seen.

Magnification $\times 98{,}000$

Plate 64 Kinocilia from the Tracheal Epithelium of the Rat

A peculiar differentiation of the ciliary membrane is demonstrated by freeze-etching. This differentiation consists of several strands of membrane-associated particles (→), visible on both fracture faces, and which are found exclusively at the base of the kinocilium. Convex faces of the ciliary membrane are A-faces, concave ones, B-faces (see Plates 15 and 44). In contrast to the membrane of brush border microvilli, the ciliary membrane has very few particles.

Magnification $\times 89{,}000$

Selected Reference

GILULA, N.B., SATIR, P.: The ciliary necklace. A ciliary membrane specialization. J. Cell Biol. **53**, 494–509 (1972).

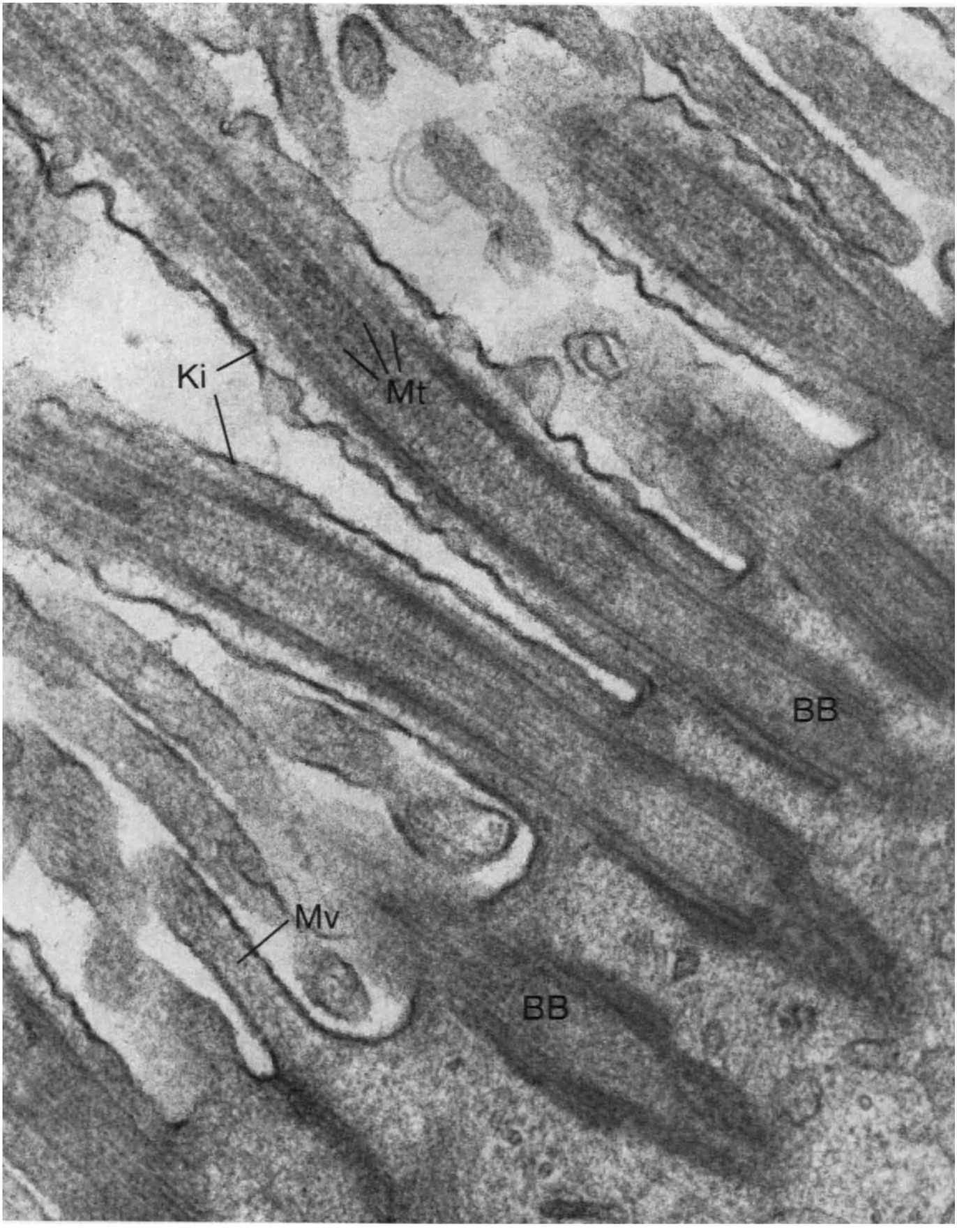
Ki
Mt
BB
Mv
BB

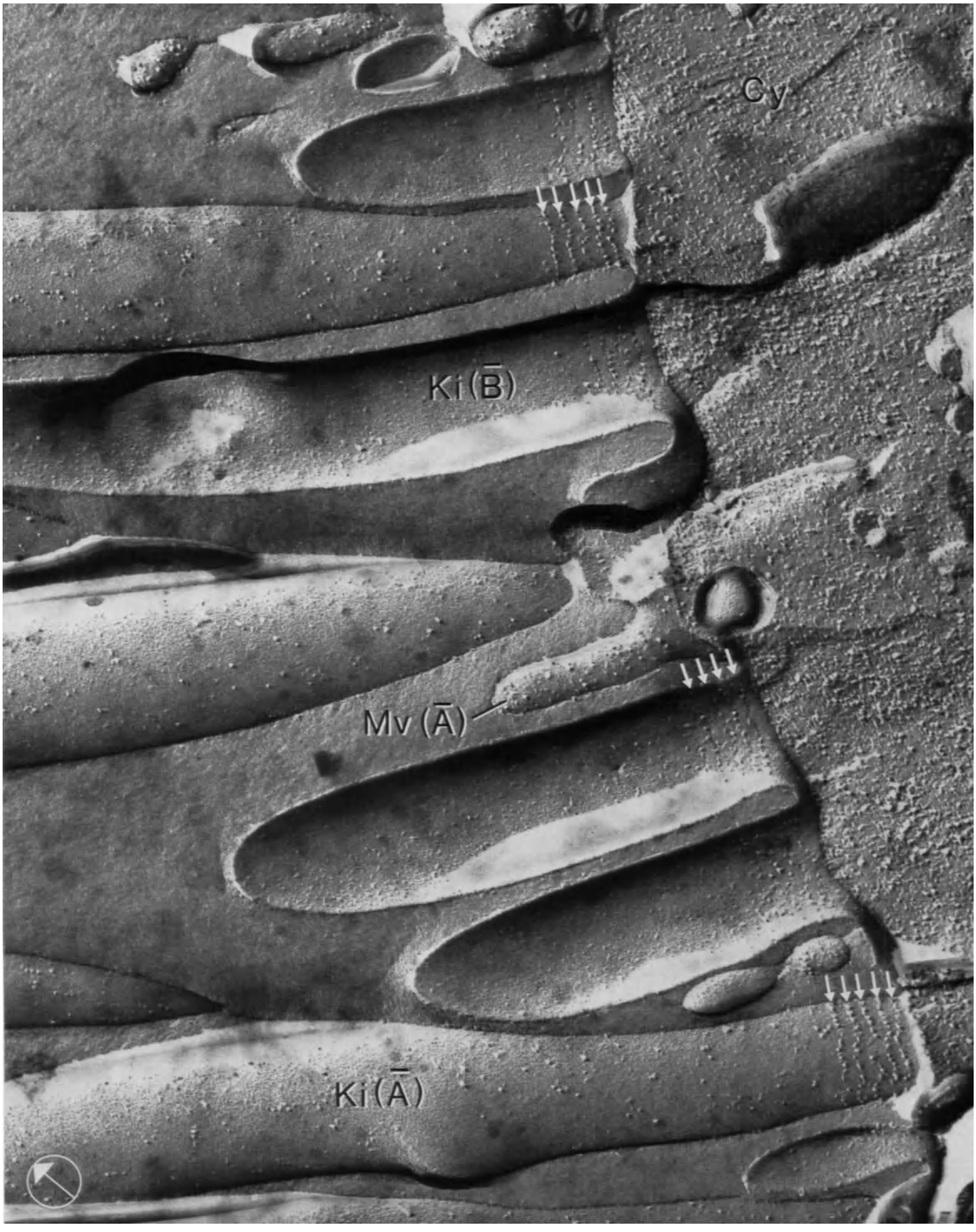

Plate 64

Lung

Plate 65 Alveolar Lining of the Rat Lung

The alveolar lining is formed by flattened and cuboidal cells resting on a basal lamina (BL). The cuboidal cells, one of which is illustrated here, are also called the great alveolar cells or type II pneumocytes. Their free surface is provided with short microvilli (Mv) and their cytoplasm contains characteristic multilamellar bodies (LB). Multilamellar bodies are released from the cell and spread over the alveolar surface, acting there as surfactant.

Magnification $\times 21{,}000$

Plate 66 Alveolar Lining of the Rat Lung

The fracture has exposed the great alveolar cell cytoplasm and one can see that the lamellar bodies have been split in a very characteristic way. The fracture plane followed successive layers (much as it does in the case of myelin) which are visible as smooth faces separated by steps of various heights. This appearance, due to the high content in phospholipids of the multilamellar bodies, allows one to differentiate them clearly from the other cytoplasmic organelles.

Magnification $\times 32{,}000$

Selected References

Belton, J.C., Branton, D., Thomas, H.V., Mueller, P.K.: Freeze-etch observations of rat lung. Anat. Rec. **170**, 471–484 (1971).

Smith, D.S., Smith, U., Ryan, J.W.: Freeze-fractured lamellar body membranes of the rat lung great alveolar cell. Tissue and Cell **4**, 457–468 (1972).

Untersee, P., Gil, J., Weibel, E.R.: Visualization of extracellular lining layer of lung alveoli by freeze-etching. Respiration Physiol. **13**, 171–185 (1971).

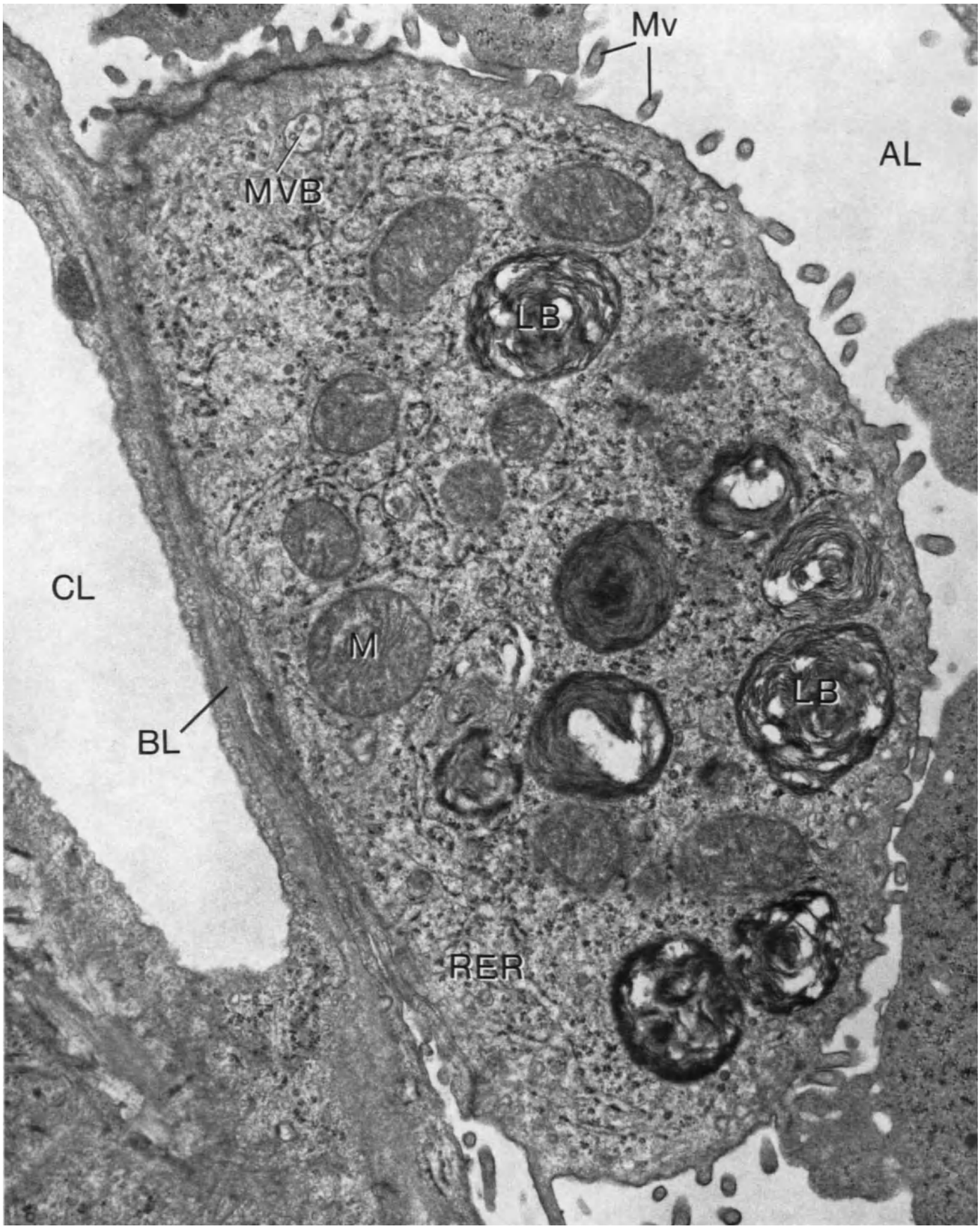

Plate 65

Plate 66

Muscle

Plate 67 Cardiac Muscle from the Mouse

The cardiac muscle is a striated muscle particularly rich in mitochondria (M). These occur in clusters between areas occupied by the myofibrils (Mf) (cross-sectioned). This muscle is also richly vascularised and one capillary is illustrated here (CL). Its wall is formed by attenuated endothelial cells (EC) which show an intense endocytotic activity (→), especially on the side facing the muscle cells. Endocytotic activity can also be seen at the surface of the muscle cells.

Magnification ×21,000

Plate 68 Cardiac Muscle from the Rat

Well emphasized here are the endocytotic pits (P) present in the A-face of the endothelial cell (EC). In the muscle cell, mitochondrial profiles (M), as well as myofibrils (Mf) can be recognized. Cross fractured myofibrils appear as tiny dots standing on a smooth fracture face. The large membrane face exposed above the capillary is the A-face of a muscle cell with a few endocytotic pits (P).

Magnification ×21,000

Selected Reference

LEAK, L.V.: Frozen-fractured images of blood capillaries in heart tissue. J. Ultrastruct. Res. **35**, 127–146 (1971).

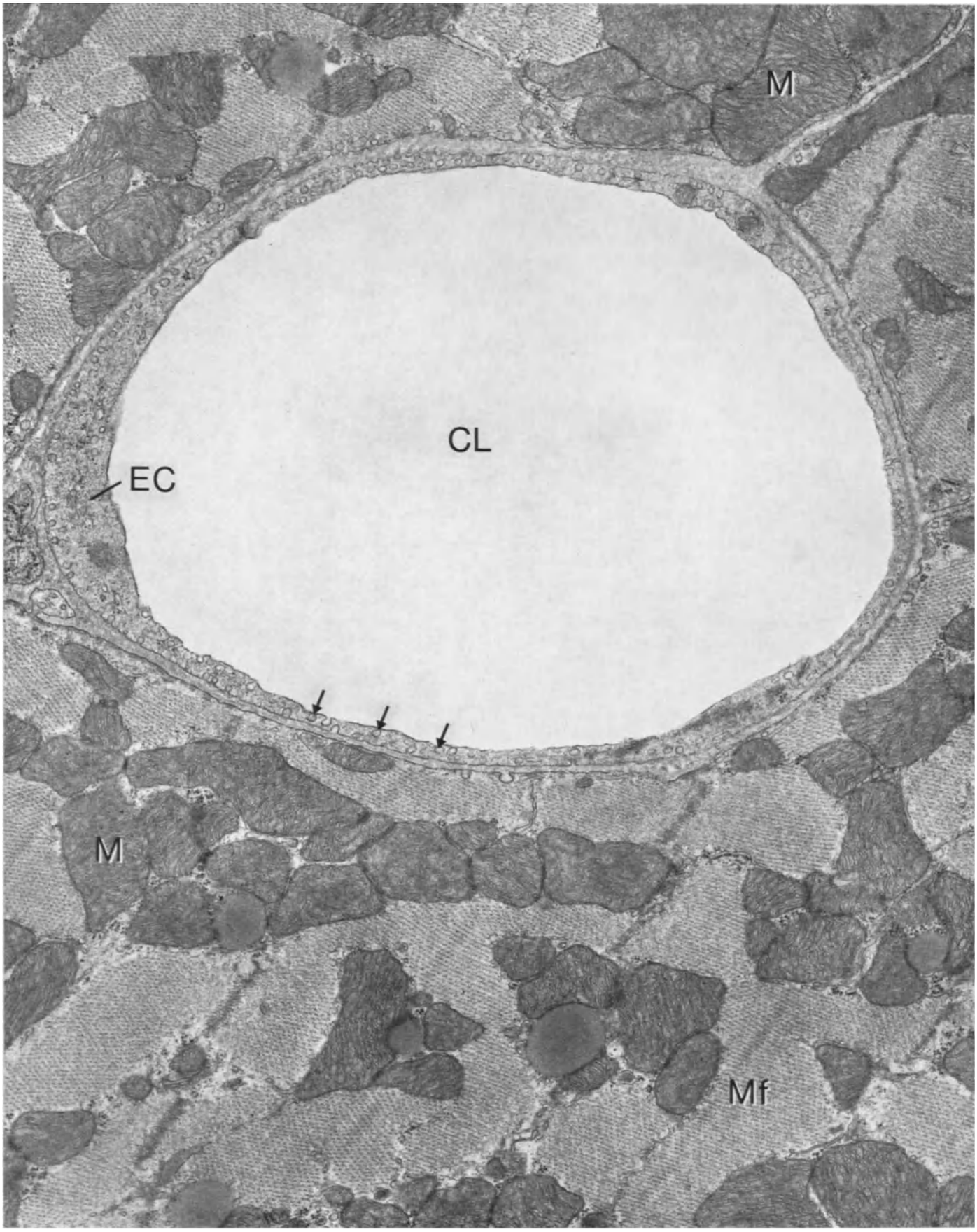
M
CL
EC
M
Mf

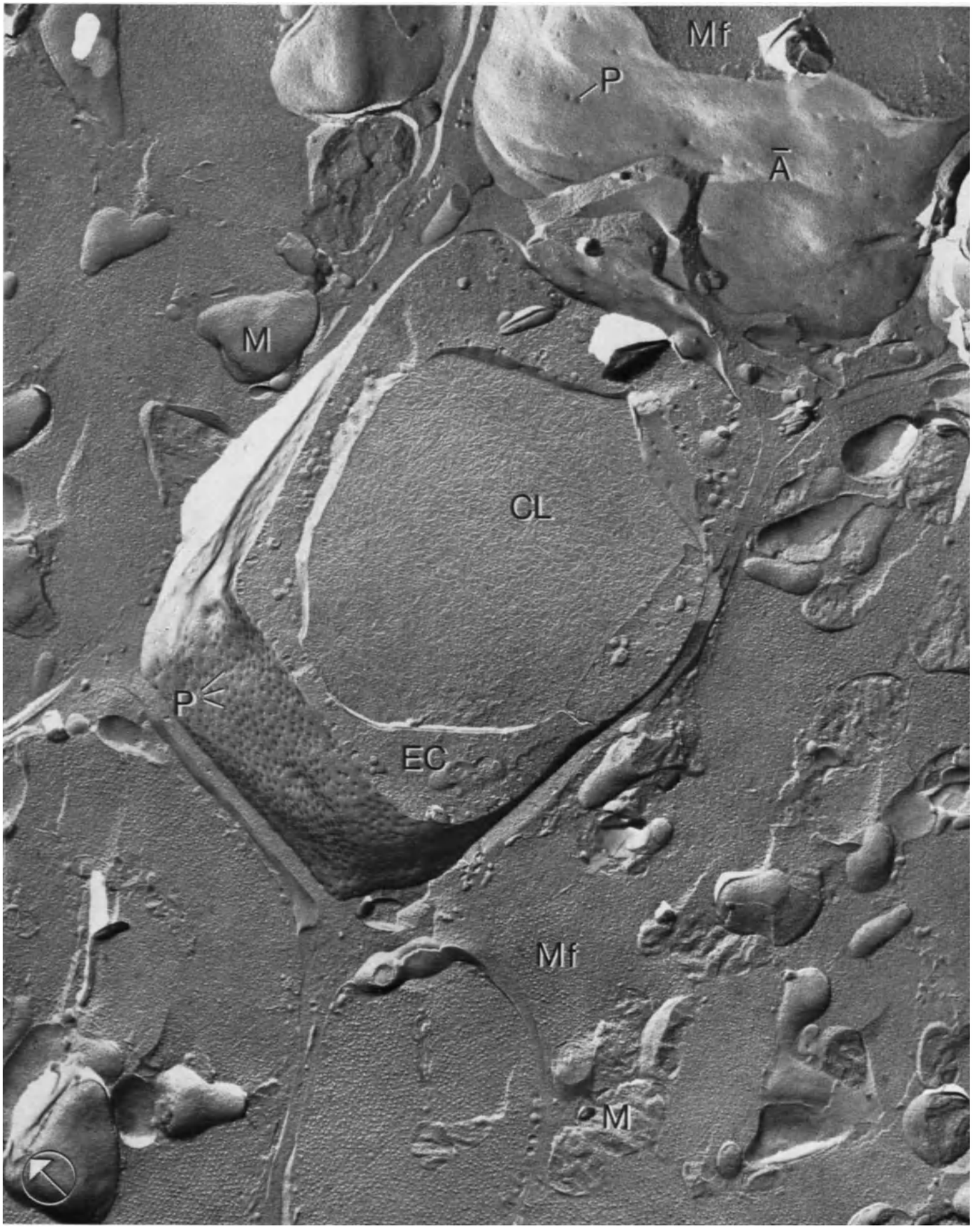
Mf
P
Ā
M
CL
P
EC
Mf
M

Plate 69 Cardiac Muscle from the Rat

The banding pattern of the sarcomeres is seen distinctly in a longitudinal section of the muscle cell. Between sarcomeres, mitochondria (M), and deposits of glycogen (Gl) are also conspicuous. At the level of the dense Z-bands, notice elements of the "dyad" (→).
Z = Z-band; A = A-band; I = I-band; H = H-band.

Magnification × 31,000

Plate 70 Cardiac Muscle from the Rat

In longitudinal orientation, myofibrils impart a definite periodicity to the fracture face of the sarcoplasm. Along the path of the myofibrils, there is a surface granularity which is locally increased at the level of the Z-bands. Granularity might represent extremities or branchings of myofibrils exposed by the fracturing process. Fracture faces from mitochondria (M) and "dyads" (→) can also be recognized.

Magnification × 36,000

Selected References

BULLIVANT, S., RAYNS, D.G., BERTAUD, W.S., CHALCROFT, J.P., GRAYSTON, G.F.: Freeze-fractured myosin filaments. J. Cell Biol. **55**, 520–524 (1972).

RAYNS, D.G.: Myofilaments and cross bridges as demonstrated by freeze-fracturing and etching. J. Ultrastruct. Res. **40**, 103–121 (1972).

WILLISON, J.H.M., COCKING, E.C., LAWRIE, R.A.: Some observations on the filaments of frozen-etched striated muscle. J. Microsc. (Lond.) **95**, 511–518 (1972).

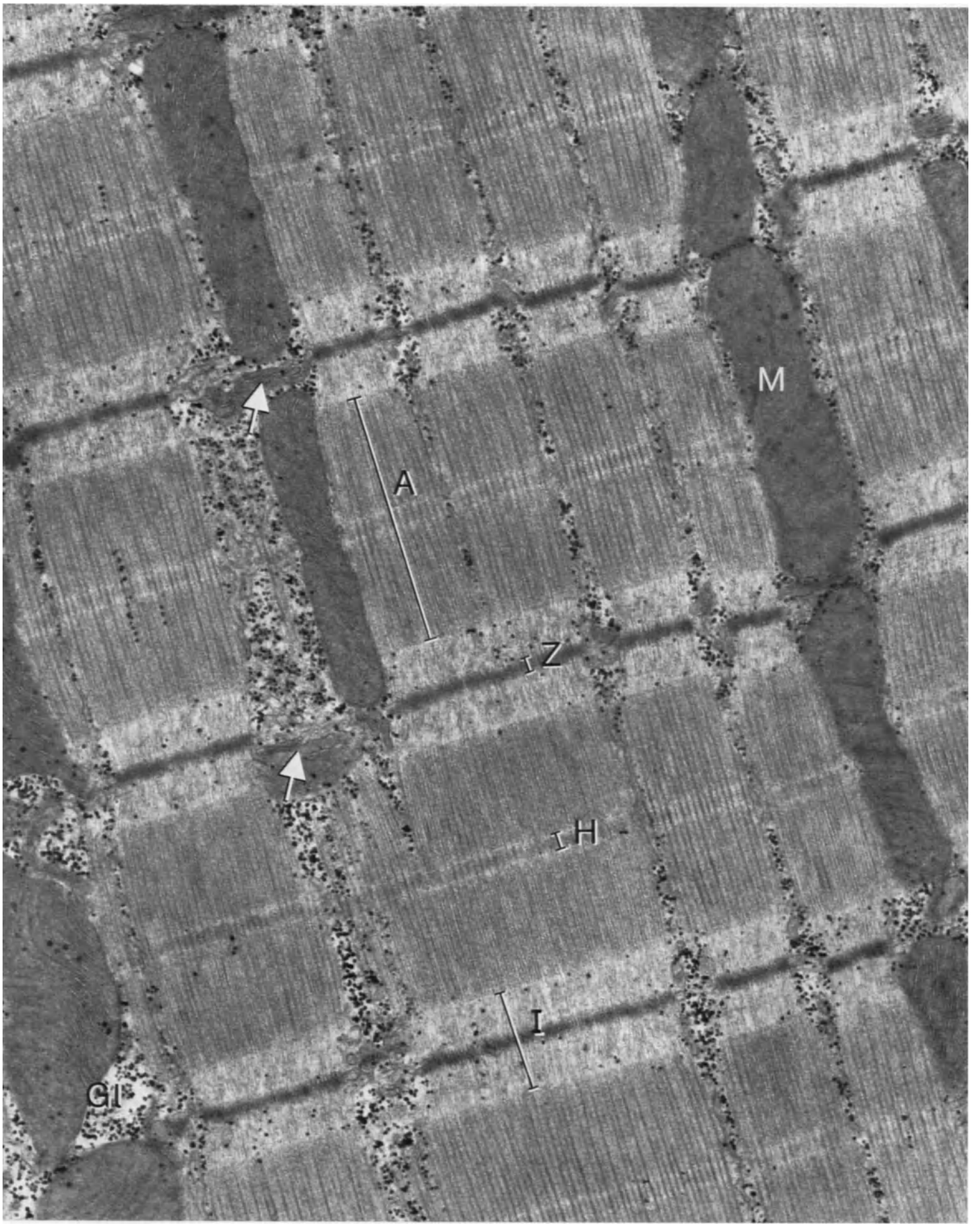
M
A
Z
H
I
GI

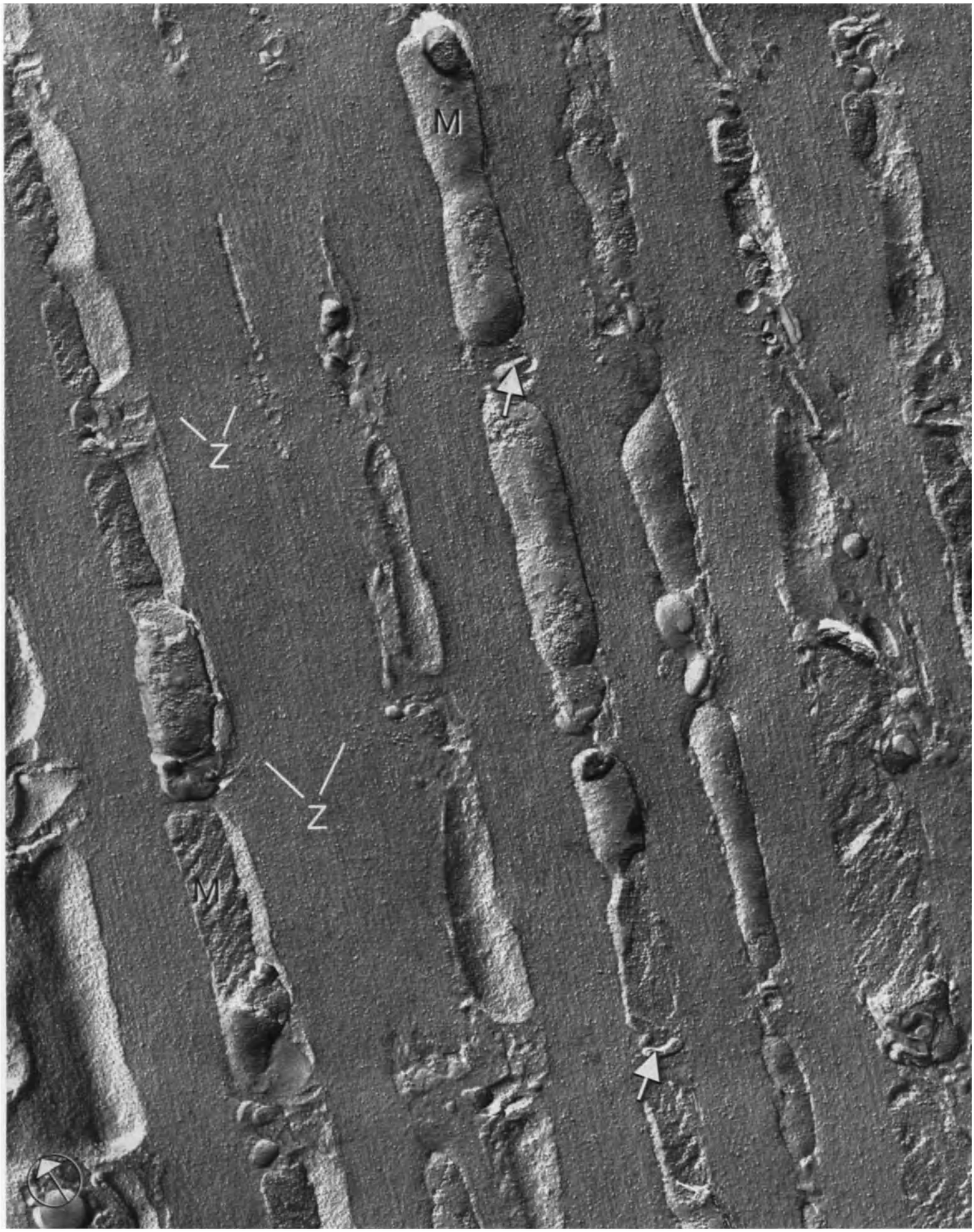
M
Z
Z
M

Plate 71 Smooth Muscle from the Human Bladder

Several smooth muscle cells (SM) sectioned transversely can be seen in this picture. The cells have an irregular outline and they are separated one from another by a wide intercellular space (ICS) containing collagen fibers (CF). The smooth muscle cell cytoplasm is packed with myofilaments (see also Plate 73). In the lower left-hand side of the picture, one distinguishes a bundle of non-myelinated axons (AA) in cross section.

Magnification ×21,000

Plate 72 Smooth Muscle from the Mouse Intestine

The fracturing process has exposed the cytoplasm of many smooth muscle cells (SM) at different levels, thus revealing also several areas of plasma membranes. In these membranes, arrays of endocytotic-like events are visible (→) (see Plates 73 and 74). Most of the membrane faces within the cytoplasm belong to mitochondria (M). In the lower part of the picture, the small circular profiles arranged in a discrete bundle represent nonmyelinated axons (AA) (see also Plates 75–76).

Magnification ×15,000

Selected Reference

DEVINE, C.E., SIMPSON, F.O., BERTAUD, W.S.: Freeze-etch studies on the innervation of mesenteric arteries and vas deferens. J. Cell Sci. **9**, 411–425 (1971).

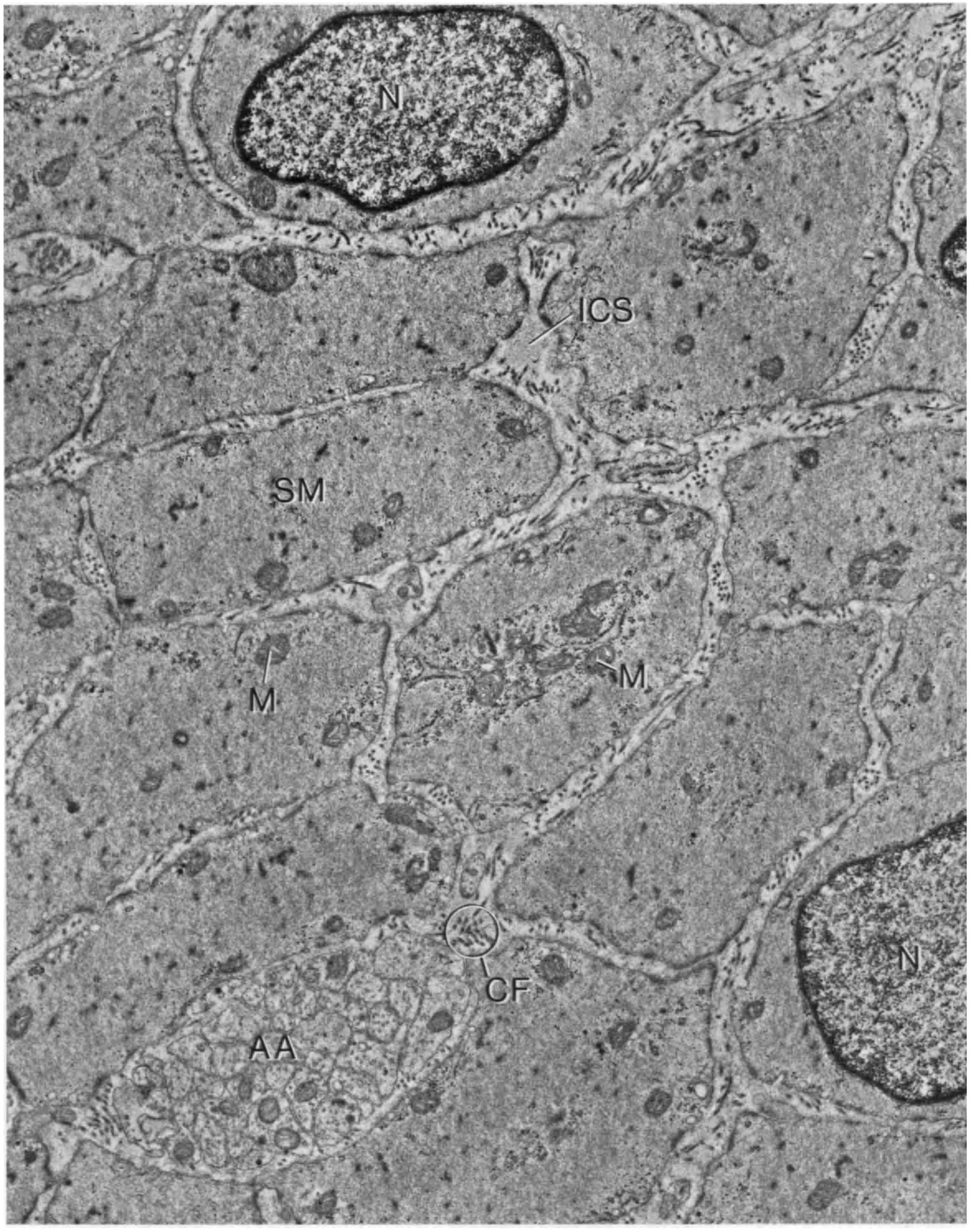
N
ICS
SM
M
M
CF
AA
N

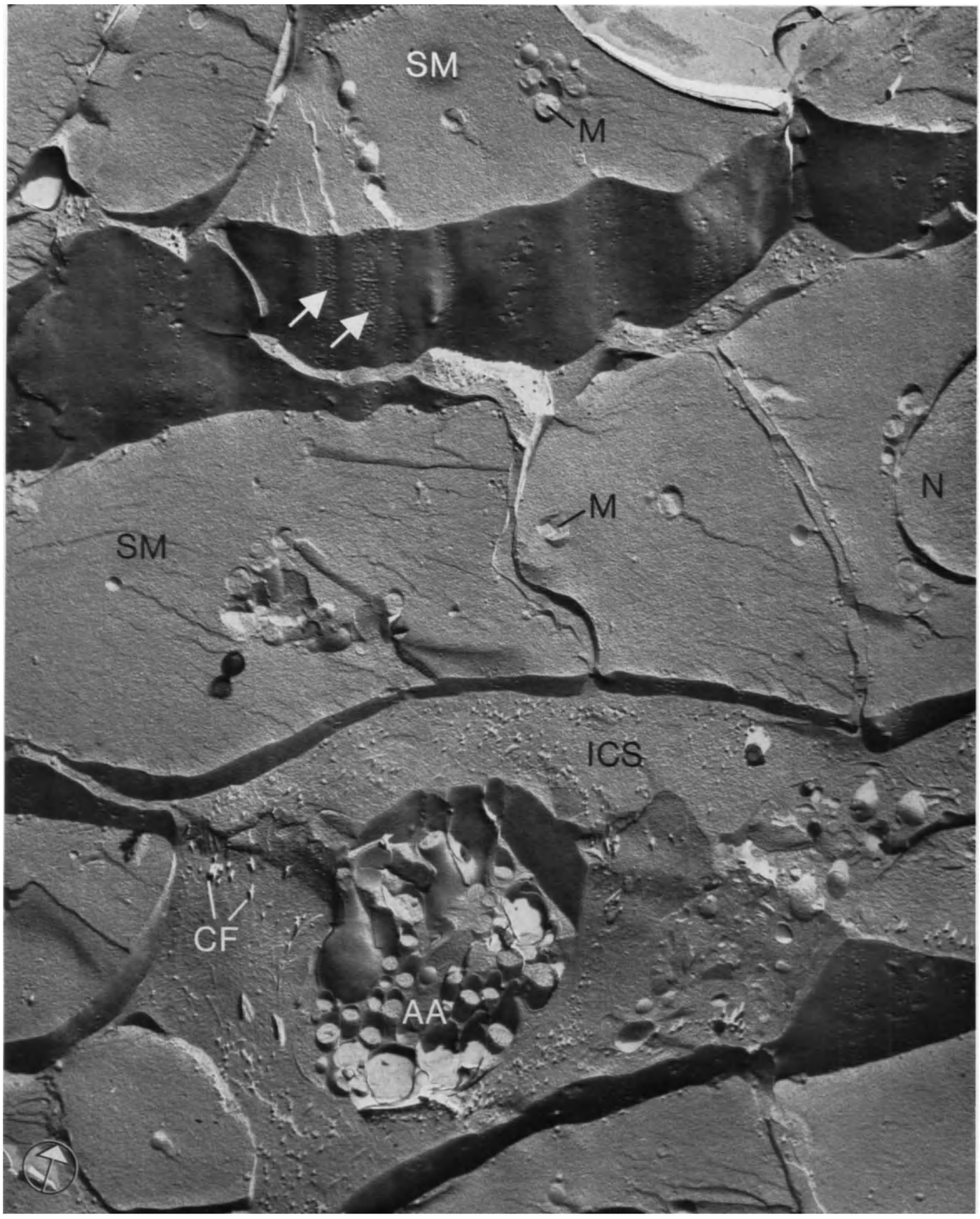
SM
M
M
N
SM
ICS
CF
AA

Plate 73 Arterial Smooth Muscle (Rat Pancreas)

Apart from the cytoplasm filled with a meshwork of myofilaments (Mf), the most noticeable feature of the smooth muscle cell is its surface. At this level, the plasma membrane shows numerous flask-like invaginations (→) resembling endocytotic vesicles. These invaginations occur in rather well delimited areas of the cell membrane (see Plate 74). Contrasting with the number of membrane invaginations, there are relatively few vesicles to be seen free in the cytoplasm.

Magnification ×43,000

Plate 74 Smooth Muscle from the Rat Intestine

The freeze-fracture has exposed a large area of the smooth muscle cell membrane before breaking through the cytoplasm. The membrane face exposed, an A-face, reveals in a striking way what was suspected in the thin-section, namely that endocytotic-like events occur in discrete regions of the cell membrane. Several rows of pits (P) are seen in the membrane and a closer look will also reveal that the membrane-associated particles are more numerous in the rows than outside. This distribution is another example emphasizing the relationship between the number and the disposition of membrane-associated particles, and a specific function of the membrane.

Magnification ×25,000. From L. ORCI and A. PERRELET: Science **181**, 868–869 (1973).

Selected References

MUGGLI, R., BAUMGARTNER, H.R.: Pattern of membrane invaginations at the surface of smooth muscle cells of rabbit arteries. Experientia (Basel) **28**, 1212–1214 (1972).

ORCI, L., PERRELET, A.: Membrane-associated particles: increase at sites of pinocytosis demonstrated by freeze-etching. Science **181**, 868–869 (1973).

WELLS, G.S., WOLOWYK, M.W.: Freeze-etch observations on membrane structure in the smooth muscle of guinea-pig taenia coli. J. Physiol. (Lond.) **218**, 11–13P (1971).

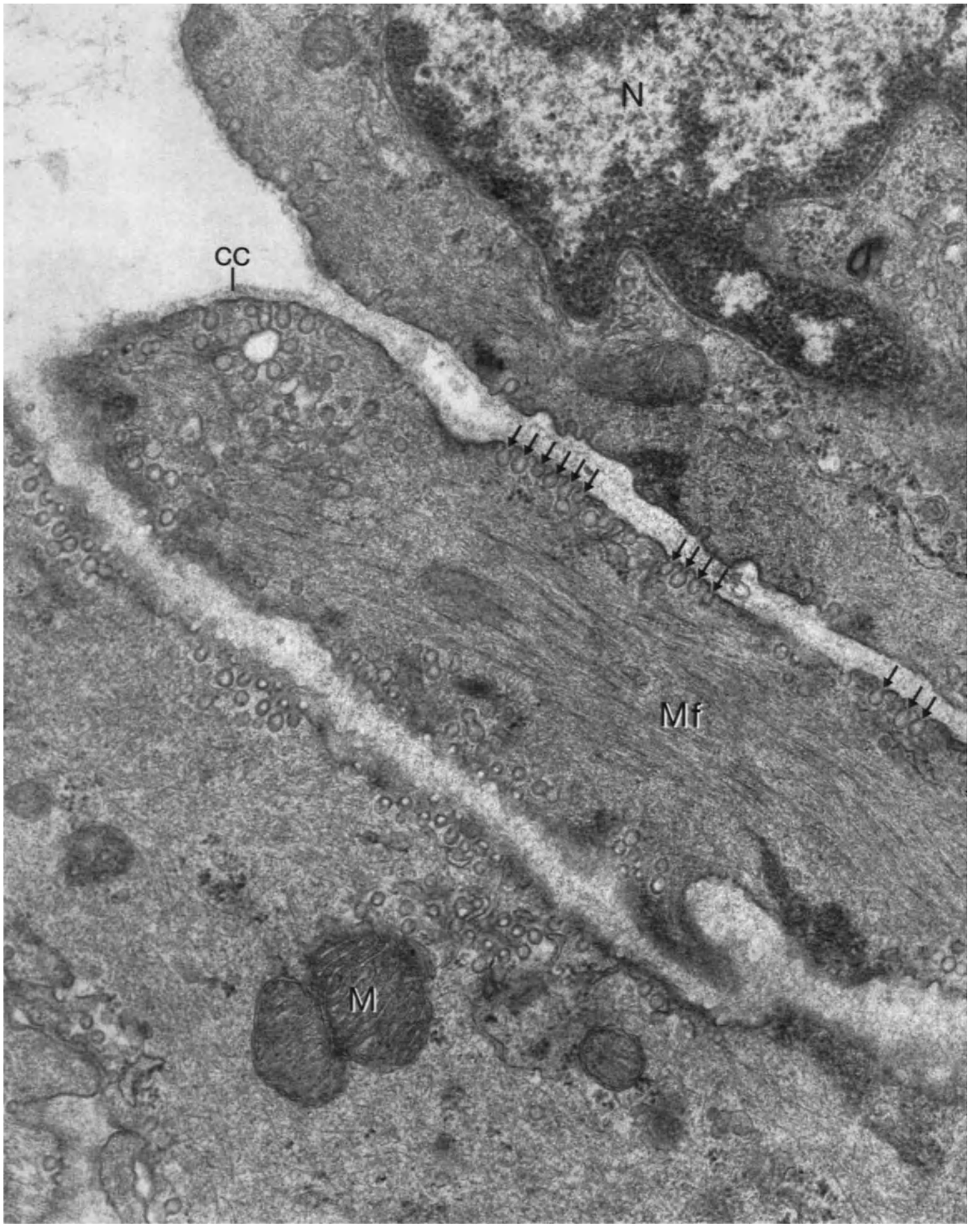
N
cc
Mf
M


CYTOPLASM
P
P
P
A

Plate 75 Non-Myelinated Axons from the Rabbit Vagus Nerve

Non-myelinated axons (AA) are contained within recesses of Schwann cells (SC). A single Schwann cell may surround several axons segregated in small bundles. Individual bundles, underlined by a basal lamina (BL), are separated from each other by wide intercellular spaces containing collagen fibers (CF). Within axons, one distinguishes cross-sectioned neurofilaments, a few vesicular profiles and some mitochondria (M). Axonal membrane is separated from the Schwann cell membrane by a narrow cleft of constant width (→).

Magnification × 35,000

Plate 76 Non-Myelinated Axons from the Human Bladder

The freeze-fractured nerve appears as a succession of membrane faces separated by steps. These latter represent the axoplasm or the Schwann cell cytoplasm in cross fracture. Due to the very close topographical relationship between the Schwann cell and the axonal membranes, it is in most cases difficult to distinguish their respective faces. In this figure, we assume that the rod-like, convex profiles represent A-faces of the axonal membrane. The four relatively large membrane areas of irregular outline (*) are attributed to Schwann cells.

Magnification × 30,000

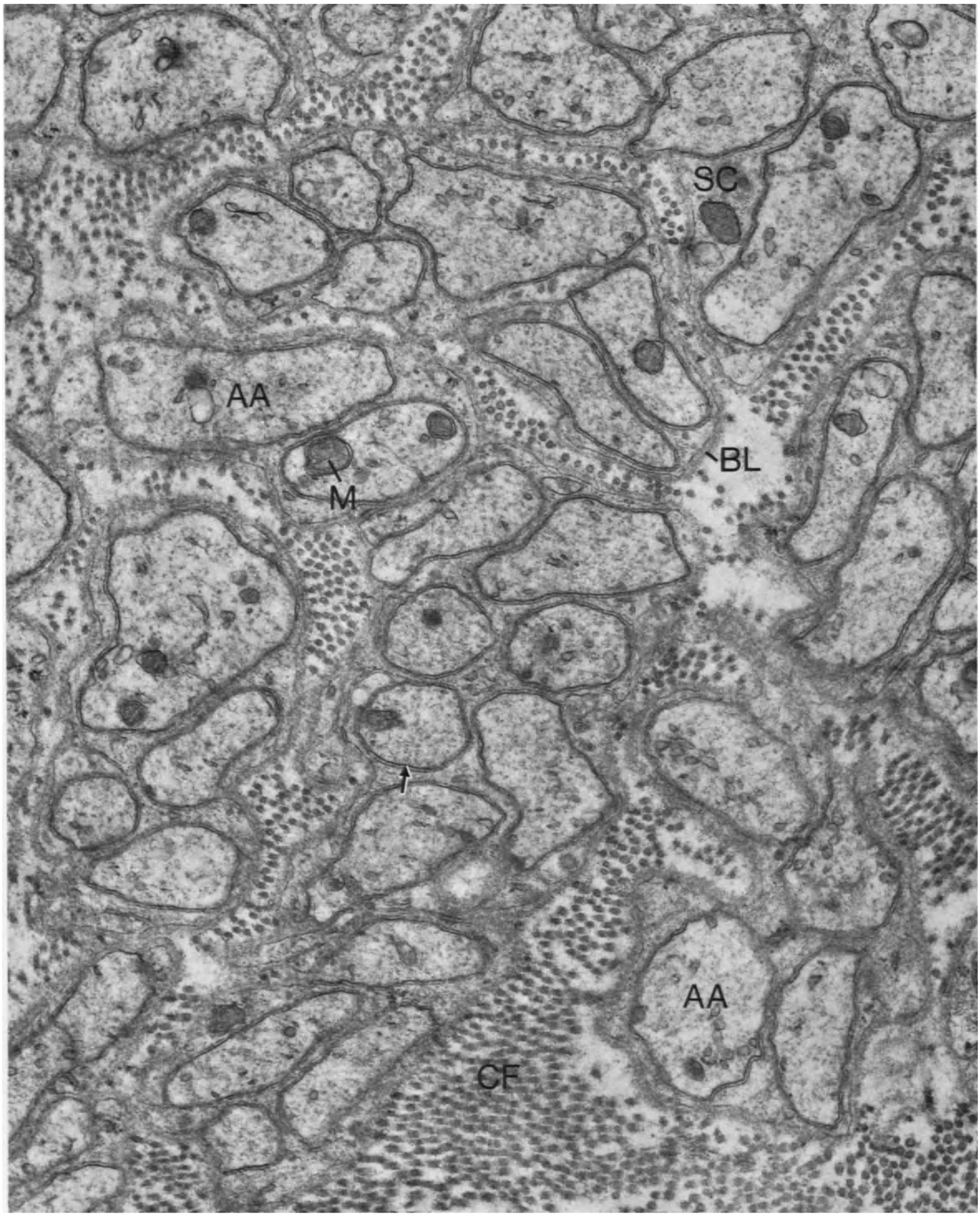
SC
AA
BL
M
AA
CF


CF
AA
Ā
Ā
AA

Plate 77 Myelinated Axon from the Superior Cervical Ganglion of the Rat

In cross section, one distinguishes the characteristic periodic lines of the myelin sheath (My) formed by the Schwann cell membrane around the axon. The Schwann cell (SC) membrane facing the intercellular space is underlined by a basal lamina (BL) outside of which several collagen fibers (CF) are visible. Within the axon (A), one recognizes neurotubules (microtubules) (Mt) and neurofilaments (F).

Magnification $\times 98{,}000$

Plate 78 Myelinated Axon from the Mouse Sciatic Nerve

In suitable areas of the replica (right-hand side of the picture, a definite periodicity is detectable in the cross fractured myelin (My). Its spacing corresponds to that seen in the sectioned material. The axon cytoplasm (A) contains a large number of protruding dots, most of which probably represent the fractured ends of neurofilaments (F).

Magnification $\times 23{,}000$

Selected References

BISCHOFF, A., MOOR, H.: Ultrastructural differences between the myelin sheaths of peripheral nerve fibres and CNS white matter. Z. Zellforsch. **81**, 303–310 (1967).

BRANTON, D.: Fracture faces of frozen myelin. Exp. Cell Res. **45**, 703–707 (1967).

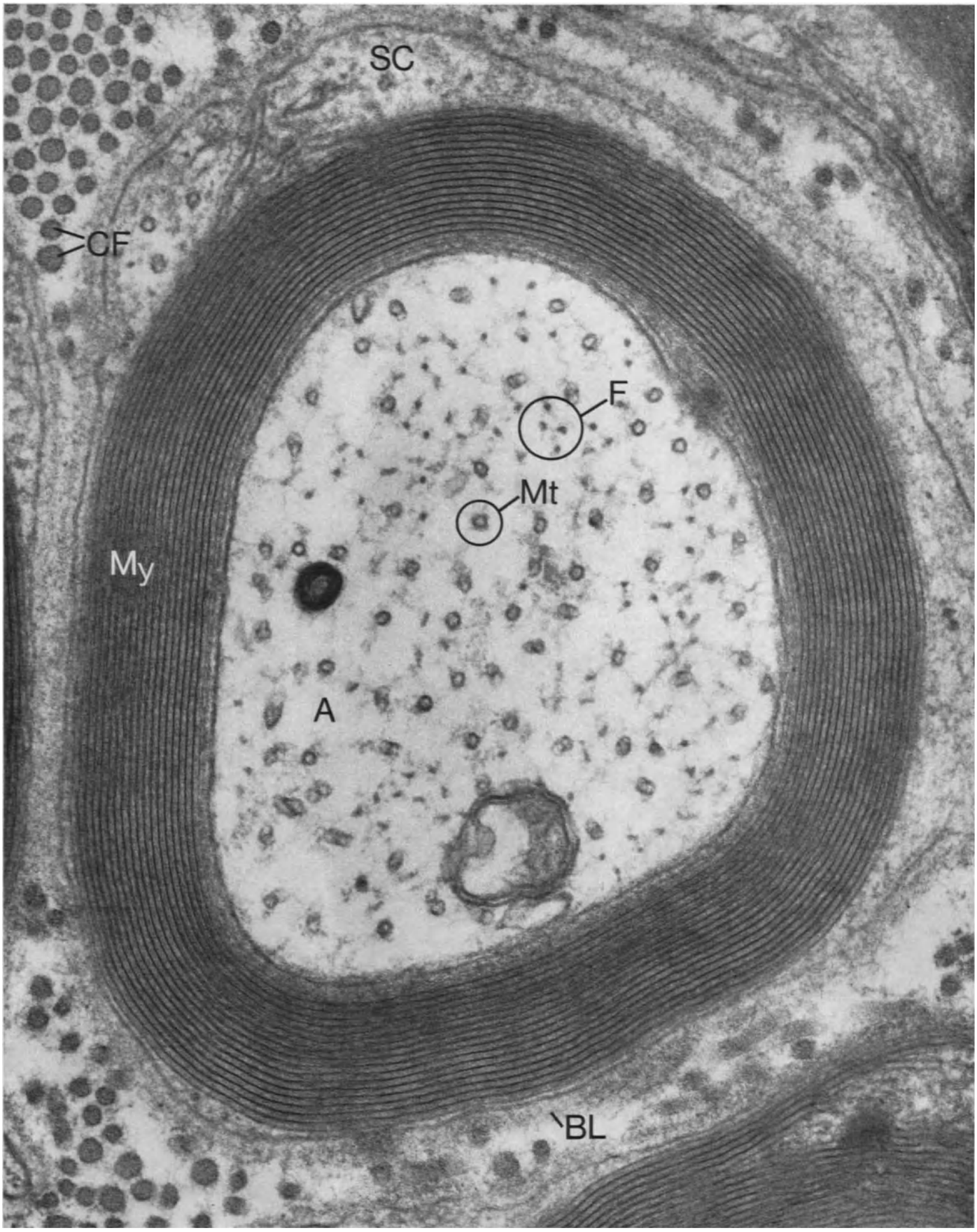
SC
CF
F
Mt
My
A
BL


My
F
A

Adipose Tissue

Plate 79 White Adipose Cell from the Rat Epididymis

In the adipose cell, the stored lipid is apparently not separated from the cytoplasmic matrix by a membrane. The cytoplasm is reduced to a thin rim containing flattened cisternae of smooth endoplasmic reticulum applied to the surface of the lipid droplet and numerous microvesicles of endocytotic origin (EV).

Magnification × 124,000

Plate 80 White Adipose Cell from the Rat Epididymis

The fracture through the lipid droplet produced a bumpy surface with a smooth texture. This appearance is characteristic of frozen lipids when they do not contain protein. The presence of protein would introduce a particulate component in the smooth background, as is best evidenced in work with artificial liposomes. The rim of cytoplasm (Cy) shows by contrast a coarse granular texture which merges with a large area of the adipose cell membrane. The A-face of the membrane has been exposed and displays a conspicuous endocytotic activity indicated by the presence of numerous pits (P).

Magnification × 98,000

Selected Reference

VAIL, W.J., PAPAHADJOPOULOS, D., MOSCARELLO, M.A.: Interaction of a hydrophobic protein with liposomes: evidence for particles seen in freeze-fracture as being proteins. Biochim. Biophys. Acta. **345**, 463–467 (1974).

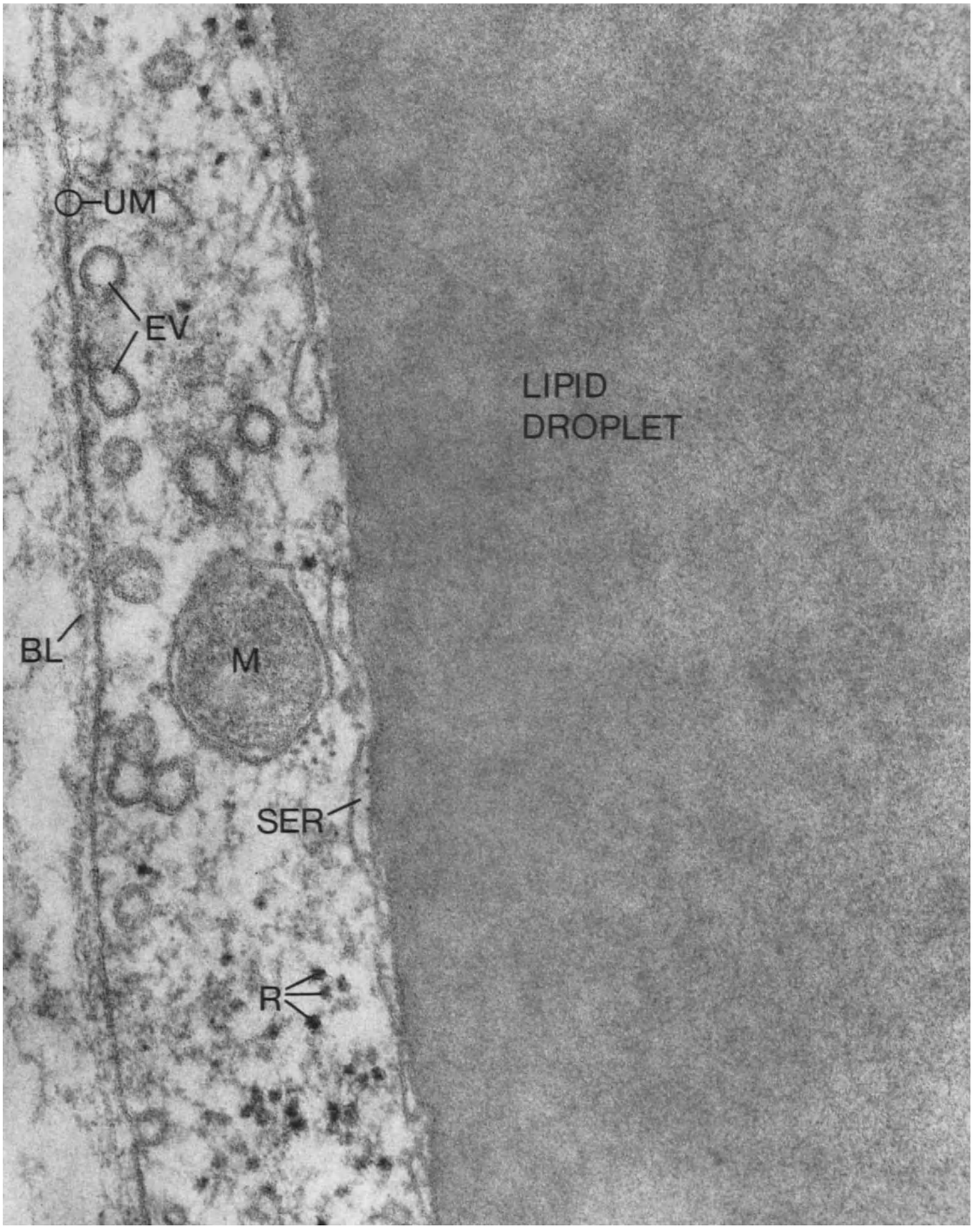
UM
EV
LIPID
DROPLET
BL
M
SER
R

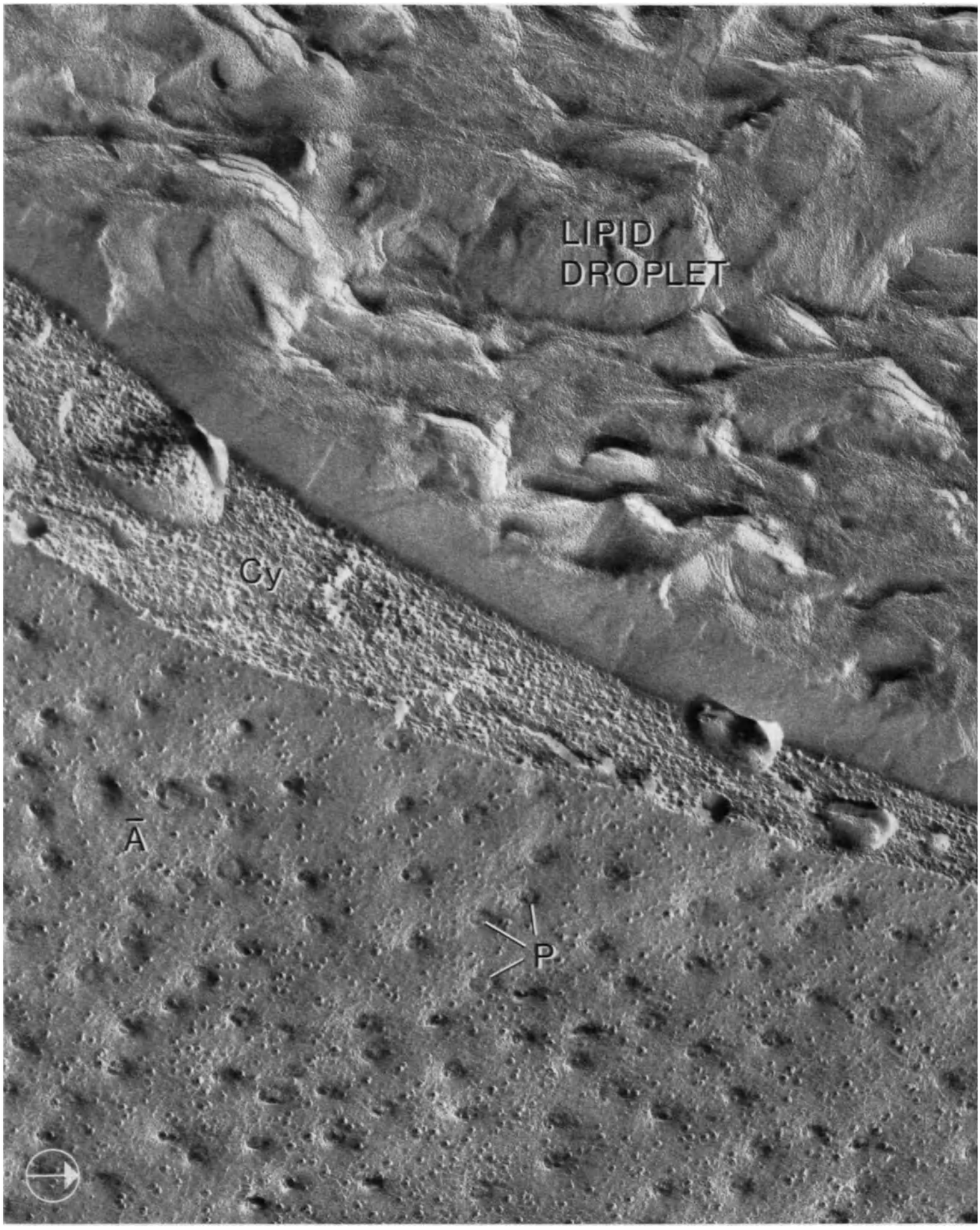
LIPID
DROPLET
Cy
Ā
P

Blood

Plate 81 Red Blood Cells from the Peripheral Blood of the Rat

Mature mammalian red blood cells (RBC) have a very simple organization consisting only of a plasma membrane enclosing a cytoplasm free of any organelle, but showing a strong electron density due to the iron of the hemoglobin molecules. The three cells shown here display various shapes since each of them has been sectioned at a different level.

Magnification × 30,000

Plate 82 Red Blood Cells in a Lung Capillary of the Rat

The freeze-fracture of a red cell with a shape comparable to that of the cell in the middle of Plate 81 gives the unusual image of a continuous A-face which is successively convex (upper part of the cell) and concave (lower part of the cell). Moreover, one can see that the richly particulated A-face is partially covered by smoother faces ($\bar{B}$). If one rejects the hypothesis of a spontaneous uncovering of the true outer surface of the red cell membrane, this image could be best explained by interpreting the smooth faces as remnants of the B-face of a neighboring red cell (removed by the fracturing process).

Magnification × 31,000

Selected Reference

WEINSTEIN, R.S., MCNUTT, N.S.: Ultrastructure of red cell membrane. Seminars in Hematology **7**, 259–274 (1970).

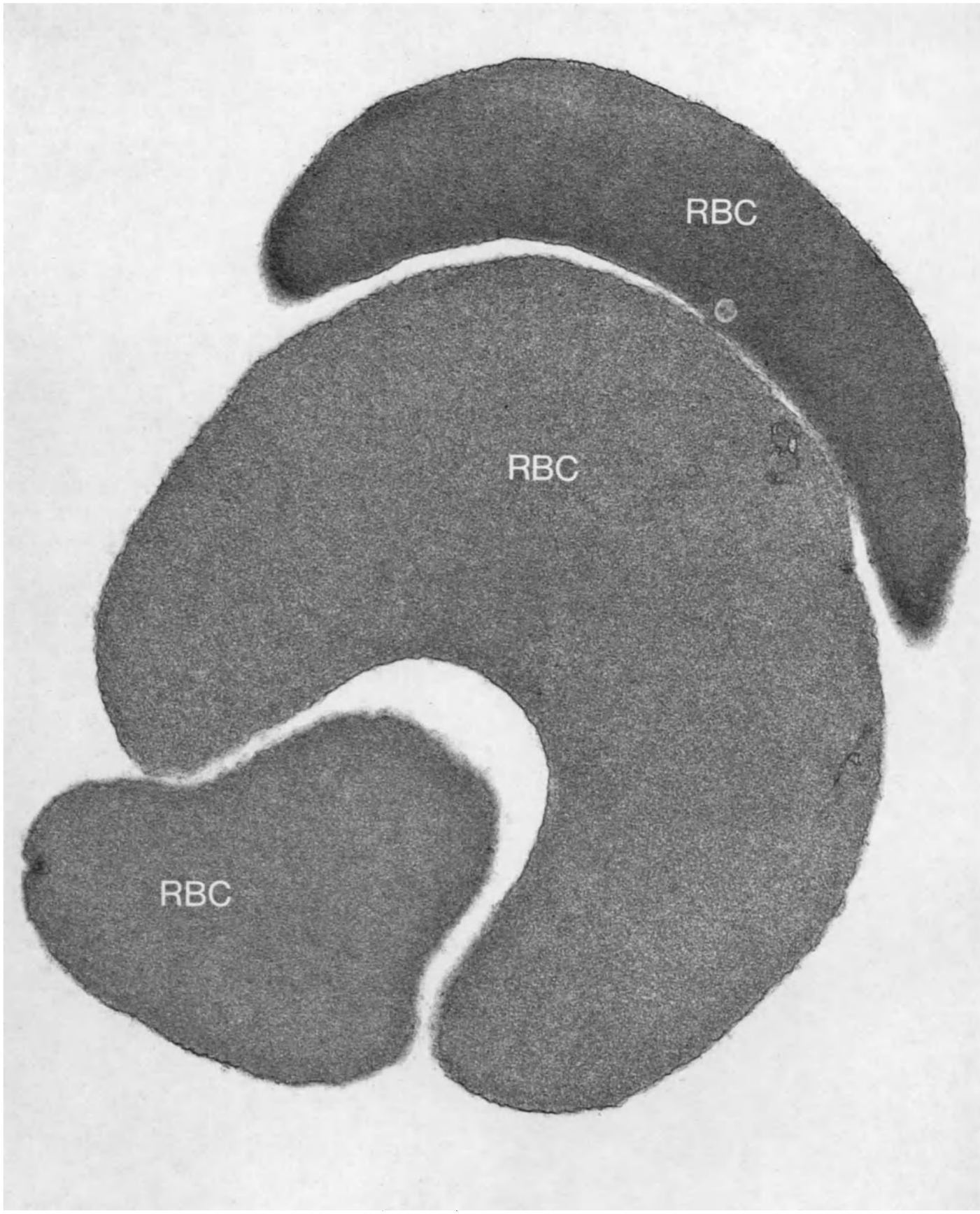
RBC
RBC
RBC


$\bar{A}$
$\bar{B}$
$\bar{A}$

Subject Index

Advanced Techniques in Biological Electron Microscopy

Edited by J. K. Koehler
With contributions by numerous experts
108 figures. XII, 304 pages. 1973
ISBN 3-540-06049-9
Cloth DM 50,—
ISBN 0-387-06049-9 (North America)
Cloth $20.50

Contemporary Research Methods in Neuroanatomy

Proceedings of an International Conference held at the Laboratory of Perinatal Physiology, San Juan, Puerto Rico, in January 1969 under the auspices of the National Institute of Neurological Diseases and Strokes and the University of Puerto Rico
Edited by W. J. Nauta, S. O. Ebbesson
190 figures. VIII, 386 pages. 1970
ISBN 3-540-04785-9
Cloth DM 122,—
ISBN 0-387-04785-9 (North America)
Cloth $34.30

Fluorescence Techniques in Cell Biology

Proceedings of the Conference on "Quantitative Fluorescence Techniques as Applied to Cell Biology" held at Battelle Seattle Research Center
Edited by A. A. Thaer, M. Sernetz
303 figures VIII, 420 pages. 1973
ISBN 3-540-06421-4
Cloth DM 48,—
ISBN 0-387-06421-4 (North America)
Cloth $19.90

Distribution rights for India:
Universal Book Stall (UBS), New Delhi

Prices are subject to change without notice

H. Elias

Normal and Pathologic Human Embryology: Textbook and Atlas

With contributions by J. E. Pauly and C. B. Severn
482 figures. Approx. 640 pages. 1975
ISBN 3-540-06229-7
Cloth DM 129,50
ISBN 0-387-06229-7 (North America)
Cloth $49.80

Distribution rights for Japan:
Igaku Shoin Ltd., Tokyo

Intracellular Staining in Neurobiology

Edited by S. B. Kater, C. Nicholson
132 figures (some in color). XIII, 332 pages 1973
ISBN 3-540-06261-0
Cloth DM 75,60
ISBN 0-387-06261-0 (North America)
Cloth $24.80

S. L. Palay, V. Chan-Palay

Cerebellar Cortex

Cytology and Organization
267 figures, incl. 203 plates. X, 348 pages 1974
ISBN 3-540-06228-9
Cloth DM 156,—
ISBN 0-387-06228-9 (North America)
Cloth $60.10

Distribution rights for Japan:
Igaku Shoin Ltd., Tokyo

Red Cell Shape

Physiology, Pathology, Ultrastructure
Proceedings of a Symposium held June 20 and 21, 1972 at the Institute of Cell Pathology, Hôpital de Bicêtre (as part of the scientific exchange program between N.I.H., U.S.A., and I.N.S.E.R.M., France)
Edited by M. Bessis, R. I. Weed, P. F. Leblond
147 figures. VIII, 180 pages. 1973
ISBN 3-540-06257-2
Cloth DM 36,—
ISBN 0-387-06257-2 (North America)
Cloth $17.80

Distribution rights for Japan:
Maruzen Co. Ltd., Tokyo

M. Bessis

Blood Smears Reinterpreted

Approx. 250 pages
In preparation
ISBN 3-540-07206-3
ISBN 0-387-07206-3 (North America)

M. Bessis

Corpuscles

Atlas of Red Blood Cell Shapes
121 figures. 147 pages. 1974
ISBN 3-540-06375-7
Cloth DM 96,—
ISBN 0-387-06375-7 (North America)
Cloth $26.20

Distribution rights for Japan:
Maruzen Co. Ltd., Tokyo

M. Bessis

Living Blood Cells and their Ultrastructure

Translated by R. I. Weed
521 figures, 2 color plates
XXI, 767 pages. 1973
ISBN 3-540-05981-4
Cloth DM 168,—
ISBN 0-387-05981-4 (North America)
Cloth $68.90

Distribution rights for Japan:
Maruzen Co. Ltd., Tokyo

Springer-Verlag
Berlin
Heidelberg
New York

Springer Journals

Calcified Tissue Research

Editorial Committee:
W. D. Armstrong, B. Engfeldt, H. Fleisch, R. M. Frank, B. A. Friedman (Secretary), R. P. Heaney, B. E. C. Nordin (Secretary), F. G. E. Pautard (Secretary), D. B. Scott (Secretary), K. M. Wilbur

Because calcified tissues serve as a support system for almost all living organisms, this periodical is strongly oriented toward an interdisciplinary approach. CALCIFIED TISSUE RESEARCH publishes research on the structure and function of bone and other mineralized systems in living organisms. It includes reports and review of studies that deal with connective tissues and cells, ion metabolism and transport, hormones, nutrition, ultrastructure, and molecular biology.

Cell and Tissue Research

Continuation of Zeitschrift für Zellforschung und mikroskopische Anatomie
Editors: W. Bargmann, D. S. Farner, A. Oksche, B. Scharrer

The introduction of electron optical, cytochemical, and quantitative methods is mainly responsible for the rapid progress now being made in research on the ultrastructure of cells and tissues. CELL and TISSUE RESEARCH, formerly ZEITSCHRIFT FÜR ZELLFORSCHUNG UND MIKROSKOPISCHE ANATOMIE, enables the reader to keep up with advances in this expanding field. The journal publishes original works dealing with all aspects of descriptive and experimental cell tissue research, including microscope studies of human and animal anatomy.

Histochemistry

Editors: P. B. Diezel, P. van Duijn, O. Eränkö, P. Gedigk, W. Gössner, W. Graumann, W. A. Jensen, Z. Lojda, B. Maurer-Schultze, A. E. F. H. Meijer, F. Moog, H. A. Padykula, A. G. E. Pearse, D. Pette, W. Sandritter, T. H. Schiebler, A. M. Seligman, M. Wolman

In its publication of original papers on the problems of histochemistry, cytochemistry, and histophysics, this journal especially features those dealing with methods-fractionation and homogenization techniques, autoradiography, polarization, optics, flourescence microscopy, etc. The material is well documented with illustrations, occasionally with color plates. As the information provided in this international journal can be applied to many fields of biological research HISTOCHEMISTRY also performs an important interdisciplinary role.

Anatomy and Embryology

Zeitschrift für Anatomie und Entwicklungsgeschichte

Editors: K. Fleischhauer, H. Frick, B. Kummer, M. Okamoto, R. Ortmann (Managing Editor), S. L. Palay, G. Raisman, K. Theiler, F. Walberg

Advanced research techniques, especially those derived from biophysics and biochemistry, have broadened the scope of anatomical research. This journal serves to inform the specialist about new research findings in the following fields: gross anatomy, histology, embryology, and experimental morphology in vertebrates.

Sample copies as well as subscription and back-volume information available upon request.

Please address:
Springer-Verlag
Werbeabteilung 4021
D-1000 Berlin 33
Heidelberger Platz 3

or

Springer-Verlag New York Inc.
Promotion Department
175 Fifth Avenue
New York, N.Y. 10010

Springer-Verlag
Berlin
Heidelberg
New York